

Radio sources in the 2dF Galaxy Redshift Survey – II. Local radio luminosity functions for AGN and star-forming galaxies at 1.4 GHz

Elaine M. Sadler¹, Carole A. Jackson², Russell D. Cannon³, Vincent J. McIntyre⁴, Tara Murphy¹, Joss Bland-Hawthorn³, Terry Bridges³, Shaun Cole⁵, Matthew Colless², Chris Collins⁶, Warrick Couch⁷, Gavin Dalton⁸, Roberto De Propris⁷, Simon P. Driver⁹, George Efstathiou¹⁰, Richard S. Ellis¹¹, Carlos S. Frenk⁵, Karl Glazebrook¹², Ofer Lahav¹⁰, Ian Lewis³, Stuart Lumsden¹³, Steve Maddox¹⁴, Darren Madgwick¹⁰, Peder Norberg⁵, John A. Peacock¹⁵, Bruce A. Peterson², Will Sutherland⁸, Keith Taylor¹¹

¹School of Physics, University of Sydney, NSW 2006, Australia

²Research School of Astronomy & Astrophysics, The Australian National University, Weston Creek, ACT 2611, Australia

³Anglo-Australian Observatory, P.O. Box 296, Epping, NSW 2121, Australia

⁴Australia Telescope National Facility, CSIRO, P.O. Box 76, Epping, NSW 2121, Australia

⁵Department of Physics, South Road, Durham DH1 3LE, UK

⁶Astrophysics Research Institute, Liverpool John Moores University, Twelve Quays House, Birkenhead, L14 1LD, UK

⁷Department of Astrophysics, University of New South Wales, Sydney, NSW 2052, Australia

⁸Department of Physics, Keble Road, Oxford OX1 3RH, UK

⁹School of Physics and Astronomy, North Haugh, St Andrews, Fife, KY6 9SS, UK

¹⁰Institute of Astronomy, University of Cambridge, Madingley Road, Cambridge CB3 0HA, UK

¹¹Department of Astronomy, Caltech, Pasadena, CA 91125, USA

¹²Department of Physics & Astronomy, Johns Hopkins University, Baltimore, MD 21218-2686, USA

¹³Department of Physics, University of Leeds, Woodhouse Lane, Leeds, LS2 9JT, UK

¹⁴School of Physics & Astronomy, University of Nottingham, Nottingham NG7 2RD, UK

¹⁵Institute for Astronomy, University of Edinburgh, Royal Observatory, Blackford Hill, Edinburgh EH9 3HJ, UK

arXiv:astro-ph/0106173v2 25 Jan 2002

26 October 2018

ABSTRACT

We have cross-matched the 1.4 GHz NRAO VLA Sky Survey (NVSS) with the first 210 fields observed in the 2dF Galaxy Redshift Survey (2dFGRS), covering an effective area of 325 square degrees (about 20% of the final 2dFGRS area). This yields a set of optical spectra of 912 candidate NVSS counterparts, of which we identify 757 as genuine radio IDs — the largest and most homogeneous set of radio-source spectra ever obtained. The 2dFGRS radio sources span the redshift range $z = 0.005$ to 0.438 , and are a mixture of active galaxies (60%) and star-forming galaxies (40%). About 25% of the 2dFGRS radio sources are spatially resolved by NVSS, and the sample includes three giant radio galaxies with projected linear size greater than 1 Mpc. The high quality of the 2dF spectra means we can usually distinguish unambiguously between AGN and star-forming galaxies. We have made a new determination of the local radio luminosity function at 1.4 GHz for both active and star-forming galaxies, and derive a local star-formation density of $0.022 \pm 0.004 \text{ M}_\odot \text{ yr}^{-1} \text{ Mpc}^{-3}$ ($H_0=50 \text{ km s}^{-1} \text{ Mpc}^{-1}$).

Key words: galaxies: radio continuum — galaxies: luminosity function — galaxies: active — galaxies: starburst

1 INTRODUCTION

Radio source surveys are ideal tools for studying the distant universe, since they are unaffected by dust obscuration and detect large numbers of galaxies over a wide span of cosmic epochs (the median redshift of galaxies detected in radio surveys is typically $z \simeq 1$; Condon 1989).

At 1.4 GHz flux densities above about 50 mJy, more than 95% of radio sources are classical radio galaxies and quasars powered by active nuclei (AGN). Below 50 mJy, the AGN proportion declines and an increasing fraction of the faint radio source population is identified with star-forming galaxies (e.g. Condon 1989, 1992). These are usually disk galaxies, sometimes interacting with neighbours, in which the radio emission arises mainly through synchrotron emission from relativistic electrons accelerated by supernova explosions. Thus radio surveys to levels of a few mJy probe both the AGN population and a population of star-forming galaxies. It is important to be able to separate these, in order to determine the local space density and redshift evolution of each population.

A new generation of radio imaging surveys (NVSS, Condon et al. 1998; FIRST, Becker, White & Helfand 1995; WENSS, Rengelink et al. 1997; SUMSS, Bock, Large & Sadler 1999) is now covering the whole sky to sensitivities of a few mJy. Radio source counts from such surveys potentially yield important information on the cosmological evolution of active and star-forming galaxies (e.g. Longair 1966, Jauncey 1975, Wall et al. 1980), but their interpretation is strongly model-dependent. The scientific return from large radio surveys is enormously increased if the optical counterparts of the radio sources can be identified, their optical spectra classified (as AGN, starburst galaxy, etc.) and their redshift distribution measured. In the past, however, this was a slow and tedious process which could only be carried out for relatively small samples.

Now, fibre-fed optical spectrographs make it possible to carry out spectroscopy of complete samples of hundreds of thousands of galaxies in the local universe. The Anglo-Australian Observatory's Two-degree Field (2dF) spectrograph can observe up to 400 galaxies simultaneously over a 2° -diameter region of sky (Lewis et al. 2001, see also www.aoa.gov.au/2df/). A Six-degree Field (6dF) spectrograph will be commissioned on the AAO's Schmidt Telescope in 2001, with 150 fibres over a 6° -diameter field, and in the northern hemisphere the Sloan Digital Sky Survey (SDSS; York et al. 2000) has begun a program of spectroscopy of 10^6 galaxies. Cross-matching radio continuum surveys with these new optical redshift surveys will provide redshifts and spectroscopic data for tens of thousands of local radio-emitting galaxies, rather than the few hundred available at present.

Two recent studies show the potential of these new redshift surveys. Machalski & Condon (1999) identified 1157 galaxies in the Las Campanas Redshift Survey (LCRS) with NVSS radio sources above 2.5 mJy at 1.4 GHz. They attempted to determine the radio and infrared properties of galaxies in the LCRS redshift range of $z = 0.05 - 0.2$, but had difficulties because the LCRS was sparsely sampled, with optical spectra only being taken for about one galaxy in three. Nevertheless, Machalski & Godlowski (2000) used the LCRS to derive the local radio luminosity function for both AGN

and star-forming galaxies, and to test for evolution over the LCRS redshift range.

Sadler et al. (1999) cross-matched the NVSS radio catalogue with the first thirty fields observed in the 2dFGRS, and found that it was usually straightforward to tell from the optical spectra whether the radio emission arose from star formation or an AGN (unlike LCRS, the 2dFGRS has a spectroscopic completeness of 95%).

The present paper is the second in a series analysing the properties of NVSS radio sources which are identified with galaxies in the 2dF Galaxy Redshift Survey (2dFGRS; Colless 1999, Colless et al. 2001, see also www.mso.edu.au/2dFGRS/). When complete, the 2dFGRS will yield good-quality optical spectra for up to 4000 radio-emitting galaxies in the redshift range $z = 0$ to 0.4. Such a large sample should allow us to disentangle the effects of age, orientation and luminosity in the local AGN population, as well as providing a definitive measurement of the local radio luminosity function (RLF) for active and star-forming galaxies. Our first paper (Sadler et al. 1999; hereafter Paper I), was a preliminary investigation of a small sample of the early 2dFGRS data, and showed that the 2dFGRS radio-source population is composed of roughly similar numbers of AGN and star-forming galaxies. In this paper we analyse a 2dFGRS data set which is almost an order of magnitude larger than in Paper I, and use it to derive the local radio luminosity function for active and star-forming galaxies at 1.4 GHz.

The spectra analysed in this paper are included in the first public release of 2dFGRS data, which took place in June 2001.

Throughout this paper, we use $H_0 = 50 \text{ km s}^{-1} \text{ Mpc}^{-1}$ and $\Omega_0=1$.

2 SAMPLE SELECTION

In this paper, we analyse 2dFGRS spectra from the first two years of the survey, i.e. up to May 1999. Observations made before October 1997 were excluded because the instrument was still in a commissioning phase and the data are of variable quality. The data set analysed here comprises 210 fields, or about 20% of the total 2dFGRS area. The original selection of 2dFGRS optical targets included all non-stellar objects brighter than $b_J \simeq 19.5$ from the photographic UKST Southern Sky Survey, and should involve no explicit biases so far as radio properties are concerned.

2.1 Area covered

The 2dFGRS uses a tiling algorithm with variable overlap depending on the underlying galaxy density. Some 2dFGRS fields are also shared with a parallel QSO redshift survey, so calculating the exact area of sky observed is not straightforward until the whole survey is complete.

We therefore use the method described by Folkes et al. (1999) and estimate the area of sky covered by dividing the number of galaxies observed by the mean surface density of galaxies in the target list. The data set observed in the period October 1997—May 1999 inclusive contains 58,454 2dFGRS targets. Taking the Folkes et al. surface density of 180 galaxies deg^{-2} to the survey limit of $b_J = 19.45$ mag.

gives an effective area of 325 deg^2 for the data set we will analyse here.

2.2 Radio source identifications

We cross-matched the 2dFGRS catalogue positions with the NVSS radio catalogue and took all matches with position offsets of 15 arcsec or less as candidate radio detections. This yielded a total of 927 observations of 903 targets. Not all these will be true identifications — as discussed in Paper I, we expect most unresolved radio sources with offsets of 10 arcsec or less to be true associations with 2dFGRS galaxies, along with a smaller (and quantifiable) fraction of sources with offsets of 10–15 arcsec.

There are also three classes of objects for which the situation is more complex: (i) extended (resolved) NVSS radio sources, (ii) radio sources which are resolved by NVSS into two or more distinct components, and (iii) radio sources associated with nearby bright galaxies ($b_J < 17 \text{ mag}$). As we discuss in Section 4, these received extra attention to determine whether to accept a candidate ID as a correct one.

For completeness, and because others may wish to use our data with different selection criteria for radio-source IDs, we have tabulated 2dFGRS spectral types and redshifts for all 912 candidate radio-source IDs with radio-optical offsets of 15.0 arcsec or less. We showed in Paper I that, with the exception of a small number of double NVSS radio sources (see Section 4.2), there should be very few correct IDs with radio-optical offsets larger than 15 arcsec. This is confirmed in Fig. 1, which shows that by 15 arcsec from the 2dF position the number of candidate detections falls to the level expected from chance coincidences alone.

We also note that the 2dFGRS input catalogue is incomplete for galaxies brighter than $b_J \simeq 14$, and so some bright, nearby galaxies are missing from the 2dFGRS. Almost all these missing galaxies should already have redshift measurements, and can be added back into the sample once the entire 2dFGRS is complete. In calculating luminosity functions (see Section 8), we correct for the absence of these bright galaxies.

3 OPTICAL SPECTRA

As noted earlier, the spectra analysed in this paper were collected as the 2dFGRS progressed, and cover the period to May 1999. Most of these spectra are included in the first (mid-2001) public release of 2dFGRS data (see Colless et al. 2001 for details of the public-release database). In a few cases, a new spectrum taken after May 1999 may be better than the one used here and will replace it in the final database.

Although in most cases the public-release data are identical to those analysed here, some values of b_J , z and Q listed in Table 1 may change. This is because there have been revisions of the b_J magnitude scale, and a re-reduction of all the early 2dFGRS redshifts, since we began our analysis. In the great majority of cases, the database revisions produced no significant difference, especially for spectra with $Q \geq 3$. Small changes in the values of b_J or z for individual galaxies will not affect the overall results of the analysis which follows.

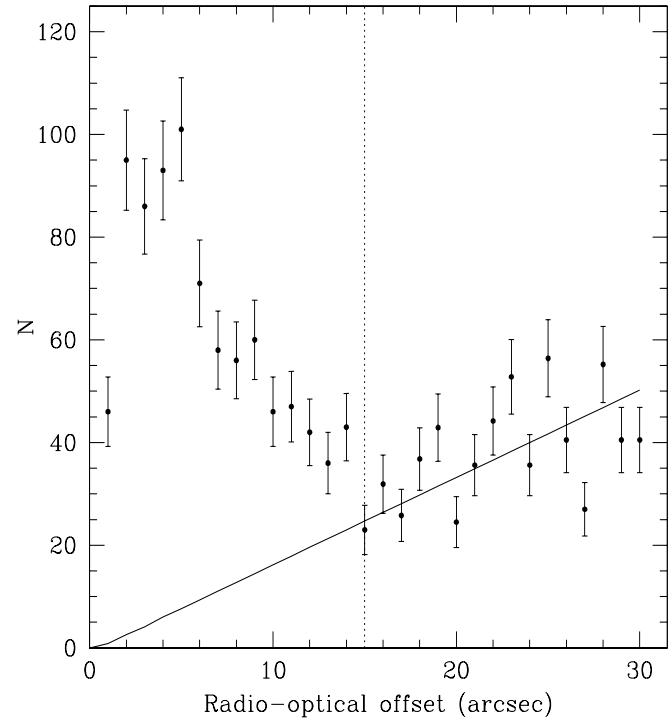


Figure 1. Number of candidate NVSS detections of 2dFGRS galaxies plotted against the offset Δ between radio and optical positions. The solid line shows the number of matches expected by chance from a sample of 58,454 2dFGRS galaxies, assuming that NVSS radio sources are randomly distributed on the sky with a surface density of 60 deg^{-2} . Note that at a separation of 15 arcsec or more, the number of matches declines to that which would be expected by chance, so we adopted a separation cutoff of 15 arcsec for candidate 2dFGRS radio sources.

3.1 Spectral classification

2dFGRS spectra of each of the 912 candidate radio-source IDs were examined and classified visually by one of us (EMS). As in Paper I, each spectrum was classified as either ‘AGN’ or ‘star-forming’ (SF) based on its 2dF spectrum. AGN galaxies have either an absorption-line spectrum like that of a giant elliptical galaxy (these we classed ‘Aa’); an absorption-line spectrum with weak LINER-like emission lines (class ‘Aae’), or a stellar continuum dominated by nebular emission lines such as [OII] and [OIII] which are strong compared with any Balmer-line emission (class ‘Ae’). ‘SF’ galaxies are those where strong, narrow emission lines of H α and (usually) H β dominate the spectrum. Objects where the spectra were too noisy for reliable classification are classed as ‘??’.

There are several independent tests of the reliability of our visual classification of the spectra: (a) the visual classifications generally agree well with the results of Principal Components Analysis (PCA) methods, as we will show in Section 3.3, (b) for galaxies with optical emission lines, our Ae/SF classifications agree well with those derived by Jackson & Londish (2000) from diagnostic emission-line ratios, and (c) most galaxies which we classify as SF are detected by IRAS and fall on the radio—FIR correlation (see section 6), whereas none of the galaxies we classified as Aa are detected

by IRAS. Thus we are confident that our visual classification of the 2dFGRS spectra allows us to distinguish AGN and star-forming galaxies in a consistent and reliable way.

3.2 Data table

Table 1 lists the entire sample of 912 candidate radio IDs, i.e. the 903 2dFGRS targets whose catalogued position is within 15 arcsec of the catalogued position of an NVSS radio source, together with a further nine extended and double radio sources which were identified separately as described in Section 4.2. The table columns are as follows:

- (1) 2dFGRS galaxy name (this is the name used in the 2dFGRS database). An asterisk following the name indicates that this galaxy appears in the Notes at the end of Table 1.
- (2) Other name — we have cross-identified with other galaxy catalogues where possible.
- (3) The optical position (J2000.0) at which the 2dFGRS fibre was placed.
- (4) The offset between 2dFGRS (optical) and NVSS (radio) positions, in arcsec.
- (5) Total blue (b_J) magnitude, from the 2dFGRS database. The magnitudes listed here are taken from the May 2000 version of the database.
- (6) Total radio flux density at 1.4 GHz, from the NVSS catalogue (Condon et al. 1998). Where a source is split into more than one component in the NVSS catalogue, this is indicated in the Notes at the end of the table and the value quoted here is the sum of all the components.
- (7) IRAS 60 μ m flux density (in Jy), where listed in the NASA Extragalactic Database (NED). Although IRAS surveyed 97% of the sky, the incompleteness near the Galactic poles is larger than in other areas. Based on the IRAS sky coverage plots given by Beichman et al. (1988), about 10% of the 2dFGRS survey area had either one or no IRAS scans and so was not catalogued. The main 2dFGRS areas missed by IRAS lie in the region between 10 and 11 h RA in the northern zone and 23 and 0 h RA in the southern zone, but there are also smaller gaps elsewhere.
- (8) Heliocentric redshift, from 2dFGRS observations unless otherwise indicated in the Notes.
- (9) 2dFGRS spectrum quality code Q, where Q=4 or 5 are excellent-quality spectra, Q=3 acceptable and Q=0, 1 or 2 poor-quality. Galaxies with Q<3 are excluded from further analysis because their redshifts are highly uncertain. Checks against repeat observations and published redshifts show that 2dFGRS redshifts with Q=3 are about 90% reliable and those with Q=4 or 5 are 99% reliable (Colless et al. 2001).
- (10) Spectral class, based on our visual classification.

3.3 Comparison of visual and PCA spectral classifications

We would eventually like to compare the 2dFGRS radio-emitting galaxies with the parent sample from which they are drawn (in order to answer questions like “what fraction of Seyfert 1 and 2 galaxies are radio-loud, and how does this vary with redshift?”), so we compared our simple visual classification of the spectra (as Aa, Ae or SF) with the Principal Components Analysis (PCA) methods developed for

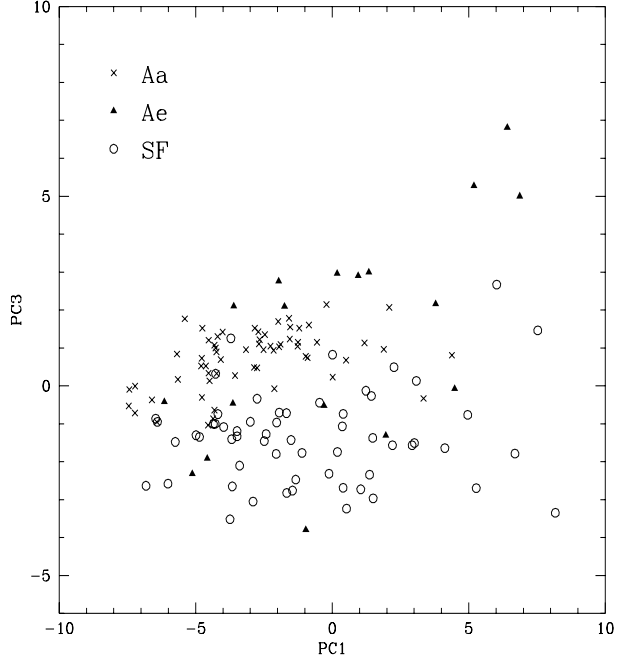


Figure 2. Plots of the first and third PCA components from 2dF spectra of radio-emitting galaxies. The three spectral classes from our visual classification are reasonably well-separated in this plot, though some Ae galaxies overlap the region populated by SF galaxies. The PCA data used in this preliminary analysis were taken from an early version of the database and there have been some significant revisions of the PCA scheme since then (Madgwick et al. 2001).

use with the 2dFGRS by Folkes et al. (1999) and Madgwick et al. (2001). PCA is an automatic method of classifying spectra which has the great advantages of being objective, quantitative and easily applied to very large samples. A series of Principal Components or eigenspectra (PC1, PC2, ...) are determined from the distribution of all the spectra in a very large multi-dimensional space; most of the information in the spectra is included in the first few PCs. This means that each spectrum can be well-represented by a set of just 3 or 4 numbers, corresponding to the relative power in the dominant PCs.

We find good agreement between the visual and automatic methods of classifying galaxy spectra. For example, in a plot of PC3 against PC1 (Fig. 2) there is a clear separation between the different visual spectral types. By combining similar plots involving PC2, it looks as if it will be possible to define an almost unique mapping between the two classification methods, making it easy to compare the properties of the 1.5% of the galaxies which are radio sources with the full 2dFGRS sample of up to 250,000 optical galaxies.

3.4 Spectral class and redshift

Fig. 3 shows how the composition of the 2dFGRS radio sources changes with redshift. As we showed in Paper I, star-forming galaxies dominate the population at low redshift while active galaxies dominate above $z \simeq 0.1$. This is because star-forming galaxies are low-luminosity radio sources ($P_{1.4} < 10^{23} \text{ W Hz}^{-1}$) which drop out of the sam-

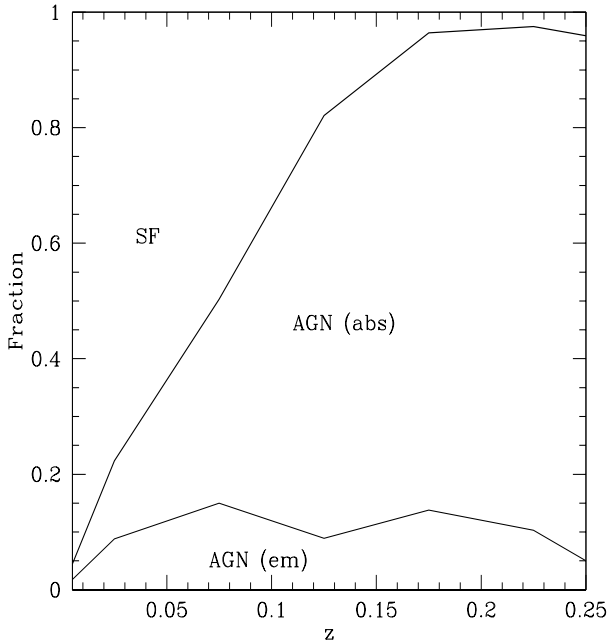


Figure 3. Change in spectral mix with redshift for 2dFGRS/NVSS galaxies. SF indicates star-forming galaxies with HII-region optical spectra and AGN (em) and AGN (abs) indicate active galaxies with and without strong optical emission lines.

ple when they fall below the NVSS radio detection limit. Conversely, most AGN have higher radio luminosities and remain in the sample out to $z \simeq 0.2 - 0.3$ where they finally drop below the 2dFGRS optical magnitude limit.

Interestingly, the fraction of emission-line AGN (Ae) galaxies remains roughly constant (at 10–15%) throughout the sample volume even though the overall AGN fraction increases dramatically with redshift. We need to keep in mind, however, that the 2 arcsec diameter 2dF fibres include an increasing fraction of the total galaxy light for more distant galaxies (see Fig. 4). As a result, galaxies with emission-line nuclei will be easier to recognise at lower redshift, where there is less dilution from the surrounding stellar galaxy, than at higher redshift. We therefore assume that the probability of recognizing a galaxy as Ae rather than Aa varies with redshift, and so we combine the Aa and Ae classes in most of our later analysis.

In star-forming galaxies, the line emission is expected to come mainly from an extended disk and dilution of the emission-line flux with redshift is less likely. Indeed we might expect star-forming galaxies to be easier to recognise at higher redshift since the 2dF aperture includes a larger fraction of the total disk light.

4 RADIO-OPTICAL IDENTIFICATIONS

We now need to determine which of the candidate radio source identifications in Table 1 are real associations between a 2dFGRS galaxy and an NVSS radio source. This is not always straightforward — as noted in paper I, we expect some chance coincidences even at the smallest radio-optical separations. In Paper I, we used a simple 10 arcsec cutoff

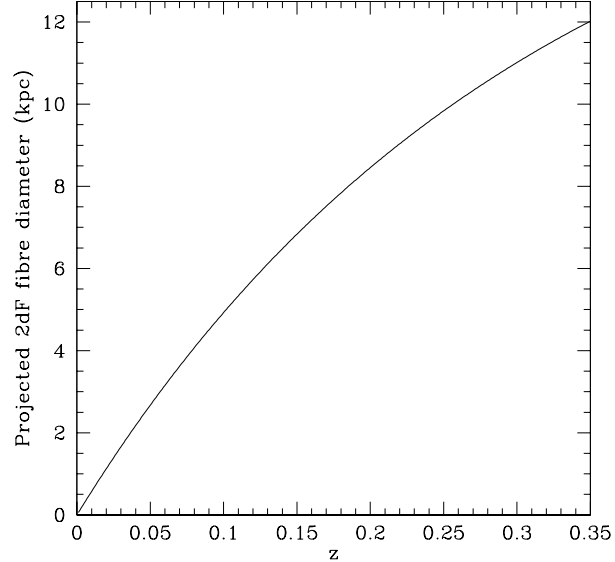


Figure 4. Projected diameter of the 2dF fibres (in kpc) for galaxies over the redshift range $z = 0$ to 0.35.

as the criterion for association. Although this will include a few objects which are not real associations and exclude some which are, the number of such objects can be quantified statistically and taken into account when calculating the luminosity function.

We use a similar 10 arcsec cutoff here, but also recognise that a simple cutoff may exclude some extended sources with complex radio structure. Thus we also inspected radio-optical overlays of all the extended sources in the candidate list and accepted some of these as genuine IDs even though the radio-optical offset was larger than 10 arcsec.

4.1 Extended radio sources

About 25% of the candidate NVSS/2dFGRS radio sources are resolved by the 45 arcsec NVSS beam, giving us an estimate of their linear size. In most such cases we still see a single radio source, but with an apparent size larger than 45 arcsec in at least one dimension. For these galaxies, the NVSS radio position is calculated by fitting a two-dimensional Gaussian to the radio image. If the fit is not perfect, the quoted position may have a much larger uncertainty than that of an unresolved radio source of similar flux density.

For all extended NVSS sources with radio-optical offsets in the range 10.0–15.0 arcsec, we inspected overlays of the radio contours onto DSS images (see Fig. 5 for examples). If the optical galaxy lay along the major axis of the extended radio source, or the radio emission appeared to be symmetric about the optical galaxy, we accepted this as a correct ID.

4.2 Double radio sources

A few NVSS radio sources are resolved into two or more distinct components, so we need to be able to recognise these,

and to search for an optical ID near the radio centroid rather than at the position of each individual component.

We first identified all the candidate double radio sources in the NVSS catalogue by using the semi-empirical link-length measure defined by Magliocchetti et al. (1998). A pair of radio sources are defined to be associated if:

- (i) the ratio of their flux densities S_1 and S_2 lies in the range $0.25 < (S_1/S_2) < 4.0$, and
- (ii) the projected separation of the two radio components is smaller than their link length r , which is calculated from the total flux density in mJy and defined as:

$$r = [(S_1 + S_2)/100 \text{ mJy}]^{0.5} \times 100 \text{ arcsec}. \quad (1)$$

This yielded a total of 525 candidate NVSS doubles in the 1700 deg^2 region of sky covered by the 2dFGRS. Of these, 59 had a 2dFGRS galaxy within 30 arcsec of the radio centroid and 17 of these galaxies had spectra taken up to 1999 May. These objects were then inspected to see whether the optical galaxy lay on or near the radio axis of the NVSS double. As a result, eight new 2dFGRS galaxies were added to the sample as optical hosts of NVSS doubles. These are listed at the end of Table 1, along with an unusual diffuse source, tentatively identified with TGN307Z092, which is discussed in Section 5.2. These nine extra galaxies bring the total number of candidate NVSS/2dFGRS matches to 912 (of these, 56% are AGN and 35% SF galaxies).

4.3 Optically-bright galaxies

We paid special attention to the brightest 2dFGRS galaxies ($b_J = 14.0 - 17.0$ mag). For these bright galaxies, the radio-optical offset alone is not always a reliable indicator of whether the galaxy is associated with an NVSS radio source. There are three reasons for this: (i) it can be difficult to measure an accurate optical position for these galaxies from Schmidt plates since the central regions are often over-exposed, (ii) we found that the 2dFGRS fibre positions used for bright galaxies were sometimes offset from what appeared to be the optical nucleus, and (iii) much of the radio emission in these galaxies arises from star formation-related processes in a resolved disk (see Section 5 for more details), so that the centroid of the radio emission can be offset by several arcsec from the galaxy nucleus. We therefore inspected radio overlays on DSS images of all galaxies brighter than mag 17.0 and accepted those with 10.0–15.0 arcsec offsets as correct IDs if the radio emission appeared to be roughly centred on the optical galaxy. When this was done, it is noted in the final column of Table 1.

4.4 The final sample

Our final sample of accepted NVSS/2dFGRS IDs comprises all sources with radio-optical offsets of 10.0 arcsec or less, along with nine additional double galaxies described above and 47 additional galaxies with radio-optical offsets of 10.0–15.0 (28 of them radio sources associated with optically-bright galaxies, and 19 extended radio sources). This gives a final sample of 757 ‘accepted’ NVSS/2dFGRS IDs which we use in further analysis.

Table 2 summarises the spectral properties of the final sample. The 2dFGRS spectra are generally of excellent

** Fig. 5 available as a separate file **

Figure 5. Overlays of NVSS radio contours on DSS optical images of some of the extended radio sources identified with 2dFGRS galaxies. Each frame shows a region 6.4 arcmin across. Contours are at $1, 2, 4, 8, 16, 32, \dots \text{ mJy beam}^{-1}$, except for (h) TGS 398Z220 and (i) TGS 190Z105, where the lowest contour is at 4 mJy beam^{-1} . For TGS 190Z105, two dark lines mark the position of the faint galaxy identified as the radio source.

Table 2. Summary of spectral classifications for the galaxies listed in Table 1

	All candidates	Accepted as ID	Rejected as ID
AGN	514	441	73
SF	319	272	47
Stars	18	0	18
Low S/N spectra	61	44	17
Total	912	757	155

quality, allowing both the redshift and spectral class to be determined accurately. Of the 912 targets analysed here only 30 had spectra of quality class 1 or 2, i.e. were too noisy for a reliable redshift measurement. Eighteen targets turned out to be misclassified Galactic stars (i.e. had absorption-line spectra with $z < 0.001$), and two of the AGN were quasars (at redshifts $z = 1.5$ and 3.0).

We can use the data presented in Fig. 1 to place some quantitative limits on the reliability and completeness of the final sample. We consider three zones in radio-optical offset Δ : (a) offsets below 10 arcsec, where all matches (other than Galactic stars) are accepted as correct IDs, (b) offsets of 10–15 arcsec, where we accept only a subset of matches (those associated with bright optical galaxies or extended radio sources, where an eye inspection suggests that the match is a correct one), and (c) offsets greater than 15 arcsec, which are rejected as correct IDs.

In the first zone ($\Delta < 10$ arcsec) there are 712 matches, and we include 702 of these in the final sample. However, integrating under the line in Fig. 1 implies that ~ 75 of these are likely to be chance coincidences. In the second zone ($\Delta = 10 - 15$ arcsec) there are 191 matches, of which 47 are included in the final sample. We expect 106 chance coincidences, suggesting that the final sample should contain ~ 85 objects in this zone rather than the 47 which are actually included. Thus our selection criteria have probably excluded some genuine IDs in this zone. In the third zone ($\Delta = 15 - 30$ arcsec) there are 590 matches, all of which we reject (we do however, include eight NVSS extended double radio sources, which were selected separately as described

in Section 4.2). Integrating under the line in Fig. 1 implies that we expect ~ 575 chance coincidences in this zone, suggesting that there are few or no ‘missing’ sample members in this zone.

In summary, we estimate that our final sample of 757 radio-source IDs includes ~ 75 objects which are chance coincidences of an 2dFGRS galaxy and a background radio source, and is missing ~ 40 genuine radio-emitting galaxies which should have been included. Thus the sample is currently about 95% complete and 90% reliable (and the overall sample size is within 5% of the correct value). In principle, both the completeness and the reliability could be raised to almost 100% by measuring more accurate radio positions for the weaker ($S < 5$ mJy) radio sources in Table 1, and this will be done in the future.

4.5 Radio stars?

As noted above, our final sample of radio-source IDs rejected all the NVSS–2dFGRS matches which had spectra characteristic of Galactic stars (with redshifts $z < 0.001$). As can be seen from Table 2, 18 of the 155 rejected IDs ($12 \pm 3\%$) are Galactic stars. This is roughly twice the number expected for objects drawn at random from the 2dFGRS data set (6% of the 2dFGRS objects observed up to March 2001 were Galactic stars; Colless et al. 2001), posing the question of whether we have detected any Galactic radio stars.

At first glance, this seems unlikely. Searches for radio stars in the NVSS and FIRST radio surveys (Condon et al. 1997; Helfand et al. 1999) find a very low detection rate at high Galactic latitudes (both studies find less than one radio-detected star per 200 deg^2 for $V < 10$ mag, and Helfand et al. note that the detection probability drops steeply at fainter magnitudes).

Furthermore, the 2dFGRS stars are not randomly-selected stars but stars which have been misclassified as galaxies. Thus some of them are likely to be the chance superposition of a galaxy and a foreground star. At least one object in Table 1 (TGN 156Z046) certainly falls into this class – it was originally classified as a star with $z = 0.0005$, but examination of the spectrum showed that although the blue end of the spectrum was dominated by light from a foreground star, a higher-redshift system at $z = 0.0391$ with emission lines of H α , [NII] and [SII] and Mg and NaD absorption lines could be seen clearly at the red end.

Nevertheless, the superposition of galaxies and foreground stars is unlikely to provide a complete explanation for a larger-than-expected number of NVSS sources matched with Galactic stars because it is hard to understand why radio-emitting galaxies should be more likely than other 2dFGRS galaxies to be obscured by foreground stars. It will be interesting to see whether the ‘radio-star’ excess persists as the 2dFGRS dataset grows. If so, it is possible that there may be a rare and so-far unrecognised class of radio sources associated with faint ($b_J > 16$ mag) Galactic stars.

4.6 Other identification criteria

Machalski & Condon (1999; MC99) took a different approach to cross-identifying NVSS radio sources with optical galaxies, and calculated a probability of association based on

the radio-optical offset and the quoted errors in radio and optical positions. They considered all NVSS radio sources within 30 arcsec of an LCRS galaxy, and calculated a normalized offset

$$\rho = [(\Delta_\alpha/\sigma_\alpha)^2 + (\Delta_\delta/\sigma_\delta)^2]^{0.5} \quad (2)$$

where Δ_α and Δ_δ are the differences between radio and optical positions and σ_α and σ_δ are the combined errors in the quoted radio and optical positions. They accepted a candidate identification as a true ID if $\rho < 2.5$. This method has the advantage that it allows a larger search radius for objects with larger position errors, but the disadvantage is that the probability of finding a spurious optical ID is larger for faint sources because of the larger error box.

We looked at the effect of applying the MC99 identification criterion to our own sample. Of the 695 unresolved sources in Table 1, 543 are identified as IDs by both criteria (i.e. MC99 and our own procedure as described above). 41 sources are rejected by both criteria, 38 are accepted by us but rejected by MC99, and 73 are accepted by MC99 but rejected by us. Thus the MC99 criterion produces about 6% more IDs than our method for the same data set. This is probably not surprising — we know that our method excludes a few genuine IDs with large radio-optical separation in order to produce a sample which is as uncontaminated by chance coincidences as possible.

4.7 K-corrections

The galaxies in our sample have redshifts as high as $z = 0.3$ to 0.4, so when calculating galaxy luminosities we need to apply optical, radio and infrared K-corrections to take proper account of the effects of redshift on both the observed flux and the width of the passband.

In the optical, we follow Folkes et al. (1999) and adopt the B-magnitude K-corrections tabulated by Pence (1976), using Pence’s E/S0 values for our Aa and Ae galaxies, and the Sbc values for our SF galaxies. We also convert Pence’s $k(B)$ values to $k(b_J)$ using the relation

$$k(b_J) = k(B) - 0.28 [k(B) - k(V)]. \quad (3)$$

In the radio, we assume a mean spectral index of $\alpha = -0.7$ (where $S \propto \nu^\alpha$) and apply the usual K-correction of the form

$$K(z) = (1+z)^{-(1+\alpha)} \quad (4)$$

at redshift z .

In the far-infrared, the situation is more complex because of the wide range in IRAS ‘spectral index’ (i.e. dust temperature) observed in these galaxies (see Section 6). Because the FIR K-correction can be either positive or negative depending on what assumptions are made about the spectral energy distribution, and because many of our galaxies are weak IRAS sources with detections in only one or two bands, we chose to apply no K-correction when calculating FIR luminosities. Since most of the FIR-detected galaxies we will study are at low redshift ($z < 0.15$), the K-correction has little or no effect in any case.

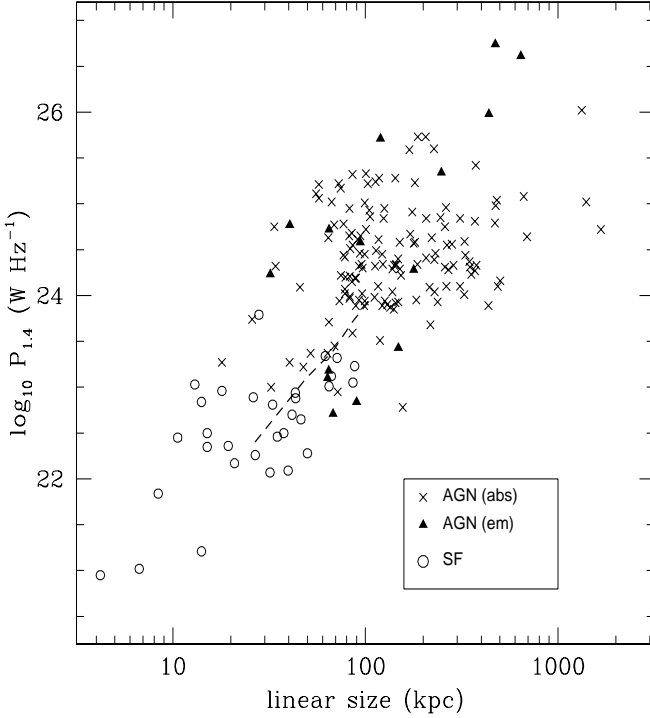


Figure 6. Relationship between radio power and projected linear size for spatially-resolved 2dFGRS/NVSS radio sources. The dashed line shows the locus of a source with an observed angular size of 20 arcsec and flux density 2.5 mJy over the redshift range $z = 0.05 - 0.3$. Most of the upper limits for unresolved sources fall to the left of this line. Sources larger than about 100 kpc will be resolved throughout the 2dFGRS sample volume.

5 RADIO STRUCTURES OF RESOLVED GALAXIES

About 25% of the radio sources associated with 2dFGRS galaxies are spatially resolved by NVSS, allowing us to measure their projected linear size. In a few cases we remeasured the angular size ourselves (usually because the NVSS source catalogue split a single source into several components), otherwise we used the NVSS catalogue value. Fig. 5 shows some of the extended NVSS sources identified with AGN and star-forming galaxies.

Fig. 6 plots radio power against projected linear size for the 182 extended NVSS radio sources with good-quality 2dFGRS spectra (i.e. with $Q \geq 3$ in Table 1). As expected, most star-forming galaxies are associated with radio sources less than about 60 kpc in diameter, i.e. no larger than a galaxy disk. The few star-forming galaxies whose radio extent is larger than this appear to be members of pairs or close groups in which more than one galaxy contributes to the radio emission. In contrast, many of the radio sources with AGN spectra are several hundred kpc in extent, consistent with classical (core plus jet) radio galaxies.

5.1 Giant radio galaxies

Our sample includes three giant radio galaxies with projected linear sizes greater than 1 Mpc, which are shown in Fig. 7. Two are newly-discovered GRGs — TGS223Z232

** Fig. 7 available as a separate file **

Figure 7. Radio contours overlaid on DSS optical images of the three giant radio galaxies (GRGs) detected in our sample: (a) TGS 223Z232 (contours 1,2,3,4,5,10,20,50 mJy beam $^{-1}$), (b) TGS 190Z081 (contours 1,2,4,8,16,32,64,128 mJy beam $^{-1}$), (c) TGS241Z299 (contours 1,2,5,10,20,50 mJy beam $^{-1}$). Each frame is 12.8 arcmin across.

($z = 0.2095$) and TGS190Z081 ($z = 0.2318$). The third, TGS241Z299, corresponds to the radio galaxy MRC B0312–271 ($z = 0.2186$) which has already been identified as a GRG by Kapahi et al. (1998).

About 50–60 GRGs are currently known (Ishwara-Chandra & Saikia 1999; Schoenmakers et al. 2000) — they are believed to represent the last stages of radio galaxy evolution, and to be unusually old or long-lived radio sources. The three GRGs in our sample represent just under 1% of the 441 AGN accepted as radio-source IDs, so they are clearly rare. It would be interesting to determine whether there is anything different about their environment (e.g. low density, lack of recent interactions with companions) which has allowed these radio sources to grow undisturbed to such a large size.

5.2 Unusual radio sources

Fig. 8 shows two unusual radio sources discovered in our data set. The diffuse radio source shown in Fig. 8(a) is resolved into four separate components in the NVSS catalogue, and one of these was originally picked up as a possible match for the 2dFGRS galaxy TGN307Z090. Inspection of the radio contours showed that this is a large (~ 6.5 arcmin diameter) source with very low radio surface brightness.

The source is clearly real, since it was independently detected at Green Bank (also at 1.4 GHz) by White & Becker (1992). The single-dish flux density of 189 mJy suggests that NVSS may have missed some flux. At present, nothing is known about the radio spectral index. While the identification is uncertain at this stage, the radio centroid is closer to the 2dFGRS galaxy TGN307Z092 than to its companion TGN307Z090. At the redshift of TGN307Z092 ($z = 0.0465$), the source has a projected linear size of 310 kpc and a 1.4 GHz radio power of $1.3 \times 10^{24} \text{ W Hz}^{-1}$. Its radio surface brightness is, however, unusually low. The nature of the source remains uncertain, though it may be a relic radio galaxy whose central engine has turned off (e.g. Komissarov & Gubanov 1994).

Fig. 8(b) shows the radio emission associated with the 16th magnitude star-forming galaxy TGS 119Z122 at $z = 0.0090$. The NVSS flux density at 1.4 GHz is 11.7 mJy.

** Fig. 8 available as a separate file **

Figure 8. Radio contours overlaid on DSS optical images of two unusual radio sources in our sample. Each frame is 8.6 arcmin across. (a) Overlay of NVSS radio contours on a DSS image of TGN 307Z092 and its fainter companion TGN 307Z090 (contour levels 1,2,3,4,6,8,10,12 mJy beam $^{-1}$), (b) NVSS contours overlaid on an image of TGS119Z122 (PKS 2225–253; contour levels 1,2,4,6,8 mJy beam $^{-1}$).

However, the same object is listed in the Parkes catalogue as PKS 2225–253, with flux densities of 230 and 130 mJy at 2.7 and 5.0 GHz respectively. The Parkes observations were made by Wall, Wright & Bolton (1976), and the observing dates are given by them as 1974.0 and 1974.8 for the 2.7 GHz and 5.0 GHz observations respectively. Thus the source was detected at two different frequencies and on two different occasions separated by several months, and appears to have been real. The optical identification with a 16th magnitude galaxy was first made by Savage & Wall (1976).

The radio luminosity of PKS 2225–253 has declined dramatically since the 1974 Parkes observations. One possibility, since TGS 119Z122 is actively forming stars, is that the bulk of the Parkes emission came from a radio-loud supernova like SN 1986J or SN 1998Z (e.g. Weiler et al. 1998), which has since faded. However, the early Parkes observations imply a 5 GHz radio power around 4×10^{22} W Hz $^{-1}$, which is a factor of three higher than the peak luminosity of any known radio supernova including the gamma-ray burst object SN1998bw (Kulkarni et al. 1998). A transient Galactic radio source seems unlikely at $b = -58^\circ$, and the nature of the catalogued Parkes source remains unclear.

6 IRAS DETECTIONS AND STAR-FORMING GALAXIES

6.1 IRAS detections of 2dFGRS galaxies

In the well-known correlation between far-infrared (FIR) and radio continuum emission in star-forming galaxies (e.g. de Jong et al. 1985, Helou et al. 1985), the FIR/radio ratio $S_{60\mu\text{m}}/S_{1.4\text{GHz}}$ has a mean value of ~ 105 (Condon & Broderick 1988). By a happy coincidence, this is very close to the ratio between the 280 mJy limit of the IRAS Faint Source Catalogue (FSC; Moshir et al. 1990) at 60 μm and the 2.5 mJy detection limit of the NVSS at 1.4 GHz. As a result, we expect most star-forming galaxies detected as radio sources by NVSS to be detected as 60 μm sources in the IRAS FSC, and vice versa.

In practice, as noted earlier in Section 3.2, about 10% of the 2dFGRS survey region was either unobserved by IRAS or had only single-scan coverage. Thus the absence of an

Table 3. Summary of spectral classifications for radio-source IDs which were also detected by IRAS

2dF spectral class	Galaxies
SF	161
Ae	16
Aae	5
Low S/N	1
Total	183

individual galaxy from the IRAS catalogue does not necessarily mean that it has a 60 μm flux below the FSC limit.

Table 3 summarises the spectral properties of the 183 accepted radio-source IDs from Table 1 which were also detected at 60 μm by IRAS. Most galaxies detected at 60 μm (83%) were also detected by IRAS at 100 μm .

All the 2dF spectra of galaxies detected as IRAS sources show optical emission lines, in agreement with earlier studies (e.g. Allen et al. 1985, Lawrence et al. 1986). The great majority (89%) are classified as SF, with the remainder (11%) being emission-line AGN with Seyfert-like spectra.

Extrapolating from our current sample suggests that the full 2dFGRS database, when complete, will contain spectra of ~ 1000 IRAS galaxies. While this is smaller than targeted redshift surveys such as the IRAS PSCz (Saunders et al. 2000), which has more than 15,000 redshifts, it reaches to lower IRAS flux densities (and a higher median redshift) than most earlier surveys, as can be seen from Fig. 9. Since the general properties of IRAS galaxies are already well-explored by earlier studies, we focus here on the radio properties of star-forming galaxies in the 2dFGRS.

6.2 The FIR–Radio Correlation

We calculated the FIR luminosity for each galaxy detected by IRAS, using the FIR flux defined by Helou et al. (1985):

$$S_{\text{FIR}} = 1.26 \times 10^{-14} \times [2.58 S_{60} + S_{100}], \quad (5)$$

where S_{60} and S_{100} are the 60 and 100 μm flux densities in Jy ($1 \text{ Jy} = 10^{-26} \text{ W Hz}^{-1} \text{ m}^{-2}$) and S_{FIR} is in W m^{-2} .

Fig. 10 plots FIR luminosity versus 1.4 GHz radio power for the IRAS-detected galaxies in our sample. Most galaxies fall close to the FIR–radio correlation for normal galaxies derived by Devereux & Eales (1989),

$$\log_{10} P_{1.4\text{GHz}} = 1.28 \log_{10} L_{\text{FIR}} + 8.87, \quad (6)$$

but the scatter increases strongly for the most luminous galaxies.

As can be seen from Table 4, the fraction of galaxies with AGN-like optical spectra increases with FIR luminosity and so it seems likely that the increased scatter in the FIR–radio correlation results from an increasingly diverse mix of pure star-forming galaxies and AGN or composite objects at higher FIR luminosities.

6.3 IRAS colours and 2dF spectral types

As noted by de Grijs et al. (1985), galaxies with active nuclei tend to have hotter IRAS colours (as measured by the

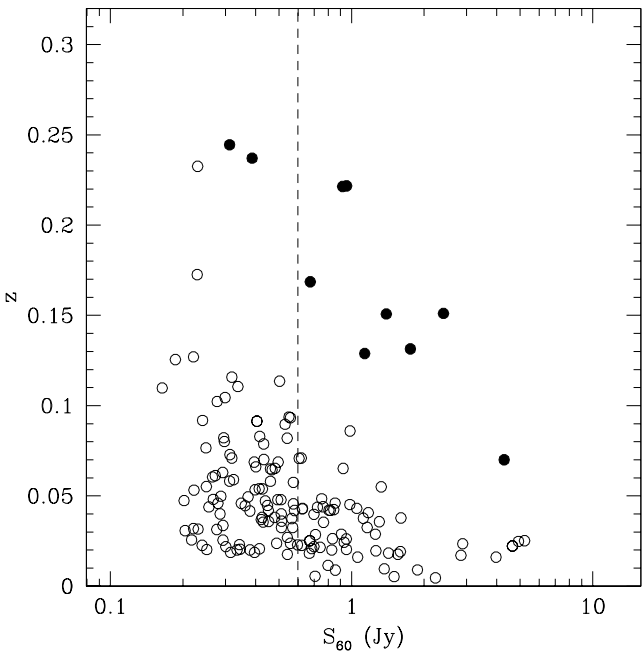


Figure 9. Plot of IRAS 60 μm flux density versus redshift for IRAS-detected 2dFGRS radio sources. ULIRGs with $L_{\text{FIR}} > 10^{12} L_{\odot}$ are shown by filled circles, and other galaxies by open circles. The vertical line at 0.6 Jy corresponds to the flux limit of the PSCz survey (Saunders et al. 2000).

Table 4. Summary of spectral properties for three bins in FIR luminosity. Hot IRAS galaxies are those with $\log_{10}(S_{60}/S_{100}) > -0.3$ (de Grijp et al. 1985)

$\log_{10}(L_{\text{FIR}})$ (L_{\odot})	Fraction with AGN spectra	Fraction with hot IRAS colours
>11.5	60%	(9/15)
10.5–11.5	9%	(11/118)
<10.5	2%	(1/49)
		92% (11/12)
		46% (45/99)
		27% (11/41)

flux ratio S_{60}/S_{100}) than ‘normal’ star-forming galaxies, and galaxies with Seyfert nuclei generally have $S_{60}/S_{100} > 0.5$.

Fig. 11 shows a FIR ‘colour-magnitude diagram’ for galaxies in our sample. The IRAS flux densities for weaker sources have typical errors of 10–15%, so the IRAS colours can have uncertainties of 30% or more. However, there is still a general increase in the fraction of galaxies with ‘hot’ IRAS colours at higher FIR luminosity (see also the summary in Table 4), consistent with an increasing contribution from active nuclei at higher FIR luminosity.

6.4 Ultraluminous IRAS galaxies

Ten of the IRAS galaxies in our sample (listed in Table 5) have FIR luminosities above $10^{12} L_{\odot}$, and can be considered ‘ultraluminous IRAS galaxies’ (ULIRGS; e.g. Sanders & Mirabel 1996). Most of these galaxies are already known as ULIRGs from other surveys, but there are two newly-discovered ULIRGs, TGN 152Z171 and TGN 131Z280. Fig. 12 shows their spectra.

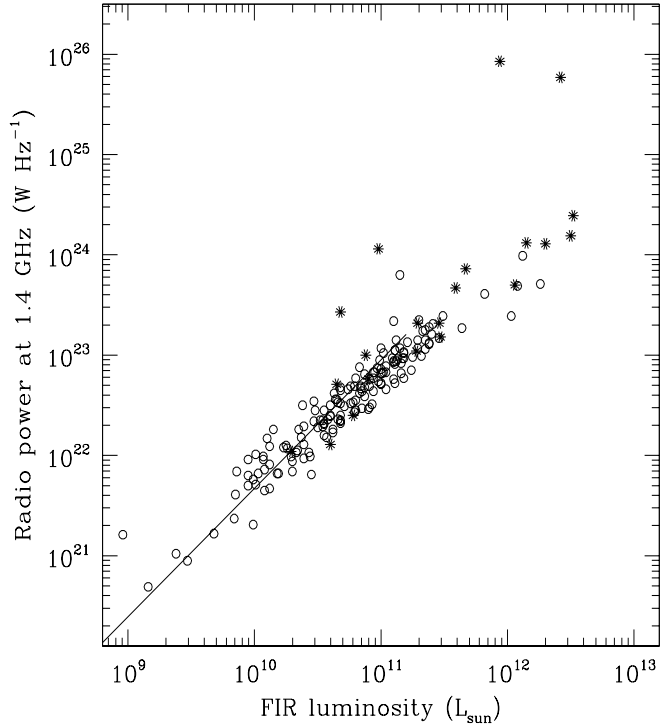


Figure 10. Relation between FIR and radio continuum luminosity for radio-source IDS from Table 1. Galaxies with SF spectra are shown as open circles and those with AGN spectra as stars. The solid line shows the FIR–radio correlation for normal galaxies derived by Devereux & Eales (1989). Note that because of the requirement that they lie above the 2.8 mJy NVSS detection limit, most of our 2dFGRS star-forming galaxies have star-formation rates which are significantly higher than the majority of ‘normal’ galaxies.

All the galaxies in Table 5 have unresolved radio sources in the NVSS, though because of the relatively large distances of these galaxies this only sets fairly unrestrictive limits (typically 100–200 kpc) on the linear size of the associated radio emission.

7 ROSAT DETECTIONS

Bauer et al. (2000) have cross-matched the NVSS source catalogue with the ROSAT Bright Source Catalogue (RSBC) of X-ray sources (Voges et al. 1999). They showed that the relatively low surface density of NVSS sources allows reliable identification of the radio counterparts of RSBC sources despite uncertainties of 10 arcsec or more in the X-ray positions. The more accurate radio positions then allow a reliable optical identification to be attempted. Bauer et al. showed that the RSBC/NVSS radio sources were dominated by AGN with an average redshift of $\langle z \rangle \simeq 0.1$.

We cross-matched the galaxies in Table 1 with the ROSAT All-Sky Survey (RASS) catalogue, taking a simple cutoff of 30 arcsec as our matching radius rather than the more complex criteria prescribed by Bauer et al. (2000). This gave the six matches listed in Table 6, four of which are also in the Bauer et al. list (the other two fall below the $0.1 \text{ ct s}^{-1} \text{ X-ray}$ limit imposed by Bauer et al. for their sample).

Table 5. Ultra-luminous IRAS Galaxies (ULIRGs) in the sample

2dFGRS name	IRAS name	Spectral class	z	Abs. mag.	$\log_{10} P_{1.4}$ (W Hz $^{-1}$)	$\log_{10} S_{60}/S_{100}$	$\log_{10} L_{\text{FIR}}$ (L_{\odot})	Notes
TGS206Z015	IRAS 00335-2732	SF	0.0700	-20.71	23.39	0.13	12.03	S92; Megamaser
TGS209Z156	IRAS 00482-2720	SF	0.1289	-21.04	23.69	-0.21	12.08	K98, V99, C99
TGS238Z241	IRAS 03000-2719	Ae	0.2214	-22.52	24.39	-0.35	12.52	C96
TGN152Z171	IRAS F09521-0400	Ae	0.2371	-22.03	24.12	-0.19	12.15	New ULIRG
TGN314Z018	IRAS 11598-0112	Ae	0.1511	-22.01	24.19	-0.05	12.50	S92; ROSAT
TGN131Z280	IRAS 12532-0322	Ae	0.1686	-22.18	23.70	-0.08	12.06	New ULIRG
TGN137Z043	IRAS 13270-0331	Ae	0.2217	-22.16	25.77	0.08	12.42	C95
TGN206Z237	IRAS 14121-0126	Ae	0.1508	-21.35	24.11	-0.17	12.30	C95
TGS178Z172	IRAS 22206-2715	SF	0.1314	-21.98	23.71	-0.12	12.26	C96
TGS180Z060	IRAS F22301-2822	SF	0.2445	-21.92	23.99	>-0.47	12.12	C96

References: C95: Clowes et al. (1995); C96 Clements et al. (1996); C99 Clements et al. (1999); K98 Kim & Saunders (1998); S92: Strauss et al. (1992); V99 Veilleux et al. (1999)

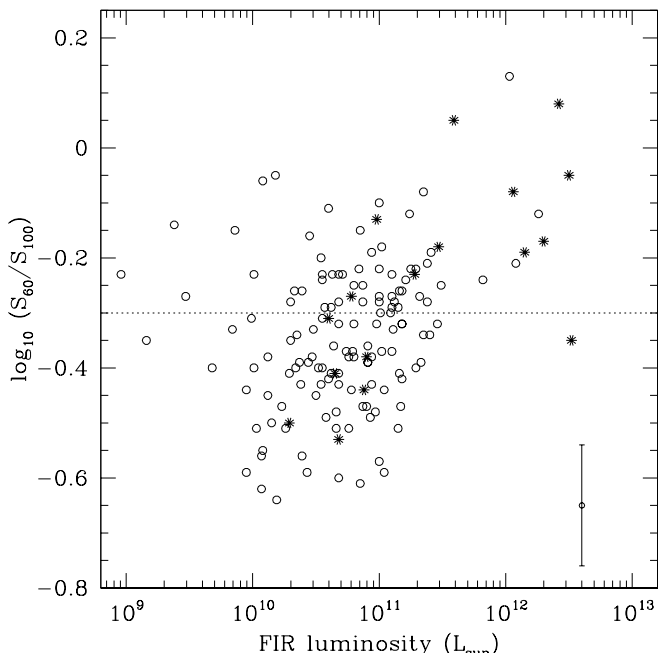


Figure 11. Plot of IRAS ‘colour’ ($\log_{10}(S_{60}/S_{100})$) versus FIR luminosity for galaxies in our sample. ‘Warm’ galaxies are defined by de Grijp et al. (1985) as those with $S_{60} > 0.5 S_{100}$, and they find that most Seyfert galaxies have ‘warm’ IRAS colours. The boundary between warm and cool galaxies as defined by de Grijp et al. is shown by the dashed horizontal line, and a typical error bar for the weakest IRAS sources ($S_{60} \approx 0.3$ Jy) is shown in the lower right-hand corner. As in Fig. 10, open circles and stars denote galaxies classified spectroscopically as SF and AGN respectively.

All six galaxies in Table 6 have strong emission lines and spectra classed as Ae, but in other respects they are a diverse population, including three powerful, double-loped radio galaxies, two Seyfert 1 galaxies with less powerful radio emission, and one ultra-luminous IRAS galaxy (ULIRG, see Table 5 and Fig. 13).

Bauer et al. identified 1512 extragalactic RSBC/NVSS sources with Galactic latitude $|b| > 15^\circ$ in the 10.3 sr NVSS survey area. This corresponds to a surface density of about

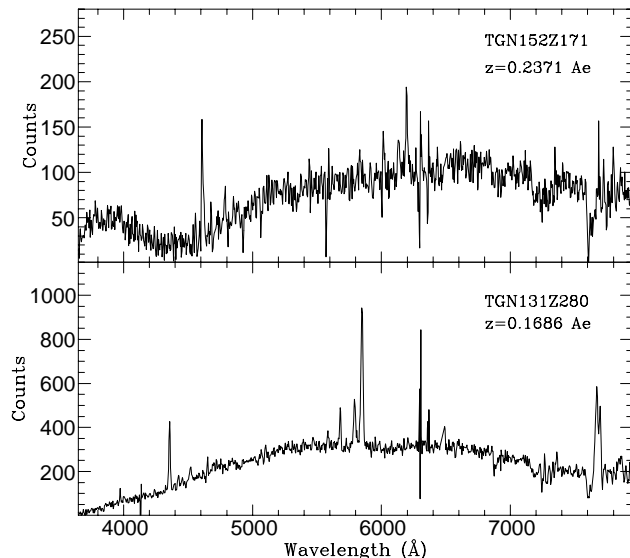


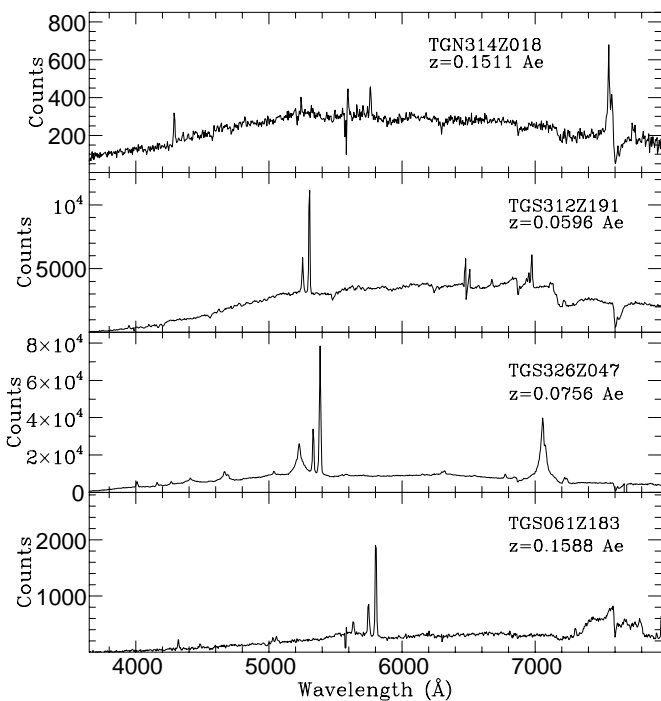
Figure 12. 2dFGRS spectra of the two newly-discovered ULIRGs in our sample, TGN152Z171 ($B_J = 18.85$) and TGN131Z280 ($B_J = 17.93$). Both spectra show residuals due to incomplete subtraction of the atmospheric airglow line at 6300 Å.

0.05 objects per square degree, or about four times higher than the corresponding surface density derived from the RSBC/NVSS/2dFGRS objects in Table 6 (0.012 objects per square degree).

Where are the missing RSBC/NVSS objects? We expect most of them to fall within the 2dFGRS volume, since Bauer et al. note that their objects are mostly local with a mean redshift of about 0.1. Closer examination of the Bauer et al. objects in the 2dFGRS area suggests that about half the missing objects are bright, nearby galaxies which were excluded from the 2dFGRS. Most of the remainder appear to be Seyfert galaxies excluded because of their compact, stellar appearance on sky survey plates, along with a few higher-redshift QSOs.

Table 6. Galaxies detected as X-ray sources in the ROSAT All-Sky Survey (RASS)

2dFGRS name	ROSAT name	Spectral class	z	Abs. mag.	$\log_{10} P_{1.4}$ (W Hz $^{-1}$)	RSBC count rate (s $^{-1}$)	Notes
TGS312Z191	1RXS J023513.9–293616	Ae	0.0596	–22.43	24.58	0.36±0.03	Radio galaxy MRC 0234–287
TGN314Z018	1RXS J120226.9–012908	Ae	0.1511	–22.01	24.19	0.14±0.03	ULIRG
TGN401Z254	1RXS J133253.5+020047	Ae	0.2162	–22.14	26.74	0.25±0.03	Radio galaxy PKS 1330+02
TGS326Z047	1RXS J214636.3–305132	Ae	0.0756	–21.48	22.84	0.84±0.07	Seyfert 1
TGS407Z205	1RXS J215809.2–312341	Ae	0.0933	–23.01	23.17	0.08±0.02	Seyfert 1
TGS061Z183	1RXS J220924.2–245326	Ae	0.1588	–21.51	25.98	0.05±0.02	Radio galaxy PKS 2206–251

**Figure 13.** 2dFGRS spectra of four NVSS galaxies detected as X-ray sources in the ROSAT All-Sky Survey. All show optical emission lines with line ratios characteristic of active galaxies, but as noted in the text they are otherwise a diverse class of objects.

8 THE LOCAL RADIO LUMINOSITY FUNCTION (RLF) AT 1.4 GHz

8.1 Calculation of the local RLF

We now calculate the radio luminosity function (RLF) for 2dFGRS–NVSS galaxies with $z \leq 0.3$, both for the sample as a whole and for the AGN and SF subclasses. We assigned spectral types to the 19 unclassified galaxies with measured redshifts as follows: galaxies with b_J fainter than magnitude 17.0 and radio power above 10^{23} W Hz $^{-1}$ were assigned to the Aa (absorption-line AGN) class, otherwise they were assumed to be star-forming (SF). Using these criteria, we classify 18 of the low S/N galaxies as Aa and only one as SF.

To calculate the local RLF, we use the $1/V_{\max}$ method (Schmidt 1968), as discussed by Condon (1989). V_{\max} is calculated from the joint optical and radio limits of the

sample, i.e. a radio cutoff of 2.8 mJy and optical cutoffs at $b_J = 14.0$ mag (bright) and 19.4 mag (faint). Table 7 lists the derived local RLF for the whole sample, and for the AGN and SF classes separately. At this stage, we make no corrections for incompleteness and the only normalisation is the effective area of 325 deg 2 derived in Section 2.1.

Fig. 14 shows the derived RLF, together with earlier values derived by Condon (1989) and Machalski & Godlowski (2000). An advantage of the 2dF/NVSS sample is that all the data are drawn from a single radio survey and a set of homogeneous optical spectra from a single instrument. Most previous determinations of the local RLF used data from several radio surveys to span the equivalent range in radio power. The good overall agreement with earlier derivations confirms our earlier calculation that the incompleteness in our final sample is small (< 10%).

8.2 Comparison with earlier work

Figures 14 and 15 shows a comparison between our values of the local RLF and those derived by Machalski & Godlowski (2000) for a sample of 1157 radio-identified galaxies from the LCRS. This is the only other determination which uses a comparably-large data set of homogeneous optical spectra.

As can be seen from Fig. 14, the overall agreement between our total (i.e. AGN plus SF) RLF and that of MG is extremely good. This is remarkable given the differences between the two samples:

- Our criteria for determining radio-source IDs differ from those used by Machalski & Condon (1999; hereafter MC99), as noted in Section 4.6.
- All the 2dFGRS redshifts were determined spectroscopically, whereas most of the redshifts listed by MC99 were estimated from optical magnitudes (so that some individual values may have large errors).

Such good agreement between two independent samples chosen in different ways suggests that the RLF is a very robust indicator of the overall density of radio sources in the local universe.

As can be seen from Fig. 15, however, the agreement between our results and those of Machalski & Godlowski (2000; hereafter MG) breaks down when we split our sample into AGN and SF galaxies. We find that the space density of AGN radio sources continues to rise as we go to radio powers as low as 10^{22} W Hz $^{-1}$, with no sign of a turnover (see Fig. 15). In contrast, MG find a decreasing density of radio AGN below 10^{24} W Hz $^{-1}$, which is reflected in the divergence of the two AGN LFs in Fig. 15. This turnover in the MG LF for

Table 7. The local radio luminosity function at 1.4 GHz

$\log_{10} L_{1.4}$ (W Hz $^{-1}$)	N	All galaxies	N	AGN	N	Star-forming galaxies
		$\log_{10} \Phi$ (mag $^{-1}$ Mpc $^{-3}$)		$\log_{10} \Phi$ (mag $^{-1}$ Mpc $^{-3}$)		$\log_{10} \Phi$ (mag $^{-1}$ Mpc $^{-3}$)
26.6	1	-7.96 $^{+0.30}_{-1.0}$	1	-7.96 $^{+0.30}_{-1.0}$		
26.2	1	-8.01 $^{+0.30}_{-1.0}$	1	-8.01 $^{+0.30}_{-1.0}$		
25.8	8	-6.86 $^{+0.13}_{-0.19}$	8	-6.86 $^{+0.13}_{-0.19}$		
25.4	14	-6.57 $^{+0.10}_{-0.14}$	14	-6.57 $^{+0.10}_{-0.14}$		
25.0	21	-6.38 $^{+0.09}_{-0.11}$	21	-6.38 $^{+0.09}_{-0.11}$		
24.6	57	-5.87 $^{+0.05}_{-0.06}$	57	-5.87 $^{+0.05}_{-0.06}$		
24.2	79	-5.72 $^{+0.05}_{-0.05}$	75	-5.74 $^{+0.05}_{-0.05}$	4	-6.98 $^{+0.18}_{-0.30}$
23.8	110	-5.46 $^{+0.04}_{-0.04}$	101	-5.49 $^{+0.04}_{-0.05}$	9	-6.64 $^{+0.12}_{-0.18}$
23.4	93	-5.14 $^{+0.04}_{-0.05}$	66	-5.32 $^{+0.05}_{-0.06}$	27	-5.62 $^{+0.08}_{-0.09}$
23.0	106	-4.56 $^{+0.04}_{-0.04}$	44	-4.98 $^{+0.06}_{-0.07}$	62	-4.77 $^{+0.05}_{-0.06}$
22.6	80	-4.14 $^{+0.05}_{-0.05}$	22	-4.73 $^{+0.08}_{-0.10}$	58	-4.27 $^{+0.05}_{-0.06}$
22.2	58	-3.70 $^{+0.05}_{-0.06}$	8	-4.52 $^{+0.13}_{-0.19}$	50	-3.77 $^{+0.06}_{-0.07}$
21.8	28	-3.49 $^{+0.08}_{-0.09}$	2	-4.69 $^{+0.23}_{-0.53}$	26	-3.52 $^{+0.08}_{-0.09}$
21.4	4	-3.59 $^{+0.18}_{-0.30}$			4	-3.51 $^{+0.18}_{-0.30}$
21.0	1	-3.74 $^{+0.30}_{-1.00}$			1	-3.74 $^{+0.30}_{-1.00}$
20.6	1	-3.26 $^{+0.30}_{-1.00}$			1	-3.26 $^{+0.30}_{-1.00}$
Total	662		420		242	
$\langle V/V_{\max} \rangle$	0.528 ± 0.011		0.542 ± 0.014		0.503 ± 0.019	

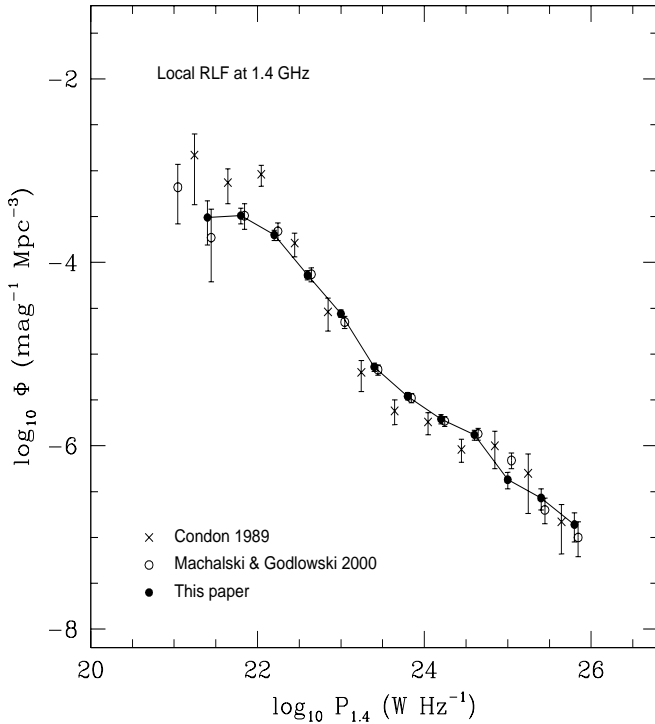


Figure 14. Local RLF derived from the 662 galaxies in Table 1 which are accepted as correct IDs and have radio flux density $S_{1.4} \geq 2.8$ mJy, optical magnitude $14.0 \leq b_J \leq 19.4$ and redshift $0.001 < z < 0.3$. Previous derivations by Condon (1989) and Machalski & Godlowski (2000) are shown for comparison. Between 10^{22} and 10^{24} W Hz $^{-1}$, our values and those of Machalski & Godlowski are sometimes so close that they are indistinguishable in the diagram.

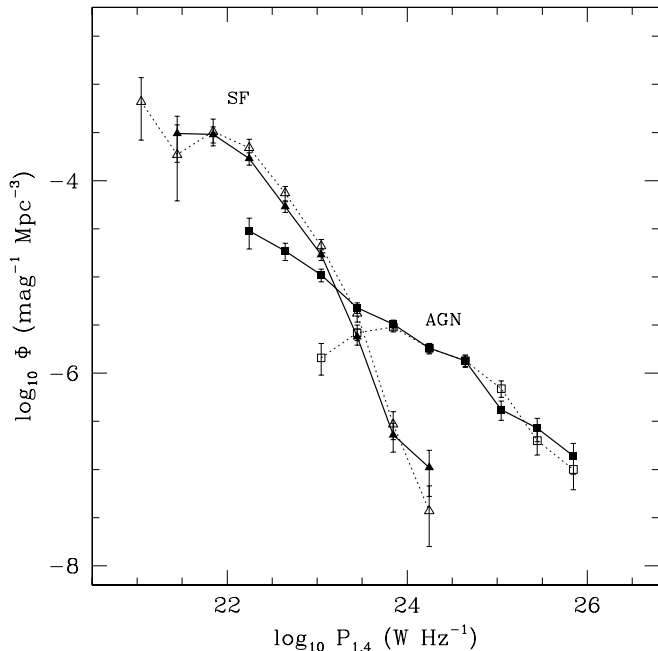


Figure 15. Local RLF derived for AGN and SF galaxies separately. Filled points connected by solid lines show our own data for AGN (squares) and SF galaxies (triangles). The local RLFs for AGN and SF galaxies derived by Machalski & Godlowski (2000) are plotted using open symbols connected by dotted lines.

AGN has also been discussed by Brown et al. (2001), who ascribe it to incompleteness in the AGN data used by MG. The good agreement between the faint end of our local RLF for AGN and that derived by Sadler et al. (1989) for nearby galaxies can be seen in Figure 18, and strongly supports the

view that our values are correct and that the MG sample is incomplete for low-luminosity AGN.

Thus, although we and MG agree on the overall density of radio sources in the local universe, we disagree on the relative fraction of AGN and SF galaxies below 10^{24} W Hz $^{-1}$. There are two possible explanations for this, a *selection difference* (i.e. the different criteria for inclusion in the two samples select roughly the same *number* of galaxies, but do not necessarily select the same *kind* of galaxies), and a *classification difference*. Our AGN/SF classification is based on optical spectra, whereas MG used the classifications from MC99, which take into account several factors including the radio-optical flux ratio, angular extent of the radio emission, and IRAS data where available.

There are 92 galaxies in common between our set of radio-source IDs in Table 1 and the LCRS data set used by MC99. Of these, we agree on the classification of 69 (40 AGN, 29 SF), i.e. 75% of the galaxies in common. Of the 25% of galaxies where there is disagreement, most are classified by us as AGN and by MC99 as SF (i.e. for a data set classified by both groups, we find more AGN, and fewer SF galaxies, than MC99).

A detailed comparison of the 2dFGRS and LCRS data sets is outside the scope of this paper, but it seems likely that both selection differences and misclassification of low-power AGN as SF galaxies contribute to the incompleteness of the MG AGN data at low radio powers. The identification criteria used by Machalski & Condon (1999) may exclude some genuine radio IDs with flux densities above 5 mJy and radio-optical position offsets of less than 10 arcsec (see Section 4.6), and the radio-optical flux ratio which they use in their classification may misclassify some low-power AGN as SF galaxies (especially since the radio sources in low-power AGN are rarely spatially resolved by NVSS, and so cannot be recognised by their radio morphology in the same way as many powerful radio AGN).

8.3 Star-forming galaxies and the local star-formation density

As noted earlier, the 2dFGRS excluded most bright, nearby galaxies with $b_J < 14$ mag. To extend our sample to lower radio luminosity, we therefore combined our measured RLF with the local RLF derived by Condon (1989) for galaxies in the Revised Shapley Ames Catalogue (RSA; Sandage & Tammann 1981). In doing this, we also increased the values of Φ listed in Table 7 by 5% to correct for the $\sim 5\%$ spectroscopic incompleteness of the 2dFGRS (i.e. the spectra in Table 1 with $Q \leq 2$ for which no reliable redshift could be measured). As can be seen from Fig. 16, our results agree well with the Condon RSA values in the small region of overlap. We then fitted an analytic function of the type described by Saunders et al. (1990):

$$\Phi(L) = C \left[\frac{L}{L_*} \right]^{1-\alpha} \exp\left(-\frac{1}{2} \left[\frac{\log_{10}(1+L/L_*)}{\sigma} \right]^2\right) \quad (7)$$

to the combined data, and Table 8 summarizes the results.

We can now use the RLF for star-forming galaxies to estimate the local star-formation density (i.e. the zero-point of the Madau diagram; Madau 1996). Following Cram et al.

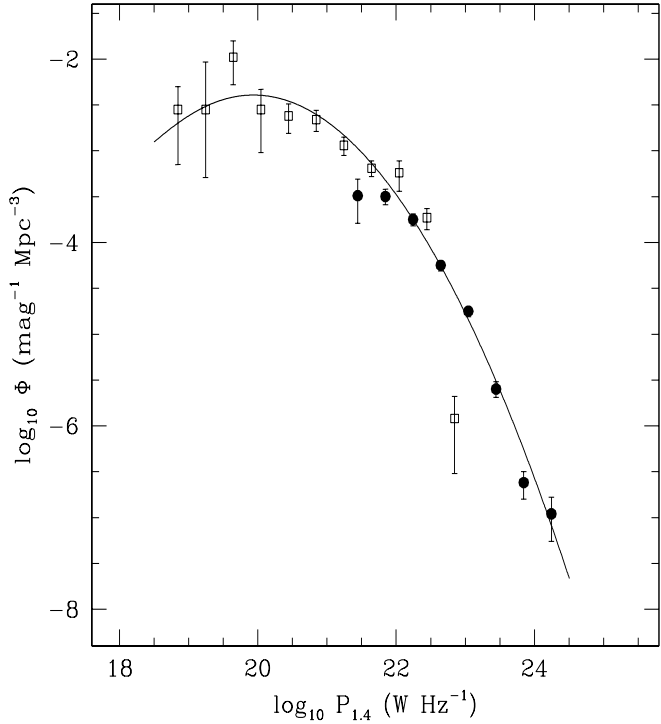


Figure 16. Local RLF for star-forming galaxies, combining data from our sample (filled circles) with values from Condon (1989) for nearby star-forming galaxies from the Revised Shapley Ames Catalogue (open squares). The NVSS/2dFGRS values of Φ have been increased by 5% to take into account the 95% redshift completeness of the 2dFGRS. The solid line shows the best-fitting analytic function as described in the text.

Table 8. Parametric fits to the local RLFs for AGN and SF galaxies, using the Saunders et al. (1990) fitting function as described in the text

Parameter	SF galaxies	AGN	Units
$\log_{10} L_*$	19.55 ± 0.03	24.59 ± 0.03	W Hz $^{-1}$
α	0.840 ± 0.020	1.58 ± 0.02	
σ	0.940 ± 0.004	1.00 ± 0.13	
$\log_{10} C$	-2.41 ± 0.04	-5.89 ± 0.02	mag $^{-1}$ Mpc $^{-3}$
χ^2	1.86	0.91	

(1998) and Haarsma et al. (2000), we assume a Salpeter-like initial mass function

$$\Psi(M) \propto M^{-2.35} \quad (8)$$

over the range 0.1 to $100 M_\odot$, and convert from a radio luminosity to a star-formation rate (SFR) via the relation

$$\text{SFR } (M_\odot \text{ yr}^{-1}) = \frac{\text{L}_{1.4} \text{ (W Hz}^{-1})}{8.85 \times 10^{20}} \quad (9)$$

(Sullivan et al. 2001). The local star-formation density at any given SFR is then

$$\rho_{\text{SF}} = \text{SFR } (L_{1.4}) \times \Phi(L_{1.4}) \quad (10)$$

where Φ is the local RLF from Tables 7 and 8, multiplied by 1.05 to correct for incompleteness as noted above. Fig.

17 shows the results — our data imply that the greatest contribution to the local star-formation density comes from galaxies with star-formation rates around $10 M_{\odot} \text{ yr}^{-1}$.

As can be seen from Fig. 17, our radio-derived values for the local star-formation density are in excellent agreement with the values derived from H α by Gallego et al. (1995; hereafter G95) for galaxies with star-formation rates up to $20-30 M_{\odot} \text{ yr}^{-1}$.

For galaxies with the highest star-formation rates ($>30 M_{\odot} \text{ yr}^{-1}$), however, we find a significantly higher density than G95. The reasons for this are not completely clear — our SF galaxies with high derived SFRs appear to be genuine star-forming galaxies which follow the FIR-radio correlation (see Fig. 10). Where measurements of diagnostic emission-line ratios have been carried out on the 2dF spectra, these also confirm the SF classification (Jackson & Londish 2000).

Our sample volume for galaxies with a high SFR is larger than that surveyed by G95. Their survey covered 471 deg^2 to a depth of $z \leq 0.045$ (beyond which the H α /[NII] lines were shifted out of their passband), i.e. a maximum volume of about $9 \times 10^5 \text{ Mpc}^3$. The equivalent volume for the SF galaxies in our current (325 deg^2) sample is set by the redshift at which the observed radio flux density falls below our 2.8 mJy cutoff. For a galaxy with a star-formation rate of $\sim 100 M_{\odot} \text{ yr}^{-1}$, this redshift is $z \simeq 0.084$, giving a volume of $4.5 \times 10^6 \text{ Mpc}^3$, or five times the volume surveyed by G95.

Because of this increase in sample volume for stronger radio sources, the 2dFGRS/NVSS SF sample is dominated by galaxies with high star-formation rates (well over half the SF galaxies we detect have derived star-formation rates above $30 M_{\odot} \text{ yr}^{-1}$, compared to only 5% of the G95 galaxies) so we would expect to have better statistics than G95 for galaxies with high SFRs, assuming that the radio luminosity continues to scale linearly with star-formation rate.

It is possible that at high star-formation rates the H α emission line is increasingly obscured by dust, so that optical surveys underestimate the number of galaxies with very high star-formation rates. Deep VLA studies of galaxy clusters at $z \sim 0.4$ (Smail et al. 1999) and local galaxies with ‘post-starburst’ optical spectra (Miller & Owen 2001) suggest that some galaxies may have star-forming regions which are largely hidden by dust. Follow-up observations of the galaxies in Table 1 for which the radio data imply high star-formation rates would therefore be valuable.

Integrating under the curve in Fig. 17 gives a local star-formation density of $0.022 \pm 0.004 M_{\odot} \text{ yr}^{-1} \text{ Mpc}^{-3}$, which is slightly higher than the value of $0.013^{+0.007}_{-0.005}$ derived by G95 from H α data. The difference arises mainly because our sample contains more galaxies with high star-formation rates ($>30 M_{\odot} \text{ yr}^{-1}$). For galaxies with star-formation rates up to $50 M_{\odot} \text{ yr}^{-1}$, we derive a local density of $0.017 \pm 0.004 M_{\odot} \text{ yr}^{-1} \text{ Mpc}^{-3}$, in excellent agreement with the G95 value.

8.4 Active galaxies and radio galaxies

As in Section 8.3, we combined the NVSS/2dFGRS sample with published data for bright, nearby galaxies to extend our results to lower radio power. Fig. 18 shows the results — the NVSS/2dFGRS data points agree well with the RLF for nearby ($B < 14.0$ mag) elliptical and S0 galaxies from Sadler

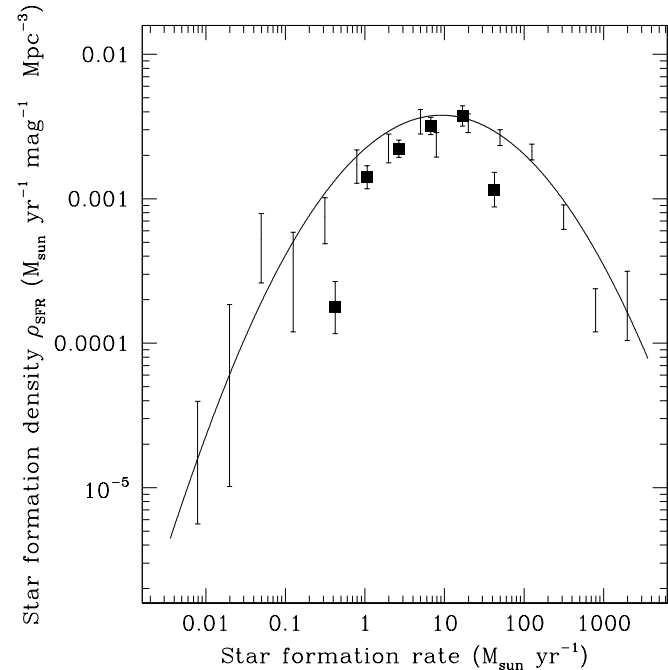


Figure 17. Local star-formation density (in $M_{\odot} \text{ yr}^{-1} \text{ mag}^{-3}$) for galaxies with star-formation rates between 0.01 and $1000 M_{\odot} \text{ yr}^{-1}$. The solid line is derived from the fit to the local RLF for star-forming galaxies (Table 8) after correcting for spectroscopic incompleteness. Error bars from the individual data points used to derive the fit are also shown. Filled squares show the values of local star-formation density derived from H α measurements by Gallego et al. (1995).

et al. (1989). Once again, we fitted an analytic function as described in Section 8.3, and the results are given in Table 8. However, it is remarkable that the space density of radio-emitting AGN is also well fitted by a single power-law of the form

$$\Phi(P_{1.4}) \propto P_{1.4}^{-0.62 \pm 0.03} \quad (11)$$

over almost five decades in luminosity from $10^{20.5}$ to $10^{25} \text{ W Hz}^{-1}$, before turning down above $10^{25} \text{ W Hz}^{-1}$. As pointed out by Sadler et al. (1989), the AGN RLF must also turn down below $10^{20} \text{ W Hz}^{-1}$ in order not to exceed the space density of luminous galaxies.

8.5 Black holes in radio AGN

Franceschini, Vercellone & Fabian (1998) examine the relation between galaxy luminosity, black hole mass and radio power in nearby active galaxies, and conclude that the radio power of an AGN is both a good tracer of supermassive black holes and an estimator of their mass (though Laor (2000) notes that the correlation between radio power and black hole mass shows considerable scatter).

Following the precepts of Franceschini et al., we can estimate the local mass density of black holes from our AGN RLF with the following conversion factors:

$$\log_{10} M_{\text{BH}} (M_{\odot}) = 0.376 \log_{10} P_{1.4} (\text{W Hz}^{-1}) + 0.173 \quad (12)$$

and

$$\log_{10} \Phi_{\text{BH}} = \log_{10} \Phi_{1.4} + 0.425 \quad (13)$$

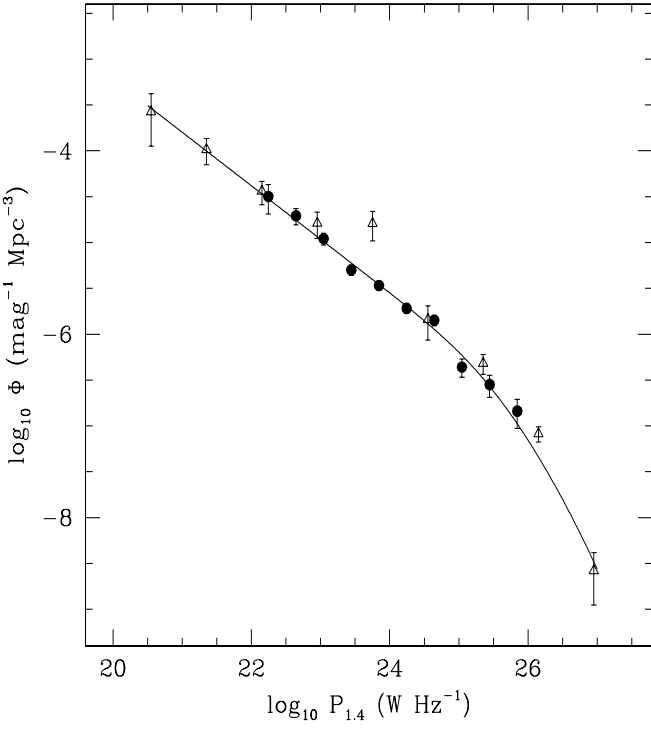


Figure 18. Local RLF for active galaxies, combining data from our sample (filled circles) with values from Sadler et al. (1989) for nearby E/S0 galaxies (open triangles). The Sadler et al. values have been converted to 1.4 GHz assuming a spectral index of $\alpha = -0.7$. As in Fig. 16, the NVSS/2dFGRS values of Φ have been increased by 5% to take into account the 95% redshift completeness of the 2dFGRS, and the solid line shows the best-fitting analytic function (see Table 8).

This yields the mass density distribution shown in Fig. 19. In contrast to the star-formation density plot shown in Fig. 17, the total mass density of black holes does not converge but continues to increase down to the lowest values (a few times $10^7 M_\odot$) so far probed by radio surveys. Integrating over the values in Fig. 19 gives a total mass density of massive black holes ($M_{\text{BH}} > 7.6 \times 10^7 M_\odot$) in galactic nuclei of

$$\rho_{\text{BH}} = 1.8^{+0.4}_{-0.6} \times 10^5 M_\odot \text{ Mpc}^{-3} \quad (14)$$

which is within the range $1.4 - 2.2 \times 10^5$ derived by Chokshi & Turner (1992) from the optical luminosity function of QSOs. We note that the value derived here is actually a lower limit, since the derived black-hole mass density is still increasing at the lowest values of M_{BH} we can measure. Thus a comparison of black-hole mass densities for radio galaxies in the local universe and high-redshift QSOs suggests that local radio-emitting AGN are the direct descendants of most or all of the high- z QSOs.

8.6 Redshift evolution of the radio luminosity function

Although the 2dFGRS probes to redshifts of $z \sim 0.3$ to 0.4 where we might expect to see cosmic evolution of the radio-source population, only the most luminous objects in our sample can be seen to these distances, and hence we

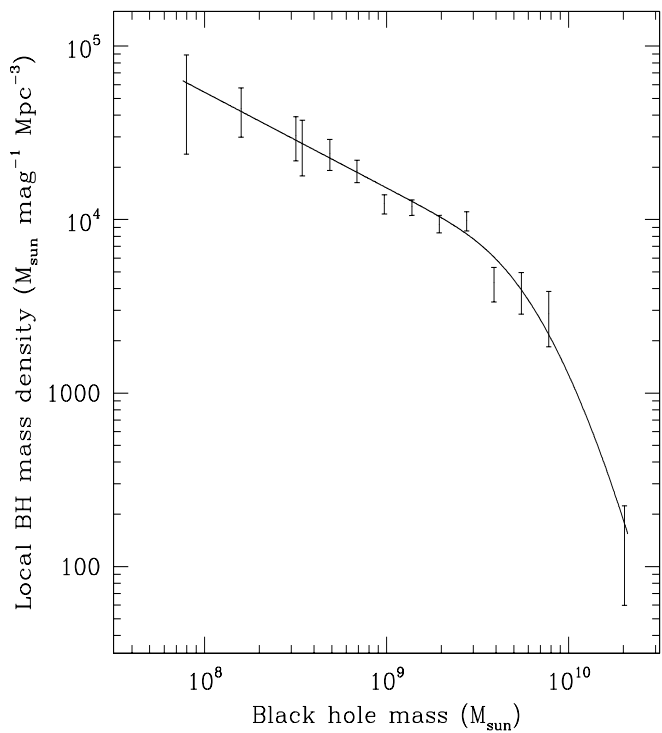


Figure 19. Local mass density (in $M_\odot \text{ mag}^{-1} \text{ Mpc}^{-3}$) of black holes, derived from the local radio luminosity function for AGN (Tables 7 and 8) together with the mean relation between radio power and black hole mass from Franceschini et al. (1998). As in Fig. 17, error bars are shown for the individual points used to derive the fit in Table 8.

Table 9. Values of $\langle V/V_{\text{max}} \rangle$ from RLF calculations split into bins in radio power

$\log_{10} P_{1.4}$ (W Hz $^{-1}$)	— AGN —		— SF —	
	n	$\langle V/V_{\text{max}} \rangle$	n	$\langle V/V_{\text{max}} \rangle$
22–23	46	0.50 ± 0.05	141	0.48 ± 0.03
23–24	195	0.55 ± 0.02	65	0.54 ± 0.04
24–25	145	0.55 ± 0.02	4	0.53 ± 0.12

can only test for evolutionary effects over a narrow range in luminosity. There are already hints that we are seeing evolution in the most powerful AGN in our sample – Table 9 shows the mean values of V/V_{max} for AGN and star-forming galaxies split into bins in radio luminosity. For AGN with $\log_{10} P_{1.4} > 10^{23} \text{ W Hz}^{-1}$, $\langle V/V_{\text{max}} \rangle$ is significantly higher than the expected value of 0.50, implying that the space density of these objects is higher at higher redshift.

Because the number of objects which we can use to probe evolutionary effects is small, we defer discussion of the RLF evolution to a later paper in this series which will analyse the full set of 2dFGRS data.

9 DISCUSSION AND CONCLUSIONS

9.1 Main results

We have shown how combining data from large radio continuum and optical redshift surveys allows us to derive accurate local radio luminosity functions (RLFs) for AGN and star-forming (SF) galaxies. Both AGN and star-forming galaxies are significant contributors to the local RLF below 10^{24} W Hz $^{-1}$ (at higher radio powers, almost all the sources are AGN), so good-quality optical spectra are needed to classify the radio sources correctly.

This paper establishes an accurate local benchmark for future studies of the cosmic evolution of both AGN and star-forming galaxies at higher redshift. The full data set of ~ 4000 radio-source spectra which will become available when the 2dFGRS is completed should be large enough to measure the evolution of radio galaxies to $z = 0.35$ and the most luminous star-forming galaxies to $z = 0.2$.

9.2 2dFGRS radio-source populations needing further investigation

We showed in Section 6 that there may be a substantial local population of radio-luminous star-forming galaxies (with implied star-formation rates of $50 M_\odot \text{ yr}^{-1}$ or more) which are not seen in H α emission-line surveys. Determining whether these ‘‘high SFR’’ galaxies are dust-enshrouded starbursts or misclassified AGN is important if we are to have an accurate census of star formation in the local universe (if they are indeed starbursts, the ‘‘high SFR galaxies’’ contribute about 20% of the local star-formation density). High-resolution radio imaging, together with infrared spectroscopy, should allow us to determine whether the radio emission seen by NVSS arises mainly from dusty star-forming regions.

Optical spectra of the remaining NVSS/ROSAT sources in the 2dFGRS area (see Section 7) would be valuable in determining whether some radio AGN have been excluded from the 2dFGRS because they have a bright nucleus which leads to them being classified as stars rather than galaxies on sky survey plates. We estimate that no more than five or six potential members of the current sample have been excluded in this way, but it would be useful to confirm this.

9.3 Prospects for deeper radio and optical observations in the 2dFGRS area

Since the overlap between 2dFGRS galaxies and NVSS radio sources is relatively small — about 5% of NVSS radio sources in the 2dFGRS area are associated with 2dFGRS galaxies, and 1–2% of 2dFGRS galaxies are detected by NVSS — it is tempting to speculate on what could be achieved with deeper radio and optical observations in the 2dFGRS area.

Radio observations to sub-mJy sensitivities at 1.4 GHz would increase the detection rate for galaxies in the 2dFGRS sample, particularly for star-forming galaxies since many of these lie close to the 2.8 mJy NVSS detection limit (see Section 3.4). For example, observations with a 3σ detection limit of 0.4 mJy at 1.4 GHz could detect galaxies with a star-formation rate of $\sim 17 M_\odot \text{ yr}^{-1}$ at $z = 0.1$, which is significantly lower than the limit of $\sim 120 M_\odot \text{ yr}^{-1}$ at the

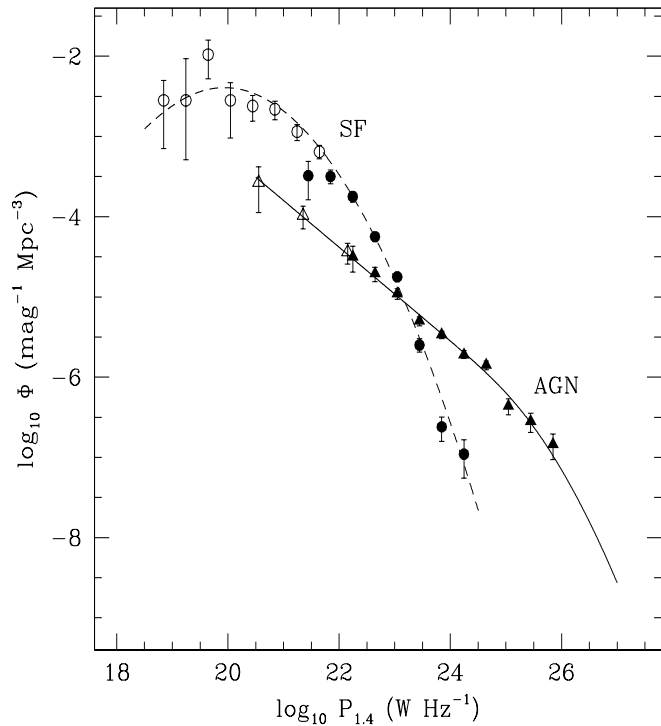


Figure 20. Local radio luminosity functions for AGN and star-forming galaxies, combining 2dFGRS data with nearby RSA spirals (SF) from Condon (1989) and nearby E/S0 galaxies (AGN) from Sadler et al. (1989). Note that both AGN and SF galaxies contribute significantly at all radio powers below $\sim 10^{25}$ W Hz $^{-1}$ at 1.4 GHz.

same redshift for galaxies near the NVSS detection limit of 2.8 mJy.

About 30% of all NVSS radio sources have an optical counterpart visible on the digitised sky survey (i.e. brighter than $b_J \sim 23$ mag). Deep 2dF spectroscopy should be possible to $b_J = 21$ mag (and even fainter for emission-line objects) with integration times of 4–8 hours rather than the 40–60 minutes used by the 2dFGRS, and careful attention to sky-subtraction techniques (Cannon 2001). This would allow spectroscopy of the host galaxies of powerful AGN (and hence studies of their cosmic evolution) to redshifts of $z \sim 0.7$ rather than the $z \sim 0.35$ limit of the 2dFGRS.

9.4 Implications for deep radio surveys to μ Jy levels

Fig. 20 shows the local radio luminosity functions (RLFs) for star-forming (SF) galaxies and AGN over the whole range in radio power for which data are currently available. The two RLFs cross over (i.e. AGN and SF galaxies contribute equally to the local radio-source population) at $P_{1.4} \simeq 10^{23.2}$ W Hz $^{-1}$. Both AGN and SF galaxies contribute at least 20% of the radio-source population over the range $10^{22.5} - 10^{23.7}$ W Hz $^{-1}$.

Fig. 21 shows the radio luminosity range probed at different redshifts by 1.4 GHz surveys with flux-density limits of 2.8 mJy (NVSS), 100 μ Jy (e.g. Gruppioni et al. 1997, Hopkins et al. 1998) and 20 μ Jy (e.g. Haarsma 2000). Extrapol-

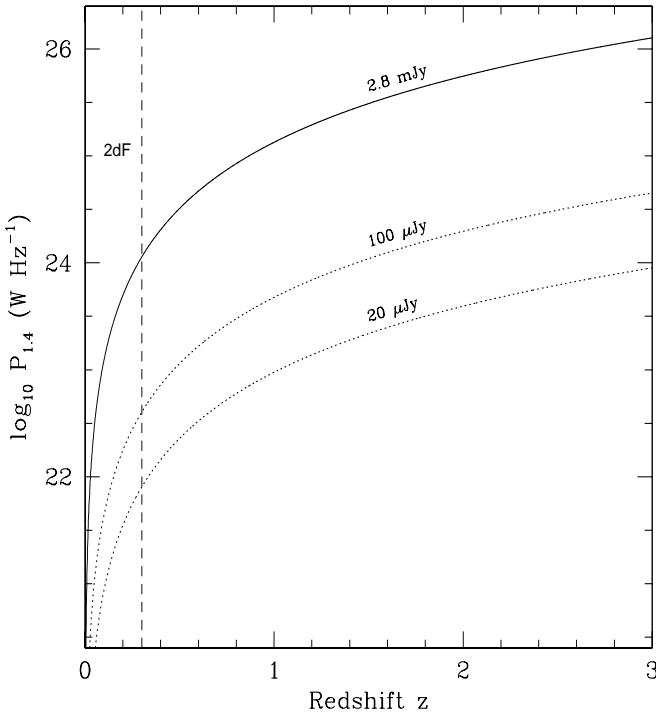


Figure 21. Radio luminosity limits at high redshift for NVSS (2.8 mJy limit) and deeper 1.4 GHz surveys (100 μ Jy and 20 μ Jy limits). The vertical line at $z=0.3$ marks the effective redshift limit of the 2dFGRS. Note that at $z \sim 1$ the deepest surveys so far carried out detect galaxies with radio luminosities above about $10^{23} \text{ W Hz}^{-1}$, i.e. in the regime where we expect a mixture of AGN and star-forming galaxies.

olating from the local RLF suggests that all μ Jy-level radio surveys should find a mixture of AGN and star-forming galaxies at all redshifts, i.e. there is no observational regime in which we can simply assume that a faint radio source arises from a starburst. Deep radio continuum surveys in the Hubble Deep Field (Richards et al. 1998; Garrett et al. 2000) suggest that the μ Jy radio-source population is composed of a mixture of 70–90% spiral and irregular/merging galaxies and 10–30% ellipticals.

A mixture of star-forming galaxies and AGN is probably present even at flux densities below 1 μ Jy — Hopkins et al. (2000) remark that in their simulations of the faint radio-source population to a flux density limit of 0.1 μ Jy, the proportion of AGN is still significant. If this is true, then optical/IR spectroscopy will play a key role in disentangling the faint radio-source population probed by future deep radio surveys, and partnerships between radio and optical telescopes in mapping out the distant universe will increase in importance in the years to come.

10 ACKNOWLEDGMENTS

The 2dF Galaxy Redshift Survey was made possible through the dedicated efforts of the staff of the Anglo-Australian Observatory, both in creating the 2dF instrument and in supporting it on the telescope. This research has made use of the NASA/IPAC Extragalactic Database (NED) which

is operated by the Jet Propulsion Laboratory, Caltech, under contract with NASA. We thank Prof. Lawrence Cram for helpful conversations about the derivation of star-formation rates from radio data, and the referee, Dr I. Snellen, for several perceptive comments which improved the final version of this paper.

REFERENCES

- Allen, D.A., Roche, P.F., Norris, R.F. 1985, MNRAS, 213, 67P
 Bauer, F.E., Condon, J.J., Thuan, T.X., Broderick, J.J., 2000, ApJS, 129, 547
 Becker, R.H., White, R.L., Helfand, D.J. 1995, ApJ, 450, 559
 Beichman, C.A., Neugebauer, G., Habing, H.J., Clegg, P.E., Chester, T.J. 1988, IRAS Catalogs and Atlases, Version 2. Explanatory Supplement
 Bock, D.C-J., Large, M.I., Sadler, E.M. 1999, AJ, 117, 1593
 Brown, M.J.I., Webster, R.L., Boyle, B.J. 2001, AJ, 121, 2381
 Cannon, R., 2001, AAO Newsletter, 96, 13
 Chokshi, A., Turner, E.L. 1992, MNRAS, 259, 421
 Clements, D.L., Sutherland, W.J., Saunders, W., Efstathiou, G.P., McMahon, R.G., Maddox, S., Lawrence, A., Rowan-Robinson, M. 1996, MNRAS, 279, 459
 Clements, D.L., Saunders, W.J., McMahon, R.G. 1999, MNRAS, 302, 391
 Clowes, R.G., Campusano, L.E., Leggett, S.K., Savage, A. 1995, MNRAS 275, 819
 Colless, M. 1999, Phil Trans R Soc Lon A, 357, 105
 Colless, M. et al. 2001, MNRAS, in press (astro-ph/0106498)
 Condon, J.J., Broderick, J.J. 1988, AJ, 96, 30
 Condon, J.J. 1989, ApJ, 338, 13
 Condon, J.J. 1992, ARAA, 30, 575
 Condon, J.J., Kaplan, D.L., Yin, Q.F. 1997, AAS, 191.1402
 Condon, J.J., Cotton, W.D., Greisen, E.W., Yin, Q.F., Perley, R.A., Taylor, G.B., Broderick, J.J. 1998, AJ, 115, 1693
 Cram, L.E. 1998, ApJ, 506, 85
 de Grijp, M.H.K., Miley, G.K., Lub, J., de Jong, T. 1985, Nature, 314, 240
 de Jong, T., Klein, U., Wielebinski, R., Wunderlich, E 1985, A&A, 147, 6
 Devereux, N.A., Eales, S.A. 1989, ApJ, 340, 708
 Folkes, S., et al. 1999, MNRAS, 308, 459
 Franceschini, A., Vercellone, S., Fabian, A.C. 1998, MNRAS, 297, 817
 Gallego, J., Zamorano, J., Aragon-Salamanca, A., Rego, M. 1995, ApJ, 455, L1
 Garrett, M.A., de Bruyn, A.G., Giroletti, M., Baan, W.A., Schilizzi, R.T. 2000, A&A, 361, L41
 Gruppioni, C., Zamorani, G., de Ruiter, H.R., Parma, P., Mignoli, M., Lari, C. 1997, MNRAS, 286, 470
 Haarsma, D.B., Partridge, R.B., Windhorst, R.A., Richards, E.A. 2000, ApJ, 544, 641
 Helfand, D.J., Schnee, S., Becker, R.H., White, R.L., McMahon, R.G. 1999, AJ, 117, 1568
 Helou, G., Soifer, B.T., Rowan-Robinson, M. 1985, ApJ, 298, L7
 Hopkins, A.M., Mobasher, B., Cram, L., Rowan-Robinson, M. 1998, MNRAS, 296, 839
 Hopkins, A., Windhorst, R., Cram, L., Ekers, R. 2000, Experimental Astronomy, 10, 419
 Ishwara-Chandra, C.H., Saikia, D.J. 1999, MNRAS, 309, 100
 Jackson, C.A., Londish, D.M. 2000, PASA, 17, 234
 Jauncey, D.L. 1975, ARAA, 13, 23
 Kapahi, V.K., Athreya, R.M., van Breughel, W., McCarthy, P.J., Subrahmanya, C.R. 1998, ApJS, 118, 275
 Kim, D.-C., Sanders, D.B. 1998, ApJS, 119, 41
 Komissarov, S.S., Gubanov, A.G. 1994, A&A, 285, 27

- Kulkarni, S.R., Frail, D.A., Wieringa, M.H., Ekers, R.D., Sadler, E.M., Wark, R.M., Higdon, J.L., Phinney, E.S., Bloom, J.S. 1998, Nature, 395, 663
- Laor, A. 2000, ApJ, 543, L111
- Lawrence, A., Walker, D., Rowan-Robinson, M., Leech, K.J., Penston, M.V. 1986, MNRAS, 219, 687
- Lewis, I.J. et al. 2001, in preparation
- Longair, M.S. 1966, MNRAS, 133, 421
- Machalski, J., Condon, J.J. 1999, ApJS, 123, 41
- Machalski, J., Godlowski, W., 2000, A&A, 360, 463
- Madau, P., Ferguson, H.C., Dickinson, M.E., Giavalisco, M., Steidel, C.C., Fruchter, A. 1996, MNRAS, 283, 1388
- Madgwick, D. et al. 2001, MNRAS, submitted (astro-ph/0107197)
- Magliocchetti, M., Maddox, S.J., Lahav, O., Wall, J.V. 1998, MNRAS, 300, 257
- Miller, N.A., Owen, F.N. 2001, ApJ, 554, L25
- Moshir, M., et al. 1990, IRAS Faint Source Catalogue Version 2.0
- Pence, W. 1976, ApJ, 203, 39
- Rengelink, R.B., Tang, Y., de Bruyn, A.G., Miley, G.K., Bremer, M.N., Röttgering, H.J.A., Bremer, M.A.R. 1997, A&AS, 124, 259
- Richards, E.A., Kellermann, K.I., Fomalont, E.B., Windhorst, R.A., Patridge, R.B. 1998, AJ, 116, 1039
- Sadler, E.M., Jenkins, C.R., Kotanyi, C.G. 1989, MNRAS, 240, 591
- Sadler, E.M., McIntyre, V.J., Jackson, C.A., Cannon, R.D. 1999, PASA, 16, 247 (Paper I)
- Sandage, A., Tammann, G.A., 1981, *A Revised Shapley-Ames Catalogue of Bright Galaxies*, Washington, Carnegie Inst.
- Sanders, D.B., Mirabel, I.F. 1996, ARAA, 34, 749
- Saunders, W., Rowan-Robinson, M., Lawrence, A., Efstathiou, G., Kaiser, N., Ellis, R. S., Frenk, C. S., 1990, MNRAS, 242, 318
- Savage, A., Wall, J.V. 1976, AuJPA, 39, 39
- Schoenmakers, A.P., Mack, K.-H., de Bruyn, A.G., Röttgering, H.J.A., Klein, U., van der Laan, H. 2000, A&AS, 146, 322
- Schmidt, M. 1968, ApJ, 151, 393
- Smail, I., Morrison, G., Gray, M.E., Owen, F.N., Ivison, R.J., Kneib, J.-P. 1999, ApJ, 525, 609
- Ellis, R. S.
- Strauss, M.A., Huchra, J.P., Davis, M., Yahil, A., Fisher, K.B., Tonry, J. 1992, ApJS, 83, 29
- Sullivan, M., et al. 2001, submitted to MNRAS
- Veilleux, S., Kim, D.-C., Sanders, D.B. 1999, ApJ, 522, 113
- Voges, W., Aschenbach, B., Boller, T., Bräuninger, H., Briel, U., Burkert, W., Dennerl, K., Englhauser, J., Gruber, R., Haberl, F., Hartner, G., Hasinger, G., Kürster, M., Pfeffermann, E., Pietsch, W., Predehl, P., Rosso, C., Schmitt, J.H.M.M., Trümper, J., Zimmermann, H.U. 1999, A&A, 349, 389
- Wall, J.V., Wright, A.E., Bolton, J.G. 1976, AuJPA, 39, 1
- Wall, J.V., Pearson, T.J., Longair, M.S. 1980, MNRAS, 193, 683
- Weiler, K.W., Montes, M.J., Panagia, N., Sramek, R.A. 1998, ApJ, 500, 51
- White, R.L., Becker, R.H. 1992, ApJS, 79, 331
- York, D.G. et al. 2000, AJ, 120, 1579

Table 1. Candidate 2dFGRS/NVSS radio sources (continued).

(1) 2dFGRS name	(2) Other name	(3) Position α (J2000)	(4) Offset (arcsec)	(5) b_J (mag)	(6) $S_{1.4}$ (mJy)	(7) $S_{60\mu m}$ (Jy)	(8) Redshift z	(9) Q	(10) Class	(11) Comments
TGN305Z105		11 26 06.26 -01 50 03.1	1.7	15.38	5.6	0.362	0.0446	5	SF	
TGN051Z030		11 25 08.23 -06 30 04.2	3.1	16.30	5.3		0.0633	4	Aa	
TGN110Z168	NGC 3679	11 26 08.65 -05 35 11.8	2.0	14.33	17.3	1.367	0.0096	4	SF	Extended radio source
TGN110Z117	IC 693	11 26 48.56 -05 00 14.8	6.5	14.45	4.0	0.430	0.0355	4	SF?	
TGN305Z050		11 27 15.47 -00 51 55.6	13.1	18.47	2.7		0.0770	3	SF?	
TGN110Z073*		11 27 22.24 -05 29 53.5	5.0	14.97	8.0	1.256	0.0288	4	SF	Extended radio source
TGN235Z130		11 27 27.59 -02 32 50.5	0.7	18.36	22.7		0.1446	3	??	
TGN374Z187		11 27 36.64 +00 23 40.7	4.2	15.46	3.3	0.372	0.0494	4	SF	
TGN306Z196*		11 27 54.34 -01 13 32.1	6.2	15.49	8.8		0.0427	4	Ae	Extended radio source
TGN236Z189		11 27 57.22 -02 24 18.9	8.1	18.43	8.7		0.0620	4	Ae	
TGN306Z194*		11 27 57.55 -01 12 42.8	3.1	15.45	5.4		0.0434	4	Ae?	
TGN236Z069		11 28 19.36 -02 50 19.5	12.4	19.38	5.7		0.1208	3	SF?	
TGN110Z005		11 28 29.65 -05 44 19.0	11.9	18.88	13.6		0.0250	4	SF	
TGN236Z156		11 29 17.98 -01 42 29.4	13.1	15.52	12.8	0.938	0.0431	4	SF	Extended radio source – correct ID
TGN306Z137		11 29 39.73 -01 02 15.9	11.6	18.03	14.5		0.1161	4	Aa	
TGN170Z077		11 29 45.19 -03 34 19.9	14.8	17.98	6.3		0.0756	4	SF?	
TGN306Z114		11 30 04.14 -01 02 58.4	10.3	17.43	3.5		0.1220	4	Aa	
TGN374Z091		11 30 06.90 -00 07 16.3	3.6	18.38	3.4	0.319	0.1158	4	Aae?	
TGN171Z104		11 30 08.58 -04 01 51.6	4.3	14.78	5.8		0.0369	4	Aa?	
TGN306Z105		11 30 10.36 -01 26 55.4	5.0	17.21	51.2		0.1198	4	Aa	
TGN374Z080		11 30 21.41 +00 58 22.2	3.3	17.81	668.2		0.1326	4	Ae	Extended radio source
TGN306Z066		11 30 51.26 -01 06 28.0	9.0	17.17	2.8		0.0478	3	SF	
TGN306Z064		11 30 52.63 -01 29 39.9	8.8	16.32	3.3	0.313	0.0729	4	SF	
TGN237Z005		11 31 50.60 -02 52 04.6	5.9	19.21	3.8		0.1463	4	Ae?	
TGN237Z004		11 31 57.75 -02 55 20.3	1.9	14.76	3.8	0.706	0.0055	4	SF	
TGN172Z010		11 32 11.16 -04 01 50.7	12.8	17.16	40.5		0.1197	4	Aa	Extended radio source – correct ID
TGN374Z008	NGC 3719	11 32 13.29 +00 49 04.6	8.2	14.61	4.8		0.0198	4	Aae?	
TGN375Z004		11 32 22.98 +00 52 21.0	3.8	19.33	25.9		0.1971	3	Aa	Extended radio source
TGN375Z002		11 32 29.91 -00 32 39.3	5.0	18.82	6.1		0.1327	5	Aa	
TGN237Z277		11 32 36.60 -02 17 05.8	8.3	17.61	4.0		0.0497	4	SF	
TGN306Z237		11 32 38.73 -01 31 49.9	10.4	17.65	2.7		0.0996	4	SF	
TGN171Z342		11 32 43.16 -03 53 48.1	5.8	16.08	4.7	0.698	0.0398	4	SF	
TGN237Z276		11 32 43.24 -02 11 59.9	2.3	16.55	5.9		0.0421	4	SF	
TGN172Z341		11 32 53.52 -04 00 51.2	13.1	16.56	9.5		0.0466	4	Aa?	Extended radio source – correct ID
TGN171Z319		11 32 56.20 -03 57 23.5	9.9	17.66	3.2		0.1131	4	Aae?	
TGN171Z310		11 33 04.30 -04 41 56.4	1.3	17.96	5.0		0.1380	4	Aa	
TGN171Z312*	PKS 1130-037	11 33 05.11 -04 00 49.8	5.5	15.75	1025.6		0.0519	4	Aa	Extended radio source
TGN172Z321		11 33 26.97 -03 47 08.0	3.7	17.78	4.3		0.1859	4	Ae?	
TGN236Z215	MCG +00-30-010	11 33 34.68 -02 16 49.0	0.8	15.89	11.3	1.173	0.0407	4	SF	
TGN172Z303		11 33 59.00 -03 36 20.2	9.2	15.44	4.2		0.0523	4	SF?	

Table 1. Candidate 2dFGRS/NVSS radio sources (continued).

(1) 2dFGRS name	(2) Other name	(3) Position α (J2000)		(4) Offset (arcsec)	(5) b_J (mag)	(6) $S_{1.4}$ (mJy)	(7) $S_{60\mu m}$ (Jy)	(8) Redshift z	(9) Q	(10) Class	(11) Comments
TGN306Z214		11 34 09.25	-01 35 42.9	5.8	15.94	3.1	0.620	0.0226	4	SF	
TGN171Z243		11 34 19.29	-03 54 05.7	9.4	18.71	4.4		0.0424	3	SF	
TGN307Z213		11 34 19.75	-02 02 26.0	4.3	18.58	5.6		0.1124	4	SF?	
TGN112Z288		11 34 26.27	-04 37 50.8	2.4	18.74	3.1	0.405	0.0914	4	SF	
TGN172Z276		11 34 26.68	-04 37 36.8	12.9	17.42	3.1		0.0001	4	star	
TGN172Z277		11 34 26.72	-03 16 43.2	5.7	18.71	3.2		0.1056	3	Aae?	
TGN171Z218		11 34 48.36	-04 02 46.8	11.3	16.28	16.4		0.0281	4	SF	
TGN237Z096		11 34 49.34	-03 20 57.8	3.3	16.55	2.2		0.0401	4	SF	
TGN112Z249		11 35 15.32	-04 42 08.7	3.5	17.79	20.8		0.1076	4	Aa	Extended radio source
TGN171Z183		11 35 25.11	-04 30 13.5	8.0	17.42	3.0		0.0645	4	Ae?	
TGN172Z242		11 35 34.96	-03 44 01.6	4.1	17.51	48.9		0.0006	3	star	
TGN172Z225		11 35 58.20	-04 28 28.8	0.6	18.93	200.8		0.2726	3	Aa?	
TGN238Z163		11 36 13.94	-02 52 14.6	2.1	16.42	6.4	0.984	0.0452	4	SF	
TGN171Z142		11 36 20.58	-03 46 56.8	12.7	19.35	9.1		0.2239	3	Aa?	Extended radio source – correct ID
TGN307Z122		11 36 25.41	-00 59 29.9	8.4	18.57	6.6		0.0771	3	SF?	
TGN172Z174		11 37 05.86	-04 06 01.6	6.4	19.32	6.6		0.2234	4	Aa?	
TGN112Z127		11 37 20.96	-05 36 07.0	3.2	14.95	7.5	0.565	0.0375	4	SF	
TGN307Z095		11 37 24.52	-02 05 51.8	6.2	17.56	5.1	0.432	0.0788	4	SF	
TGN307Z090*		11 37 29.21	-00 51 04.4	4.0	19.19	65.0		0.0439	4	SF	Not this ID – see Table Notes
TGN238Z120		11 37 45.32	-02 51 54.6	6.0	17.57	3.8		0.1206	4	Aa	
TGN307Z055		11 38 28.63	-00 37 43.8	7.9	19.21	2.8		0.1910	4	SF	
TGN307Z053	UGC 06608	11 38 33.27	-01 11 05.1	5.9	14.76	4.6	0.684	0.0208	4	SF?	
TGN238Z269		11 38 48.78	-02 05 07.5	13.7	19.39	26.5		0.0741	4	SF	
TGN238Z259		11 39 04.19	-01 47 45.1	7.3	17.54	3.1		0.1052	4	Aae?	
TGN238Z258		11 39 05.56	-02 37 29.0	0.7	18.46	5.9		0.1693	4	Aa	
TGN113Z259		11 39 10.39	-05 20 14.0	2.8	15.78	5.7	0.494	0.0479	4	Ae?	
TGN238Z251		11 39 15.00	-02 41 09.7	1.4	17.31	4.2		0.1035	4	Ae?	
TGN238Z073		11 39 24.05	-03 13 29.4	9.4	19.29	6.9		2	??	Extended radio source	
TGN113Z221		11 39 51.94	-05 00 47.5	2.4	16.91	4.2		0.1016	4	Aae?	
TGN376Z126		11 40 06.83	-00 27 58.0	13.3	18.93	3.3		0.0753	4	Aa	
TGN113Z178		11 40 48.60	-05 54 53.9	7.2	17.53	16.1		0.0001	4	star	
TGN113Z165		11 41 00.91	-06 07 04.6	7.2	15.92	3.6		0.0299	4	SF	
TGN238Z202		11 41 26.55	-02 34 05.6	0.9	19.28	46.3		0.1602	4	Ae?	Extended radio source
TGN113Z125		11 41 33.16	-04 50 39.7	1.8	17.49	8.3	1.119	0.0376	4	SF	Extended radio source
TGN308Z109		11 41 44.63	-00 41 17.7	9.6	17.77	4.6		0.0502	5	SF	
TGN239Z082		11 41 45.43	-03 29 02.8	9.6	18.76	2.8		0.1412	4	SF	
TGN113Z111		11 41 47.26	-05 52 04.8	10.9	17.90	3.8		2	??		
TGN240Z319		11 42 30.91	-02 15 06.0	3.6	16.18	9.0		0.0478	4	Aa	
TGN239Z061		11 42 34.61	-03 05 31.4	5.3	17.46	3.3		0.0554	4	SF?	
TGN240Z127		11 42 37.93	-03 06 45.2	8.1	17.01	2.4		0.0554	4	SF?	

Table 1. Candidate 2dFGRS/NVSS radio sources (continued).

(1) 2dFGRS name	(2) Other name	(3) Position α (J2000) δ		(4) Offset (arcsec)	(5) b_J (mag)	(6) $S_{1.4}$ (mJy)	(7) $S_{60\mu m}$ (Jy)	(8) Redshift z	(9) Q	(10) Class	(11) Comments
TGN114Z337		11 43 10.16	-05 32 56.2	3.9	18.88	11.0		0.1502	4	SF	
TGN173Z052		11 43 18.68	-03 25 54.2	2.2	19.16	6.5	0.751		2	SF?	
TGN113Z019		11 43 24.06	-05 37 23.5	5.8	18.25	3.1		0.1495	3	Aa?	
TGN239Z044		11 43 26.66	-02 53 07.5	10.1	17.91	3.9		0.1155	4	Ae	
TGN239Z228		11 43 30.41	-01 45 25.1	12.7	18.65	60.7		0.1067	4	Aa	Extended radio source – not this ID
TGN239Z221		11 43 38.89	-01 38 50.0	2.8	17.37	4.8	0.626	0.0430	4	SF	
TGN113Z005		11 43 45.15	-05 36 35.3	0.8	16.99	9.2		0.0791	3	Aa?	
TGN309Z233		11 44 04.77	-02 02 27.9	4.6	17.90	3.9		0.0677	4	SF?	
TGN114Z270		11 44 16.36	-05 57 45.5	3.2	15.42	15.7		0.0492	4	Aa?	Extended radio source
TGN240Z277		11 44 25.98	-01 57 26.5	0.6	16.87	6.4		0.0766	4	Aa	
TGN239Z017		11 44 54.66	-02 47 51.6	8.0	18.40	5.1		0.1148	4	Aae	
TGN239Z172		11 44 57.35	-02 30 17.3	3.7	16.15	9.5	0.931	0.0459	4	SF	
TGN239Z171		11 44 58.50	-02 19 31.1	1.4	18.16	2.6		0.1219	4	Aae	
TGN239Z013		11 45 13.84	-02 59 39.7	0.6	17.88	105.0		0.1070	4	Aae	
TGN239Z158		11 45 25.87	-02 23 33.5	9.8	18.30	52.5		0.1289	4	Aa	Extended radio source
TGN239Z154		11 45 30.87	-02 27 09.0	11.8	17.70	146.8			2	Aa	Extended radio source – correct ID
TGN240Z219		11 46 03.12	-02 14 46.4	8.5	19.30	5.1		0.1216	4	SF?	
TGN114Z092		11 46 46.03	-05 08 05.5	13.8	18.80	3.2		0.1341	4	SF	
TGN242Z140		11 52 31.36	-02 14 21.5	8.2	19.09	4.2		0.1649	4	??	
TGN175Z316		11 53 11.79	-04 05 16.2	3.1	17.91	10.4		0.0928	4	Aae	Extended radio source
TGN176Z250	NGC 3952	11 53 40.55	-03 59 46.0	7.4	14.37	8.6	1.502	0.0053	4	SF	Extended radio source
TGN176Z227		11 54 27.49	-04 24 38.3	6.5	19.21	6.1		0.1598	4	Aa	
TGN176Z204		11 55 01.23	-03 36 47.5	0.3	18.11	42.7		0.1660	4	Aae	
TGN176Z175		11 55 38.37	-04 11 01.0	8.9	19.44	4.4		0.2724	4	Aae	
TGN176Z174		11 55 41.35	-03 59 05.8	2.6	19.34	13.1		0.2126	4	Aa	
TGN312Z230		11 56 31.71	-01 53 06.7	14.4	16.84	3.9		0.0892	4	SF?	Bright galaxy – correct ID
TGN176Z071		11 58 02.63	-03 44 36.7	9.3	15.12	3.9	1.262	0.0196	4	SF	
TGN312Z215		11 58 44.93	-01 48 03.3	9.0	19.17	4.6		0.0880	3	??	
TGN243Z131		11 59 06.34	-02 07 19.1	7.3	18.19	3.0		0.0880	4	SF	
TGN243Z124		11 59 20.01	-02 22 34.6	13.5	19.34	6.1		0.1884	4	??	
TGN244Z145		12 00 21.91	-02 01 53.4	13.5	18.25	40.8		0.1464	4	Aa	Extended radio source – not this ID
TGN244Z100		12 01 49.72	-01 53 27.2	8.8	17.29	3.9		0.0908	5	Ae	
TGN314Z018*		12 02 26.64	-01 29 16.1	1.4	17.85	14.9	2.406	0.1511	4	Ae?	
TGN245Z023		12 07 19.79	-00 45 27.9	9.2	19.28	4.4		0.0003	4	star	
TGN120Z253		12 07 52.75	-04 35 38.5	14.1	18.08	3.9		0.1316	3	Ae	
TGN246Z105		12 08 23.87	-00 57 17.6	8.6	19.29	3.6		0.1792	4	Aa	
TGN246Z169		12 08 55.37	-01 50 06.2	6.1	18.68	4.5		0.1759	4	Aa	
TGN246Z079		12 09 25.21	-00 57 51.7	1.3	19.01	8.1		0.1304	4	Aa	
TGN179Z137		12 09 43.63	-02 05 00.3	3.0	17.64	36.1		0.1003	4	Aa	Extended radio source
TGN180Z176		12 11 03.26	-02 02 58.1	13.0	18.87	5.3		0.1104	4	Aa	

Table 1. Candidate 2dFGRS/NVSS radio sources (continued).

(1) 2dFGRS name	(2) Other name	(3) Position α (J2000)	(4) Offset (arcsec)	(5) b_J (mag)	(6) $S_{1.4}$ (mJy)	(7) $S_{60\mu m}$ (Jy)	(8) Redshift z	(9) Q	(10) Class	(11) Comments
TGN318Z043		12 16 30.06 +00 41 28.0	11.4	19.18	21.7		0.3057	3	Aa?	Extended radio source – correct ID
TGN247Z053		12 16 49.06 -00 44 31.4	3.6	16.45	9.8		0.0711	4	Aa	
TGN248Z150		12 17 04.73 -00 55 09.4	8.9	19.24	2.7		0.1973	4	Aa	
TGN318Z148		12 17 30.76 +00 23 57.1	8.8	18.60	33.7			2	??	Extended radio source
TGN122Z072	PKS 1215-033	12 17 55.26 -03 37 23.3	2.2	19.30	213.9		0.1823	3	Ae	
TGN248Z126		12 18 08.57 -01 03 52.1	8.6	14.66	3.5		0.0192	5	SF	
TGN318Z108		12 19 06.49 +00 01 37.7	4.9	18.39	4.5		0.1175	4	Aa	
TGN248Z224		12 19 20.85 -02 00 27.1	5.8	18.24	6.2		0.1312	5	Ae?	
TGN385Z027		12 20 06.13 +00 57 39.7	2.6	18.15	3.1		0.0902	4	SF	
TGN181Z175		12 20 18.37 -02 41 02.1	5.4	19.19	148.8		0.4380	4	Ae	
TGN318Z080*		12 20 32.79 +00 04 16.2	5.9	18.32	99.3		0.1585	4	Aa	Extended radio source
TGN181Z166		12 20 52.05 -02 09 24.0	4.1	17.43	6.0		0.0675	5	Aa	
TGN319Z194		12 21 04.18 +00 05 03.7	11.8	18.24	2.8		0.1073	4	SF	
TGN182Z119		12 21 13.23 -02 48 59.8	0.6	18.39	103.2		0.1135	3	Ae	Extended radio source
TGN248Z017		12 21 59.67 -01 08 00.5	5.6	19.15	57.8		0.2599	4	Aa	Extended radio source
TGN319Z151		12 22 17.69 -00 07 45.0	5.8	18.48	4.9		0.1727	4	Ae	
TGN249Z121		12 24 43.22 -00 25 08.1	12.2	18.46	4.0		0.1577	4	Aa	
TGN183Z132		12 25 34.38 -02 50 28.8	6.7	16.83	8.6		0.0671	4	SF	Extended radio source
TGN124Z221		12 25 45.35 -03 33 48.9	3.3	18.28	3.2	0.503	0.1136	5	SF	
TGN124Z214		12 25 56.40 -03 58 36.1	3.6	15.02	4.2	0.396	0.0187	5	SF	
TGN124Z197*		12 26 10.54 -03 50 47.6	6.8	17.37	104.3		0.1234	5	Aa	Extended radio source
TGN065Z155		12 26 13.53 -04 38 43.9	2.3	17.58	9.6		0.1349	5	Aa	Extended radio source
TGN249Z076		12 26 44.94 -00 37 19.1	1.4	18.08	25.1		0.1584	4	Aa	Extended radio source
TGN183Z104		12 27 00.85 -02 59 37.2	6.9	19.31	3.4		0.1064	4	Aa	
TGN183Z043		12 28 53.13 -03 10 23.0	13.2	18.72	21.8		0.0997	4	SF	
TGN124Z048		12 28 58.63 -03 38 57.4	14.6	19.17	20.3		0.1091	4	Aa	Extended radio source – not this ID
TGN125Z064		12 31 25.63 -04 29 12.5	3.4	18.28	9.2		0.0337	4	SF	Extended radio source
TGN251Z074		12 36 22.96 -00 52 04.5	2.5	18.70	9.7		0.1423	4	Aa	
TGN186Z286		12 38 50.07 -02 29 35.8	4.6	18.22	4.3		0.1373	4	Aa	
TGN185Z019		12 39 48.37 -02 47 46.3	3.6	15.53	4.7		0.0482	4	Aa	
TGN252Z151		12 43 27.38 -01 50 49.7	6.2	18.07	3.5		0.0812	4	Aae?	
TGN325Z119		12 48 17.99 +00 28 15.3	9.0	18.61	187.2		0.0827	4	Aa	Extended radio source
TGN255Z004		12 52 14.53 -00 42 08.4	11.8	18.00	3.6		0.0827	4	SF	
TGN130Z005		12 52 23.36 -04 05 26.7	4.4	17.54	105.4		0.1663	4	Aa	Extended radio source
TGN071Z240		12 54 32.77 -04 54 06.4	3.2	19.26	13.2		0.1881	4	Aa	Extended radio source
TGN130Z203		12 54 45.25 -03 06 53.2	1.9	17.93	28.4		0.1720	3	Aa	
TGN130Z346		12 54 52.33 -04 44 02.8	5.2	19.06	12.5		0.1883	4	Aa	Extended radio source
TGN326Z164		12 55 16.54 +00 14 48.5	7.8	15.49	3.1		0.0478	3	Aa	
TGN131Z280		12 55 47.82 -03 39 10.5	4.4	17.93	3.8	0.674	0.1686	4	Ae?	
TGN130Z161		12 55 50.37 -03 42 15.3	1.5	19.42	42.9		0.2190	3	??	

Table 1. Candidate 2dFGRS/NVSS radio sources (continued).

(1) 2dFGRS name	(2) Other name	(3) Position α (J2000)	(4) Offset (arcsec)	(5) b_J (mag)	(6) $S_{1.4}$ (mJy)	(7) $S_{60\mu m}$ (Jy)	(8) Redshift z	(9) Q	(10) Class	(11) Comments
TGN326Z127		12 56 17.11 -00 38 23.0	9.2	19.07	6.1		0.1352	4	Aa	
TGN326Z014		12 59 51.92 +00 20 34.1	11.5	18.71	3.4		0.1709	4	Aa	
TGN327Z215		13 00 04.66 +00 27 10.2	6.0	17.07	2.6		0.0223	3	SF	
TGN192Z187		13 05 30.87 -02 05 48.1	10.3	19.18	3.4		0.2008	4	Aa	
TGN258Z122		13 05 51.44 -01 19 04.8	12.5	17.78	3.0	0.299	0.0966	4	SF	
TGN258Z042		13 07 29.23 -01 03 16.1	10.7	17.68	2.4		0.0852	4	SF	
TGN258Z014		13 08 12.54 -01 16 56.9	14.7	17.14	3.7		0.0854	4	Aa	
TGN135Z211		13 14 36.23 -03 56 01.4	4.2	17.67	2.8	0.461	0.0650	4	SF	
TGN194Z059		13 14 37.88 -03 18 27.4	3.3	15.78	7.1	0.806	0.0421	4	SF	
TGN135Z197*		13 14 51.85 -04 09 53.2	11.3	18.56	6.9		0.1484	3	Aa	
TGN135Z148		13 15 43.77 -04 09 51.2	5.1	15.79	2.7	0.315	0.0187	3	SF	
TGN135Z133		13 15 54.69 -03 43 55.0	10.9	16.37	3.2		0.0307	4	SF	Bright galaxy – correct ID
TGN076Z131		13 17 36.86 -04 57 16.6	1.9	17.75	2.6		0.1179	4	Aae	
TGN399Z203		13 23 21.55 +01 56 31.6	4.3	17.47	3.7	0.338	0.1106	4	SF?	
TGN137Z256		13 25 42.06 -03 51 00.0	8.1	18.02	2.3		0.0357	4	Aa?	
TGN333Z215		13 26 17.67 +00 13 18.0	8.2	15.70	21.6		0.0830	4	Aa	
TGN333Z077		13 26 55.79 +00 41 53.6	3.8	17.62	4.4	0.541	0.0820	4	SF	
TGN332Z098		13 27 39.52 +00 19 17.8	5.4	17.01	4.9	0.439	0.0472	4	SF	
TGN333Z187		13 27 48.89 -00 15 34.8	6.7	17.85	2.6		0.1427	3	SF?	
TGN333Z047		13 28 38.98 +00 32 54.4	2.0	17.89	5.5		0.1048	4	Aa	
TGN401Z147		13 28 41.87 +02 01 40.5	14.2	18.28	42.1		0.1400	4	Aa	Extended radio source – correct ID
TGN137Z082		13 28 52.41 -04 26 29.9	6.2	16.11	4.9	0.510	0.0479	4	SF?	
TGN137Z043*		13 29 39.25 -03 46 50.8	0.7	18.56	253.9	0.954	0.2217	4	Ae	
TGN138Z108		13 29 56.73 -04 23 51.1	7.1	17.98	3.5		0.1150	4	Aa	
TGN138Z170		13 29 58.53 -04 39 27.7	5.8	18.63	17.5		0.1049	4	Aa	Extended radio source
TGN138Z103		13 30 01.72 -03 50 00.3	4.6	18.08	19.0		0.1057	4	Aa	Extended radio source
TGN265Z022	VIII Zw 318	13 30 32.18 -00 36 15.7	4.1	16.14	10.5	1.328	0.0549	4	SF	
TGN138Z066		13 31 12.03 -04 16 38.9	5.0	19.40	8.7		0.2210	4	Ae	Extended radio source
TGN138Z054		13 31 32.29 -03 54 34.9	10.3	17.63	3.1		0.1243	4	Aa	
TGN138Z046		13 31 36.64 -03 35 58.7	9.2	18.61	2.6		0.1094	4	Aae	
TGN401Z029		13 31 52.84 +02 01 00.4	2.3	17.44	14.0	0.986	0.0860	3	Ae	
TGN401Z254*	PKS 1330+02	13 32 53.27 +02 00 44.9	2.6	19.41	2656.8		0.2162	4	Ae	Extended radio source
TGN266Z210		13 32 54.58 -00 32 35.9	5.7	18.07	4.0	0.337	0.0870	4	SF	
TGN138Z312		13 33 15.50 -04 27 10.0	10.2	17.74	16.3		0.1116	4	Aa	Extended radio source – correct ID
TGN401Z219		13 34 01.62 +01 05 45.2	9.8	18.61	3.0		0.0227	4	SF	
TGN401Z202		13 34 25.72 +00 56 46.7	4.5	19.43	13.0		0.2480	4	Aa	Extended radio source
TGN139Z348		13 34 39.33 -04 02 45.3	4.8	17.50	14.1		0.0854	4	Aae?	
TGN266Z235		13 34 53.32 -01 32 39.7	2.6	18.93	23.3		0.0869	4	Aa	Extended radio source
TGN200Z274		13 37 36.61 -02 30 41.7	2.9	19.32	14.7		2	??	Extended radio source	
TGN267Z218		13 37 44.05 -02 10 28.0	4.2	17.37	7.4	0.834	0.0263	4	SF	

Table 1. Candidate 2dFGRS/NVSS radio sources (continued).

(1) 2dFGRS name	(2) Other name	(3) Position α (J2000)	(4) Offset (arcsec)	(5) b_J (mag)	(6) $S_{1.4}$ (mJy)	(7) $S_{60\mu m}$ (Jy)	(8) Redshift z	(9) Q	(10) Class	(11) Comments
TGN267Z210		13 38 01.49 -01 47 11.5	4.7	19.01	7.8		0.1773	4	Aa	Extended radio source
TGN200Z263		13 38 05.63 -02 24 16.7	6.5	19.37	2.9		0.2177	3	??	
TGN200Z235		13 38 49.45 -02 22 37.6	3.8	19.15	11.5		0.2187	4	Aae	
TGN335Z179		13 39 02.29 +00 29 12.7	12.3	19.01	3.4		0.1440	4	Aa	
TGN200Z219		13 39 17.31 -01 50 49.5	2.0	17.62	60.2		0.0892	4	Aa	Extended radio source
TGN139Z160		13 39 18.66 -04 48 04.2	1.6	18.38	63.1		0.1308	4	Aa	Extended radio source
TGN139Z143		13 39 37.86 -04 12 55.9	4.0	18.67	3.8		0.1232	4	Aae?	
TGN200Z048		13 39 39.67 -03 01 21.0	10.3	19.17	8.7		0.1139	3	??	Extended radio source – not this ID
TGN402Z030*	NGC 5257	13 39 52.64 +00 50 28.2	7.2	14.89	49.8	4.649	0.0223	4	SF	Extended radio source
TGN268Z285		13 39 55.94 -01 44 16.4	6.1	19.42	32.3		0.0367	3	??	Extended radio source
TGN402Z029*	NGC 5258	13 39 57.95 +00 49 58.3	8.4	15.28	43.3	4.649	0.0222	4	SF	Extended radio source
TGN139Z094		13 40 28.00 -04 21 52.6	2.9	19.09	13.9		0.1959	3	Aa	
TGN200Z020		13 40 42.63 -03 08 08.4	3.7	19.27	38.8		0.1856	4	Aae	Extended radio source
TGN139Z073		13 40 47.69 -04 35 32.5	2.9	17.86	4.0		0.1309	3	Aa	
TGN268Z092		13 43 32.04 -00 21 16.7	10.6	19.33	11.1		0.0874	4	Aae	Extended radio source – not this ID
TGN201Z096		13 43 36.69 -02 46 47.6	3.7	18.47	13.9		0.1519	3	Aa	Extended radio source
TGN201Z226		13 44 44.07 -02 24 08.2	3.0	19.07	41.1			2	??	Extended radio source
TGN269Z222		13 44 58.00 -01 28 10.1	4.4	18.62	2.9		0.1633	4	Aa	
TGN268Z220		13 45 16.84 -01 56 26.1	1.1	18.37	365.7		0.1497	4	Aae	
TGN268Z216		13 45 29.89 -01 40 03.0	6.4	18.44	4.7	0.465	0.0881	5	SF	
TGN268Z023		13 45 52.83 -00 46 07.8	2.7	18.30	20.3		0.1486	4	Aa	Extended radio source
TGN140Z151		13 45 54.73 -04 01 44.8	5.7	18.82	3.8		0.2689	4	SF??	
TGN201Z043		13 46 02.59 -03 21 57.6	7.2	18.75	3.1		0.0862	4	Aa?	
TGN201Z167		13 46 14.96 -02 12 17.7	3.3	19.31	10.4		0.1555	4	Aa	
TGN201Z035		13 46 22.18 -03 25 06.3	11.4	16.78	6.1		0.0242	4	Ae	Bright galaxy – correct ID
TGN140Z101		13 46 53.63 -03 36 13.3	0.8	19.38	139.3		0.2158	4	Aa	
TGN140Z051		13 47 45.39 -04 42 19.6	3.0	18.92	5.3		0.1595	4	Aa	
TGN337Z042		13 48 06.38 +00 49 19.9	4.9	17.93	37.1		0.0887	4	Aa	Extended radio source
TGN141Z043		13 51 52.04 -04 17 08.1	4.9	18.13	6.2	0.550	0.0937	4	SF?	
TGN337Z224		13 53 26.21 +00 02 47.8	3.4	17.53	8.0		0.1163	4	Aa	Extended radio source
TGN203Z178		13 58 20.01 -02 21 42.1	7.5	19.42	3.1		0.2201	3	Aa	
TGN203Z153		13 59 30.16 -02 27 03.0	4.3	19.41	3.8		0.2233	4	Aa	
TGN271Z113		13 59 48.20 -01 46 50.2	9.7	18.34	2.8		0.0731	4	Aa	
TGN272Z270		14 00 13.21 -00 57 46.4	12.3	16.39	4.1		0.0242	4	SF	Bright galaxy – correct ID
TGN271Z084		14 00 16.23 -01 32 08.9	8.2	19.17	3.7		0.1465	4	Ae	
TGN271Z072		14 00 31.52 -01 21 30.0	1.4	18.84	6.5		0.1713	4	Aa	Extended radio source
TGN204Z105	NGC 5400	14 00 37.30 -02 51 27.7	7.4	14.25	7.0		0.0250	4	Aa	
TGN339Z111		14 00 51.77 -00 37 49.1	9.1	19.32	5.1		-0.0001	4	star	
TGN204Z252		14 01 18.98 -02 11 27.1	10.6	18.06	3.9		0.1716	4	Ae	
TGN204Z244		14 01 38.20 -02 30 23.8	3.5	19.35	5.8		0.2169	4	Ae	

Table 1. Candidate 2dFGRS/NVSS radio sources (continued).

(1) 2dFGRS name	(2) Other name	(3) Position α (J2000)		(4) Offset (arcsec)	(5) b_J (mag)	(6) $S_{1.4}$ (mJy)	(7) $S_{60\mu m}$ (Jy)	(8) Redshift z	(9) Q	(10) Class	(11) Comments
TGN272Z254		14 01 46.70	-01 53 58.0	11.9	18.76	5.7		0.1315	4	SF	
TGN205Z093		14 08 23.43	-03 14 00.0	12.0	19.11	4.6		0.0591	4	SF	
TGN205Z206		14 09 28.84	-01 54 24.3	4.4	15.88	3.9		0.0296	4	SF?	
TGN205Z052		14 09 54.30	-02 44 34.2	5.0	18.75	12.9		0.1855	4	Aa	
TGN205Z185	UGC 09057	14 10 12.81	-02 34 19.7	11.3	14.38	13.0	0.516	0.0054	4	SF	Extended radio source – correct ID
TGN275Z005		14 12 23.46	-00 49 29.6	10.0	19.14	27.1		0.1881	4	Aa	Extended radio source – correct ID
TGN205Z158		14 13 21.10	-02 47 07.8	3.0	18.16	22.6		0.1480	4	Aa	Extended radio source
TGN275Z178		14 13 51.80	-00 37 51.2	2.0	18.93	6.2		0.1212	4	Aa	
TGN275Z166		14 14 16.25	-00 21 05.1	6.2	19.16	2.4		0.1396	5	Aa	
TGN275Z162		14 14 29.11	-00 22 30.3	3.8	18.28	12.0		0.1361	5	Aa	Extended radio source
TGN206Z079		14 14 31.29	-03 18 50.4	2.5	15.12	6.4	1.161	0.0325	4	SF	
TGN206Z237		14 14 45.50	-01 40 55.6	1.1	18.51	12.4	1.394	0.1508	4	Ae	
TGN206Z205		14 15 17.97	-02 26 42.2	0.8	16.16	19.2		0.0470	4	Aa	
TGN274Z240		14 15 26.05	-01 35 58.0	4.9	18.89	3.4		0.1255	4	Aa	
TGN275Z118		14 15 41.23	-00 38 52.6	4.6	19.06	12.7		0.1483	5	Aa	Extended radio source
TGN275Z123		14 15 41.32	-01 11 07.8	6.4	18.32	10.6		0.1477	4	Aa	Extended radio source
TGN145Z211		14 16 20.94	-04 00 25.7	13.4	16.22	27.1		0.1230	4	Aa	Extended radio source – not this ID
TGN206Z175		14 16 37.66	-02 35 22.9	13.0	19.01	3.6		0.0932	4	Aa?	
TGN207Z146*		14 16 37.87	-03 01 32.3	8.4	19.37	16.1		3.0000	4	Ae	Extended radio source
TGN206Z028		14 16 42.95	-02 56 12.4	1.7	18.74	94.2		0.2066	1	??	
TGN206Z022		14 17 08.23	-03 01 33.7	10.2	17.34	3.4		0.1310	4	SF	
TGN206Z019		14 17 20.05	-02 49 30.9	10.1	19.39	4.2		0.1753	4	Ae	
TGN275Z056		14 17 27.83	-00 25 25.2	13.4	19.15	4.4		0.1231	5	Aa	
TGN276Z186		14 18 08.82	-01 22 35.0	1.3	19.31	31.3		0.1533	5	Aa	Extended radio source
TGN145Z096		14 18 23.44	-03 55 52.8	14.7	19.40	3.8		0.1063	4	SF	
TGN145Z046		14 19 16.74	-03 46 30.5	3.5	14.94	7.9	0.762	0.0440	4	SF	
TGN145Z024		14 19 37.65	-03 36 59.5	1.4	18.17	2.6		0.1171	4	SF	
TGN145Z010		14 19 51.39	-03 51 56.1	0.7	18.00	13.0		0.1251	4	Aa	Extended radio source
TGN146Z305	IC 997	14 19 59.52	-04 27 09.0	2.5	14.29	27.3	2.891	0.0235	4	SF?	
TGN086Z206		14 20 15.69	-04 34 06.4	3.1	18.63	53.9		0.3108	1	??	Extended radio source
TGN276Z089		14 20 23.20	-00 49 10.2	10.4	17.66	2.9		0.0841	5	SF?	
TGN086Z150		14 21 03.60	-04 54 15.3	1.6	19.07	26.1		0.2573	4	Aa	
TGN146Z233		14 21 23.45	-04 00 29.5	5.1	18.30	2.6		0.1264	4	Aa	
TGN146Z219		14 21 35.36	-04 32 50.0	6.4	15.14	4.1	0.799	0.0115	4	SF?	
TGN146Z172		14 22 39.21	-03 59 48.5	10.7	18.89	14.2		0.0006	3	star	
TGN208Z039	VIII Zw 414	14 24 58.67	-03 04 01.2	8.4	14.60	3.6	0.204	0.0308	4	SF	
TGN146Z056		14 25 30.89	-04 26 51.0	4.4	15.85	3.2	0.217	0.0256	3	SF	
TGN209Z211		14 27 29.67	-02 05 33.9	8.8	18.48	5.8	0.347	0.0547	4	SF	
TGN209Z132		14 30 33.00	-02 36 54.9	13.2	19.14	6.3		0.2042	4	Aa	
TGN210Z078		14 34 09.17	-03 26 44.9	2.4	19.11	10.0		0.2228	4	Aa	Extended radio source

Table 1. Candidate 2dFGRS/NVSS radio sources (continued).

(1) 2dFGRS name	(2) Other name	(3) Position α (J2000) δ		(4) Offset (arcsec)	(5) b_J (mag)	(6) $S_{1.4}$ (mJy)	(7) $S_{60\mu m}$ (Jy)	(8) Redshift z	(9) Q	(10) Class	(11) Comments
TGN210Z071		14 34 19.24	-03 15 34.7	8.9	18.21	4.6		0.1204	3	Aa	
TGN148Z250		14 35 05.29	-04 09 08.5	10.7	19.31	24.5			2	??	Extended radio source – not this ID
TGN088Z182		14 35 14.19	-04 48 47.7	1.9	17.22	8.9		0.0585	3	Aae	
TGN148Z204		14 35 47.68	-04 07 15.3	4.4	17.44	3.6		0.1175	4	Aa	
TGN211Z063		14 39 32.61	-02 47 47.1	11.1	19.22	3.5		0.0825	3	Aae?	
TGN348Z183*		14 40 13.78	+00 00 38.7	10.7	18.65	67.2		0.1790	4	Aa	Double radio source – correct ID
TGN211Z052		14 40 14.60	-02 46 09.6	3.9	18.19	6.7		0.1299	4	Aa	
TGN211Z130		14 41 50.80	-02 20 58.1	10.7	16.63	2.3	0.243	0.0575	4	SF	Bright galaxy – correct ID
TGN149Z12		14 42 23.50	-04 12 43.8	9.3	18.53	2.7		0.0695	4	SF	
TGN149Z195		14 42 41.18	-03 50 45.0	11.5	19.35	14.0		0.2116	4	Aae	Extended radio source – not this ID
TGN149Z174		14 43 04.02	-03 38 48.4	3.8	15.77	7.1	0.574	0.0456	4	SF	
TGN211Z007		14 43 16.02	-02 54 08.9	4.4	17.28	3.4	0.249	0.0766	4	SF	
TGN149Z152		14 43 44.87	-03 31 42.9	7.0	17.02	3.1	0.448	0.0447	4	SF	
TGN211Z003		14 44 06.80	-02 50 50.4	5.4	16.50	3.1	0.312	0.0582	4	SF	
TGN149Z119		14 44 16.01	-03 19 22.5	10.3	17.81	2.6		0.0441	4	SF?	
TGN149Z091*		14 44 56.59	-03 12 01.7	9.5	17.05	388.3		0.1060	4	Aae	Extended radio source
TGN149Z039		14 46 00.88	-03 24 07.3	11.5	19.33	28.9		0.1052	4	SF?	Extended radio source – not this ID
TGN282Z198		14 46 48.72	-01 57 31.7	5.3	15.48	2.2		0.0432	4	SF?	
TGN149Z006		14 47 09.80	-03 58 01.3	14.8	17.53	8.3		0.0011	4	star?	
TGN349Z172		14 48 27.53	-00 06 45.2	3.9	19.34	4.2		0.1379	3	SF?	
TGN349Z020		14 49 37.80	+00 50 33.8	4.2	19.22	14.0		0.2116	4	Aa	Extended radio source
TGN349Z005		14 51 03.11	+00 40 58.5	6.2	17.34	4.1		0.0690	4	SF?	
TGS246Z061*		21 43 24.07	-28 45 43.1	10.7	19.23	61.5		0.0735	4	SF	Rejected as ID – see table notes
TGS326Z128		21 43 47.99	-29 28 45.4	5.7	17.86	2.8		0.1336	5	SF	
TGS326Z047*		21 46 36.06	-30 51 41.1	8.7	17.15	2.8		0.0756	5	Ae	
TGS170Z124		21 48 11.37	-27 36 52.2	4.2	19.03	4.6		0.1589	4	Aa	
TGS247Z196		21 48 11.38	-29 07 47.7	8.6	16.93	30.5		0.0728	4	Aa	Extended radio source
TGS170Z094		21 48 54.04	-27 40 34.8	5.6	16.85	4.6		0.0744	4	Aa?	
TGS248Z105		21 50 11.67	-28 59 35.8	4.8	19.28	9.5		1.5000	4	Ae	
TGS248Z210		21 50 48.78	-29 31 37.9	7.2	18.97	3.9		0.1747	4	Aa	
TGS248Z201		21 51 26.22	-29 30 56.0	9.8	19.38	3.1		0.1478	3	SF?	
TGS328Z064		21 51 28.02	-29 37 06.8	5.2	19.02	4.6		0.1765	4	Aa	
TGS248Z072		21 52 02.50	-28 57 19.5	1.4	18.85	67.3		0.2384	4	Aa	
TGS248Z174		21 53 22.92	-29 15 50.2	11.7	16.30	2.7		0.0484	3	??	Bright galaxy – correct ID
TGS248Z170	NGC 7152	21 53 59.00	-29 17 20.5	12.2	14.54	3.2	0.352	0.0219	4	SF	Bright galaxy – correct ID
TGS249Z112		21 55 38.15	-28 42 05.6	1.6	18.98	330.7	0.230	0.2326	4	Aae	
TGS249Z081		21 57 08.36	-28 23 01.8	12.1	18.62	2.6		0.0640	4	SF	
TGS114Z166		21 57 24.08	-25 37 57.1	6.8	18.60	2.4		0.0801	4	Ae?	
TGS172Z232		21 57 46.96	-26 40 09.4	1.9	19.41	2.9		0.0000	5	star	
TGS407Z205*		21 58 08.21	-31 23 49.5	6.2	16.16	3.9	0.558	0.0933	5	Ae	

Table 1. Candidate 2dFGRS/NVSS radio sources (continued).

(1) 2dFGRS name	(2) Other name	(3) Position α (J2000)		(4) Offset (arcsec)	(5) b_J (mag)	(6) $S_{1.4}$ (mJy)	(7) $S_{60\mu m}$ (Jy)	(8) Redshift z	(9) Q	(10) Class	(11) Comments
TGS406Z076		21 58 21.20	-31 45 34.7	6.7	18.79	42.7		0.3147	3	??	Extended radio source
TGS114Z308		21 58 38.46	-26 22 41.0	3.2	16.33	5.3	0.619	0.0710	5	SF	
TGS114Z303		21 58 42.34	-26 10 34.0	1.4	18.86	6.8		0.2082	5	Aa	
TGS172Z095		21 58 49.27	-27 35 09.1	4.1	16.69	3.6		0.0668	3	Aa	
TGS249Z041		21 58 49.92	-28 38 05.6	2.2	18.69	6.5		0.1796	4	Aae	
TGS172Z203		21 58 57.59	-26 47 01.7	7.0	16.70	3.0		0.0708	5	Ae	
TGS172Z202		21 58 57.98	-26 33 42.7	13.6	19.41	6.2		0.1907	3	Aa	
TGS408Z237	NGC 7163	21 59 20.26	-31 52 54.9	4.0	14.13	5.9	1.877	0.0090	3	SF?	
TGS114Z282	ESO 532-007	21 59 31.40	-26 39 36.5	9.1	15.29	3.5	0.422	0.0369	4	SF	
TGS407Z030		21 59 41.84	-32 19 05.1	3.7	17.36	6.7		0.0922	5	Ae?	
TGS249Z155		21 59 49.17	-29 26 36.4	10.6	17.82	7.7		0.0005	3	star	
TGS173Z089		21 59 52.35	-27 31 08.2	5.2	18.50	15.3		0.2052	3	Aa	Extended radio source
TGS114Z094		22 00 04.38	-25 03 54.4	4.3	18.96	117.3		0.1769	4	Aa	Extended radio source
TGS114Z264		22 00 33.95	-25 57 28.8	2.0	17.72	15.6		0.1190	5	Aa	
TGS114Z067		22 00 47.39	-25 24 07.0	2.4	19.34	15.4		0.2394	4	Aa	
TGS114Z055		22 01 07.39	-25 05 49.3	4.0	19.26	9.8		0.2102	4	Aa	
TGS115Z326		22 04 35.58	-25 57 31.7	5.1	19.19	4.5		0.1898	4	Aa	
TGS115Z083		22 05 44.60	-25 47 22.3	4.2	16.39	3.1	0.668	0.0182	4	SF	
TGS115Z271		22 06 49.89	-26 01 43.9	13.0	16.70	3.1	0.331	0.0779	4	SF	Bright galaxy – correct ID
TGS115Z044		22 07 27.40	-25 00 31.4	12.1	19.02	8.9		0.2719	3	??	
TGS174Z232		22 08 09.17	-26 30 38.9	14.9	18.63	25.0		0.1066	4	Aa	Extended radio source – not this ID
TGS061Z036	ESO 533-002	22 13 46.67	-24 20 08.4	2.3	16.06	6.6	0.480	0.0381	4	SF	
TGS061Z289		22 14 26.55	-24 55 32.1	7.7	18.52	7.6		0.0001	5	star	
TGS116Z222		22 14 46.40	-25 21 16.1	0.2	17.92	325.8		0.0870	4	Ae	
TGS062Z304		22 16 00.35	-24 54 10.4	2.8	19.34	6.7		0.0635	5	SF	
TGS062Z278		22 16 18.90	-23 59 46.2	9.7	18.73	3.9	0.265	0.0605	3	??	
TGS063Z351		22 16 34.73	-24 21 36.6	0.6	19.39	66.9			2	??	Extended radio source
TGS062Z230		22 16 52.65	-24 34 51.0	4.6	19.13	4.5		0.2598	4	Aa	
TGS063Z327		22 18 07.15	-24 12 52.6	4.2	16.99	4.1	0.542	0.0270	5	SF	
TGS063Z315		22 18 35.32	-24 10 28.5	6.7	17.69	9.0		0.0906	4	??	Extended radio source
TGS063Z307		22 18 47.24	-23 59 16.0	2.8	16.15	4.6	0.765	0.0354	5	Ae	
TGS063Z211		22 20 15.31	-24 26 04.6	2.1	17.41	21.6		0.1145	4	??	
TGS063Z188	NGC 7252	22 20 44.82	-24 40 37.7	4.5	14.39	25.3	3.975	0.0161	5	SF?	Extended radio source
TGS063Z148		22 21 35.21	-24 28 47.9	4.2	16.69	2.7	0.231	0.0316	4	SF?	
TGS063Z006	ESO 533-020	22 22 32.46	-23 31 29.5	10.5	16.30	5.9		0.0388	5	Aa	
TGS178Z179		22 22 49.47	-26 56 45.5	3.5	19.16	3.7			2	??	
TGS178Z172		22 23 28.83	-27 00 03.2	5.4	17.57	6.5	1.754	0.1314	5	SF	
TGS118Z241	ESO 533-024	22 23 42.39	-26 36 46.1	8.7	14.01	4.9		0.0253	4	Aa?	
TGS179Z073	ESO 467-056	22 25 25.79	-27 42 05.4	8.6	15.75	7.6		0.0513	5	SF	
TGS064Z326	ESO 533-026	22 25 33.94	-24 14 29.1	12.3	14.76	3.2	0.437	0.0259	4	SF	Bright galaxy – correct ID

Table 1. Candidate 2dFGRS/NVSS radio sources (continued).

(1) 2dFGRS name	(2) Other name	(3) Position α (J2000) δ		(4) Offset (arcsec)	(5) b_J (mag)	(6) $S_{1.4}$ (mJy)	(7) $S_{60\mu m}$ (Jy)	(8) Redshift z	(9) Q	(10) Class	(11) Comments
TGS064Z302	ESO 533-027	22 25 56.05	-24 43 50.1	3.4	14.98	4.0	0.513	0.0360	5	SF	
TGS179Z208		22 26 04.01	-26 45 26.8	0.1	19.14	25.7		0.2502	5	Aa	Extended radio source
TGS064Z269	ESO 533-028	22 26 39.34	-24 52 17.7	8.3	14.07	4.9	0.857	0.0089	5	SF	
TGS179Z031		22 26 53.38	-27 18 22.5	6.3	19.22	9.0		0.2072	5	Aa	
TGS256Z126		22 26 56.42	-29 01 25.9	12.7	17.91	3.2		0.0512	3	??	
TGS179Z029		22 26 57.58	-27 26 32.6	6.5	19.19	2.5		0.1612	4	Aa	
TGS119Z132		22 27 57.66	-25 29 11.8	12.9	18.98	12.6		0.0904	5	SF	
TGS256Z001		22 28 12.74	-28 34 05.7	11.5	19.27	5.2		0.0918	4	??	
TGS064Z194		22 28 13.21	-24 42 09.7	14.7	18.66	8.8			2	??	
TGS119Z122*		22 28 31.03	-25 07 53.6	2.4	16.59	11.7		0.0090	5	SF	
TGS064Z009		22 28 39.38	-23 38 19.6	3.8	18.02	7.8		0.0930	4	Aa	
TGS064Z158		22 28 42.85	-25 22 47.5	1.2	19.26	23.0		0.2094	4	Aa	Extended radio source
TGS064Z145		22 28 46.94	-23 57 10.6	4.4	16.42	15.6		0.0643	5	Aa	Extended radio source
TGS064Z003		22 29 28.59	-23 44 06.4	4.7	16.50	2.2		0.0557	5	SF	
TGS064Z093		22 30 02.45	-24 24 00.6	11.0	19.20	2.9		0.2002	5	Aa	
TGS119Z087		22 30 07.11	-24 58 22.2	12.2	14.92	4.2		0.0314	5	SF	Bright galaxy – correct ID
TGS119Z231		22 31 06.50	-25 54 42.4	0.7	19.36	27.5		0.2874	4	Aa	Extended radio source
TGS119Z216		22 31 43.13	-26 15 52.3	7.8	19.37	4.3		0.1616	4	Aa	
TGS180Z083	ESO 468-007	22 31 44.90	-27 18 06.2	8.0	16.26	3.8		0.0279	4	SF?	
TGS180Z179		22 32 26.31	-27 10 15.5	9.6	16.00	4.7	0.511	0.0400	4	SF	
TGS119Z026		22 32 26.99	-25 25 35.1	11.6	16.04	3.1	0.434	0.0365	4	SF	Bright galaxy – correct ID
TGS180Z060		22 32 55.81	-28 07 12.3	4.4	19.03	3.4	0.312	0.2445	4	SF	
TGS180Z144		22 34 05.61	-27 11 21.5	11.6	17.42	2.6	0.296	0.1291	4	Ae	
TGS180Z028		22 34 34.93	-27 29 11.2	2.7	16.39	5.3		0.0398	4	Ae	
TGS120Z091		22 34 47.27	-26 47 07.7	3.3	15.38	2.6		0.0401	5	Ae	
TGS180Z007		22 36 07.23	-27 43 30.5	11.3	15.31	3.2	0.315	0.0280	4	Ae?	Bright galaxy – correct ID
TGS181Z210		22 36 54.21	-26 56 45.9	3.8	16.31	8.5	0.844	0.0424	4	SF	
TGS181Z209		22 37 01.37	-26 50 07.6	2.8	17.07	14.9		0.0856	4	Ae	
TGS258Z046	ESO 468-019	22 37 47.06	-28 12 38.4	10.0	16.20	3.9		0.0285	4	SF	
TGS258Z139		22 38 24.98	-29 23 39.5	10.0	19.21	4.1		0.0861	4	??	
TGS182Z115		22 41 44.03	-28 14 58.2	2.2	17.93	10.6		0.0909	4	Ae?	
TGS259Z022		22 45 50.21	-28 17 59.5	10.0	18.19	8.7		0.0796	4	SF	
TGS182Z037	ESO 468-026	22 45 54.76	-28 02 57.5	4.1	15.27	5.8	0.907	0.0288	4	SF	
TGS183Z082		22 48 08.68	-27 46 05.8	11.8	19.27	7.9		0.1713	4	Aa	
TGS261Z044		22 48 38.86	-28 04 01.0	3.8	18.18	28.3		0.1716	4	Aa	Extended radio source
TGS184Z265		22 51 00.35	-27 04 03.2	5.0	17.24	5.6	0.817	0.0420	4	SF	
TGS183Z161		22 51 43.51	-27 49 02.8	7.6	18.13	4.7		0.0793	4	Aae	
TGS183Z158		22 51 44.86	-27 49 01.5	10.6	18.14	4.7			1	??	
TGS183Z179		22 52 01.97	-27 02 40.5	10.7	17.43	4.0		0.0794	4	SF?	
TGS184Z119		22 54 11.80	-27 47 43.9	11.6	18.68	20.6		0.2043	4	??	Extended radio source – not this ID

Table 1. Candidate 2dFGRS/NVSS radio sources (continued).

(1) 2dFGRS name	(2) Other name	(3) Position α (J2000)		(4) Offset (arcsec)	(5) b_J (mag)	(6) $S_{1.4}$ (mJy)	(7) $S_{60\mu m}$ (Jy)	(8) Redshift z	(9) Q	(10) Class	(11) Comments
TGS184Z238*		22 54 19.08	-26 54 58.2	2.5	18.39	35.1		0.1675	4	Aae	Extended radio source
TGS184Z099		22 54 39.85	-27 34 06.5	5.1	17.90	5.1		0.1032	4	Ae	
TGS184Z052		22 56 21.57	-27 28 28.7	2.0	19.40	3.0		0.2677	4	Aa	
TGS185Z115		22 58 01.41	-27 14 48.8	3.1	18.83	3.1		0.0970	5	Ae	
TGS185Z252		22 58 37.00	-26 40 42.6	11.0	17.96	4.1		0.1997	4	Aa	
TGS185Z224		22 59 37.56	-26 44 53.3	10.9	18.35	3.6		0.1726	4	Aa	
TGS186Z238		23 00 14.95	-27 03 54.7	13.2	19.30	4.1		0.2473	3	??	
TGS186Z139		23 01 43.66	-28 04 34.2	8.5	18.95	8.9		0.2495	4	??	
TGS190Z162		23 18 32.12	-27 08 31.2	3.5	16.79	40.9		0.0832	5	Aa	Extended radio source
TGS190Z106*		23 19 56.14	-27 29 53.5	12.0	18.46	863.7		0.0657	5	SF	Rejected as ID – see table notes
TGS190Z090		23 20 40.78	-27 31 29.6	3.0	17.71	30.7		0.1396	5	Aa	Extended radio source
TGS190Z081*		23 21 13.82	-27 24 49.4	2.2	18.73	44.0		0.2318	4	Aa	Triple radio source
TGS190Z070		23 21 38.55	-27 33 08.4	7.7	17.24	2.9		0.0528	5	SF	
TGS269Z090		23 26 11.26	-28 17 02.5	2.7	19.16	80.5		0.1547	4	Aa	
TGS191Z059		23 28 47.13	-27 16 15.6	1.7	16.01	4.7		0.0321	4	SF	
TGS191Z036		23 29 29.75	-27 47 53.6	7.3	16.96	138.7		0.1080	5	Aa	Extended radio source
TGS192Z247		23 31 36.96	-26 48 56.9	6.8	19.18	3.3		0.1864	4	Aa	
TGS192Z195		23 33 44.05	-27 04 34.9	5.7	17.78	3.9		0.1127	4	SF?	
TGS192Z053*		23 34 00.90	-27 43 00.6	10.5	18.33	65.1		0.1161	3	Aa	Extended radio source – correct ID
TGS193Z242*	ESO 536-010	23 36 49.47	-26 59 26.5	3.1	15.28	9.4		0.0293	4	SF	
TGS194Z144		23 43 41.48	-28 11 50.2	10.7	15.93	5.4		0.0536	5	Aa	Bright galaxy – correct ID
TGS194Z140		23 43 52.77	-27 28 21.7	6.8	19.27	6.9		0.2101	4	Aa	
TGS131Z292		23 46 21.25	-26 50 30.9	10.1	16.99	2.9		0.0538	5	SF	Bright galaxy – correct ID
Additional galaxies											
TGS312Z191	ESO 416-002	02 35 13.41	-29 36 16.6		15.60	249.4		0.0596	5	Ae	Extended radio source
TGS312Z045	MRC 0234-287	02 37 01.50	-28 34 53.1		18.79	283.2		0.1445	5	Aa	Double radio source
TGS467Z186	IC 1858	02 49 08.32	-31 17 19.2		14.85	132.8		0.0203	4	Aa	Extended radio source
TGS398Z220	PKS 0307-305	03 10 01.49	-30 19 40.7		16.42	1064.5		0.0684	5	Ae	Double radio source
TGS241Z299	MRC 0312-271	03 16 04.01	-26 58 06.7		17.99	489.3		0.2186	3	??	Double radio source
TGN420Z160	PKS 0956+015	09 59 20.78	+01 17 51.9		16.77	514.4		0.0976	5	Aa	Extended radio source
TGN307Z092*	CGCG 012-43	11 37 27.49	-00 50 47.7		16.63	134.9		0.0465	4	Aa	Extended, diffuse radio source
TGS061Z183	PKS 2206-251	22 09 22.93	-24 53 33.3		19.12	865.1		0.1588	4	Ae	Double radio source
TGS190Z105	PKS 2317-27	23 19 56.28	-27 28 10.7		17.85	3022.5		0.1741	4	Ae	Double radio source

Table 1. 2dFGRS/NVSS radio sources (continued).

Notes to Table 1:

N.B. Objects are listed in numerical order by object name, with northern objects (TGN) first, then southern ones (TGS).

TGN109Z024: See TGN190Z025 below.

TGN190Z025: This galaxy and TGN 190Z024 lie in the same cluster. There is a complex radio structure (see Figure) with peaks close to both these galaxies. For now, we assume that both are radio sources. Higher-resolution radio observations would be valuable.

TGN110Z073: Interacting galaxy pair.

TGN124Z197: Quoted radio flux density is the sum of three NVSS components.

TGN135Z197: This galaxy is within 30 arcsec of the 15.2 mag. galaxy NGC 5039. Some or all of the radio emission probably arises from NGC 5039 (which is also an IRAS source with a 60 μ m flux density of 0.353 Jy) rather than TGN135Z197.

TGN137Z043: Identified as an ultraluminous IRAS galaxy by Clowes et al. (1995), who note that it has a Seyfert 2 optical spectrum.

TGN149Z091: Quoted radio flux density is the sum of two NVSS components.

TGN156Z046: Galaxy with Galactic star superimposed, redshift remeasured from 2dF spectrum.

TGN165Z119: Seyfert 1 galaxy (broad Balmer emission lines).

TGN165Z189: Interacting galaxy pair.

TGN171Z312: Quoted flux density is the sum of five NVSS components.

TGN207Z146: This is a QSO at redshift 3.0.

TGN284Z051: Quoted flux density is the sum of two NVSS components.

TGN286Z081: Interacting galaxy pair.

TGN299Z119: Another faint galaxy is closer to the radio centroid.

TGN304Z086: Redshift is from repeat 2dFGRS spectrum taken in Dec 1999.

TGN306Z194: Paired with TGN306Z196, which is also detected by NVSS.

TGN306Z196: Paired with TGN306Z194, which is also detected by NVSS.

TGN307Z090: Unusual, very diffuse source. TGN307Z092 is a more likely ID. Quoted flux density is the sum of four NVSS components.

TGN314Z018: ROSAT X-ray detection.

TGN318Z080: Quoted radio flux density is the sum of three NVSS components.

TGN348Z183: Quoted radio flux density is the sum of two NVSS components.

TGN401Z254: ROSAT X-ray detection. Quoted radio flux density is the sum of four NVSS components.

TGN402Z029: See TGN402Z030.

TGN402Z030: With TGN402Z029, interacting galaxy pair Arp 240 (NGC 5257/5258) — total IRAS flux density at 60 μ m is 9.297 Jy.

We have assumed that half of this comes from each galaxy.

TGN422Z122: Quoted radio flux density is the sum of three NVSS components.

TGS119Z122: This source has a flux density of only 11.7 mJy in the NVSS catalogue, but the Parkes catalogue lists it as 230 mJy at 2.7 GHz. The Parkes source may be very diffuse and largely resolved out by the NVSS, or possibly time-varying. Further investigation is needed.

TGS184Z238: Quoted radio flux density is the sum of three NVSS components.

TGS190Z081: Quoted radio flux density is the sum of three NVSS components.

TGS190Z106: The radio source is a lobe of PKS 2317-27, and the correct optical ID is the galaxy TGS190Z105 at z=0.1730.

TGS192Z053: Quoted radio flux density is the sum of two NVSS components.

TGS193Z242: Interacting pair of galaxies.

Table 1. 2dFGRS/NVSS radio sources (continued).

- TGS209Z078: The original 2dFGRS position corresponds to a blob in the spiral arm of the bright spiral ESO 411-011.
The position and magnitude given here are for ESO 411-011.
- TGS210Z106: Radio emission extends to south and overlaps spiral companion TGS210Z108 ($z=0.0401$).
- TGS221Z095: Starburst galaxy with unusual optical tail
- TGS223Z232: Quoted radio flux density is the sum of three NVSS components.
- TGS232Z027: The original 2dFGRS position corresponds to a knot in the spiral arm of the bright spiral IC 1826.
The position and magnitude given here are for IC 1826.
- TGS234Z274: Another (faint) galaxy is closer to the radio centroid.
- TGS235Z101: Radio overlay confirms that this galaxy is the correct ID in spite of 11.1 arcsec offset.
- TGS239Z227: The redshift is taken from NED, not the (poor-quality) 2dFGRS spectrum.
- TGS246Z061: Radio overlay suggests that the correct ID is the 18th magnitude galaxy TGS246Z062 at $z=0.1723$.
This second galaxy was observed by the 2dFGRS in October 1999, so is not included in the current data set.
- TGS312Z171: There is another, fainter galaxy closer to the radio centroid.
- TGS326Z047: Seyfert 1 galaxy (broad Balmer emission lines). ROSAT X-ray detection.
- TGS397Z2016: Strong, broad emission lines.
- TGS407Z205: Seyfert 1 galaxy, broad Balmer wings. ROSAT X-ray detection.

This figure "fig5.gif" is available in "gif" format from:

<http://arxiv.org/ps/astro-ph/0106173v2>

This figure "fig7_8.gif" is available in "gif" format from:

<http://arxiv.org/ps/astro-ph/0106173v2>

Table 1. Candidate 2dFGRS/NVSS radio sources.

(1) 2dFGRS name	(2) Other name	(3) Position α (J2000) δ		(4) Offset (arcsec)	(5) b_J (mag)	(6) $S_{1.4}$ (mJy)	(7) $S_{60\mu m}$ (Jy)	(8) Redshift z	(9) Q	(10) Class	(11) Comments
TGS203Z262		00 16 41.06	-26 51 18.2	6.7	15.37	4.8		0.0560	4	Aa	
TGS202Z238		00 17 15.53	-26 39 29.2	0.9	18.12	90.5		0.1390	5	Aa	
TGS202Z085		00 17 38.37	-27 22 15.3	2.1	18.68	6.4		0.1516	4	Aa	
TGS204Z164		00 20 35.49	-27 51 44.6	0.9	19.41	57.7			2	??	
TGS203Z189		00 20 55.14	-26 35 06.7	14.9	18.66	10.2		0.2283	4	Aa	Extended radio source – correct ID
TGS203Z019		00 22 01.41	-27 33 23.0	2.5	18.86	85.1		0.2358	4	Aa	Extended radio source
TGS204Z102		00 23 47.45	-27 56 14.4	1.8	16.79	3.2		0.0759	4	Aa	
TGS204Z037		00 25 54.06	-27 23 30.4	1.8	19.41	54.0		0.2643	4	Aae	Extended radio source
TGS205Z218		00 29 06.95	-27 05 36.9	12.2	16.26	2.5		0.0626	4	Aa	
TGS206Z164	ESO 410-013	00 29 55.72	-27 29 50.6	8.8	14.58	2.9	0.293	0.0255	4	SF	
TGS206Z130		00 32 43.30	-27 47 04.0	13.3	19.22	2.7		0.1484	4	Aa	
TGS206Z038		00 35 43.58	-27 38 05.2	0.9	19.15	203.4		0.2424	4	Aa	Extended radio source
TGS206Z015		00 36 00.35	-27 15 34.0	1.2	17.44	11.3	4.294	0.0700	4	SF	
TGS207Z011	ESO 410-024	00 36 27.41	-27 47 07.0	0.2	14.19	55.0		0.0355	4	Ae	
TGS206Z005	ESO 410-025	00 36 37.33	-27 47 20.8	11.8	15.23	3.7	0.217	0.0246	4	SF	Bright galaxy – correct ID
TGS284Z002		00 36 46.92	-28 12 07.0	3.7	17.66	7.6		0.0988	4	Aa	
TGS206Z183		00 37 17.04	-27 52 35.8	11.4	19.44	2.9		0.2402	4	Aa	
TGS208Z145	ESO 411-003	00 39 18.28	-27 20 58.8	5.2	14.09	4.7	0.597	0.0229	4	SF	
TGS207Z112		00 40 23.20	-27 58 38.2	4.4	16.94	3.0		0.1084	3	SF?	
TGS208Z104		00 41 10.99	-27 51 06.5	0.9	19.05	16.3		0.2521	4	Aa	Extended radio source
TGS209Z223		00 45 20.11	-26 57 27.0	0.4	16.98	8.7		0.1211	4	Aae	
TGS209Z218	IC 1579	00 45 32.41	-26 33 55.2	2.1	14.01	4.1	0.240	0.0226	4	SF	
TGS288Z075		00 46 32.75	-28 20 54.0	3.2	17.86	2.5		0.1935	4	Ae	
TGS209Z078*	ESO 411-011	00 46 40.74	-27 53 54.5	6.0	15.89	3.5		0.0603	4	Aae?	
TGS209Z156		00 50 40.29	-27 04 40.0	1.1	18.47	6.4	1.134	0.1289	4	SF	
TGS210Z205		00 51 21.18	-26 59 21.7	4.8	16.05	4.8		0.0743	4	Aa	
TGS210Z106*		00 52 15.01	-27 19 41.2	3.3	15.07	12.7		0.0400	4	SF	Extended radio source
TGS210Z188		00 53 08.98	-27 08 11.5	7.6	18.98	17.7		0.1454	4	Aae?	Extended radio source
TGS210Z184	ESO 474-039	00 53 43.41	-27 02 59.1	2.7	14.45	15.4	1.423	0.0183	4	SF	Extended radio source
TGS211Z2020		00 58 52.32	-28 18 11.7	1.8	15.55	3.1	0.377	0.0577	4	SF	
TGS212Z241		00 58 53.43	-26 59 50.3	10.4	16.83	3.4	0.260	0.1064	4	SF	Bright galaxy – correct ID
TGS212Z217		01 01 48.13	-26 42 41.8	13.7	19.14	2.6		0.1886	4	Aa	
TGS212Z209		01 02 15.31	-26 33 21.9	7.1	19.14	3.1		0.2241	4	Aa	
TGS212Z069	ESO 412-003	01 03 46.31	-27 45 13.3	4.4	15.11	7.6	0.542	0.0176	4	SF	
TGS292Z076		01 05 27.33	-28 10 55.1	14.0	18.84	10.9		0.1882	4	Aa?	
TGS212Z046		01 05 31.65	-27 29 43.4	7.2	18.24	3.0		0.1105	4	Aa	
TGS213Z017		01 11 19.84	-27 52 49.1	12.1	18.90	5.7	0.199	0.1312	3	??	
TGS214Z124		01 12 49.62	-27 54 41.8	13.5	17.62	5.0		0.1118	4	Aa?	
TGS215Z175		01 14 21.04	-27 18 45.3	3.8	18.80	98.1			2	??	Extended radio source
TGS215Z170		01 14 48.43	-28 01 17.8	1.4	18.77	23.5			2	??	

Table 1. Candidate 2dFGRS/NVSS radio sources (continued).

(1) 2dFGRS name	(2) Other name	(3) Position α (J2000) δ		(4) Offset (arcsec)	(5) b_J (mag)	(6) $S_{1.4}$ (mJy)	(7) $S_{60\mu m}$ (Jy)	(8) Redshift z	(9) Q	(10) Class	(11) Comments
TGS147Z223		01 15 10.10	-26 32 20.7	3.6	16.17	8.0	0.722	0.0437	4	SF	
TGS294Z018		01 16 12.91	-28 19 29.4	6.7	18.76	49.8		0.1912	3	Aa	Extended radio source, in cluster
TGS294Z015		01 16 18.14	-28 19 35.9	10.4	19.01	16.7		0.0491	2	??	Extended radio source – not this ID
TGS215Z136		01 17 14.93	-28 23 48.4	4.9	19.07	9.5		0.2270	3	Aa	Extended radio source
TGS215Z268		01 22 07.72	-27 05 24.3	14.7	19.03	4.0		0.1747	3	SF?	
TGS296Z220		01 23 55.37	-28 23 21.4	6.1	16.55	2.9	0.222	0.0532	4	SF	
TGS216Z098		01 25 11.01	-27 14 48.7	3.9	14.94	4.1		0.0315	4	SF?	
TGS217Z254		01 25 13.32	-26 52 24.6	8.6	19.23	3.3		0.1992	3	Aa?	
TGS217Z075		01 27 13.98	-27 57 05.5	2.0	18.91	10.8		0.2254	4	Aa	
TGS217Z058		01 27 44.01	-27 51 54.2	8.3	19.02	19.0		0.2487	3	Aa	
TGS218Z173		01 28 17.22	-27 15 22.0	3.4	18.58	8.9		0.0914	4	Ae	
TGS218Z314		01 29 44.55	-27 05 49.6	10.4	19.30	2.6		0.1183	3	Aa?	
TGS217Z161		01 30 13.06	-27 02 50.6	4.6	16.13	2.7		0.0702	4	SF	
TGS217Z158	ESO 476-016	01 30 26.05	-26 46 49.6	3.4	14.35	2.5	0.415	0.0207	4	SF	
TGS217Z157		01 30 29.61	-27 01 31.1	1.6	19.09	46.7		0.2067	3	Aa	Extended radio source
TGS217Z013	ESO 413-008	01 30 49.18	-27 21 51.1	4.1	15.31	9.5	1.594	0.0191	4	SF	Extended radio source
TGS149Z251	ESO 476-018	01 31 14.05	-26 51 31.8	3.1	15.43	4.2		0.0192	4	Aa	
TGS219Z156		01 33 10.67	-27 36 49.5	13.5	19.16	2.5		0.2208	4	SF	
TGS219Z142		01 33 56.60	-27 31 45.3	7.3	17.06	8.5		0.1245	4	Aa	
TGS218Z048		01 34 55.76	-28 10 14.3	3.2	19.16	4.6		0.1544	3	??	
TGS219Z089		01 35 04.98	-27 17 48.5	4.5	18.67	59.7		0.2497	4	Aa	Extended radio source
TGS220Z128		01 37 51.18	-28 05 55.4	6.7	18.91	3.2		0.1306	4	Ae	
TGS220Z098	ESO 413-015	01 39 57.11	-27 57 21.5	12.4	15.49	2.8		0.0564	4	Aae	Bright galaxy – correct ID
TGS220Z097	ESO 413-018	01 40 00.45	-28 02 05.8	3.0	14.27	5.4	0.953	0.0204	4	SF	
TGS221Z290		01 42 20.90	-27 07 05.6	5.1	19.06	7.7		0.2480	4	Aa	Extended radio source
TGS220Z022		01 42 50.10	-27 50 04.3	2.8	15.62	6.4	0.574	0.0575	4	SF	
TGS220Z015		01 43 20.67	-27 17 47.5	0.8	19.32	12.5		0.2630	4	Aae	
TGS220Z009		01 43 58.99	-27 28 14.2	7.9	18.69	3.1		0.2306	4	Aae	
TGS222Z152		01 48 04.71	-28 03 24.2	13.5	19.24	16.7		0.1265	3	??	Extended radio source
TGS222Z279		01 49 00.81	-27 04 48.8	5.1	15.54	8.2		0.0292	4	SF	
TGS221Z095*	ESO 414-004	01 49 30.60	-27 42 01.5	10.6	15.99	8.0	0.775	0.0301	5	SF	Extended radio source – correct ID
TGS455Z184		01 49 54.33	-31 58 42.4	4.5	17.58	5.7		0.1486	4	Aa	
TGS222Z113		01 49 56.51	-27 49 07.5	7.7	15.48	9.2		0.0439	4	SF	Extended radio source, galaxy pair
TGS221Z089	ESO 414-006	01 49 57.12	-27 46 42.2	4.4	15.03	13.7	1.051	0.0431	5	SF	
TGS456Z002		01 49 57.35	-32 15 47.8	4.6	18.38	10.9		0.1742	3	Aa	
TGS456Z001		01 50 07.17	-32 26 44.1	2.1	16.11	10.5	1.603	0.0378	4	SF?	Extended radio source
TGS456Z091		01 51 01.79	-32 41 14.4	6.9	18.75	3.7		0.1515	4	Aa	
TGS222Z203		01 52 01.66	-26 46 57.6	4.5	19.12	3.6		0.1055	3	SF?	
TGS222Z196		01 52 18.38	-27 05 54.4	8.0	19.13	2.5			2	??	
TGS456Z184		01 52 19.74	-31 32 28.4	5.8	18.31	7.6		0.0002	4	star	

Table 1. Candidate 2dFGRS/NVSS radio sources (continued).

(1) 2dFGRS name	(2) Other name	(3) Position α (J2000)	(4) Offset (arcsec)	(5) b_J (mag)	(6) $S_{1.4}$ (mJy)	(7) $S_{60\mu m}$ (Jy)	(8) Redshift z	(9) Q	(10) Class	(11) Comments
TGS153Z268		01 52 51.36 -26 50 50.9	3.1	17.75	4.5		0.1323	4	Aae?	
TGS223Z156		01 53 11.83 -27 49 07.3	3.2	18.79	48.4			1	??	Extended radio source
TGS223Z266		01 53 50.65 -26 50 36.3	12.4	18.95	3.2			2	??	
TGS222Z177		01 53 58.35 -27 13 37.9	13.8	19.39	3.0		0.2442	3	Ae	
TGS153Z214		01 54 21.43 -26 56 20.3	8.3	19.01	32.1		0.2079	3	Aa	Extended radio source
TGS456Z123		01 55 08.10 -31 57 41.7	7.6	18.27	7.8		0.1503	3	??	Extended radio source
TGS223Z244		01 55 27.82 -26 30 03.7	3.2	18.62	10.8		0.1482	3	Aa?	Extended radio source
TGS223Z238		01 55 31.97 -26 40 18.0	2.2	17.37	3.1	0.416	0.0829	4	SF	
TGS223Z232*		01 55 46.33 -26 54 04.8	2.3	18.95	27.0		0.2095	3	Aa	Triple radio source
TGS224Z149		01 57 00.95 -27 31 34.1	10.7	17.45	23.4		0.1539	4	Aa	Extended radio source – correct ID
TGS223Z205		01 57 26.55 -27 00 35.0	3.6	16.76	2.8		0.0301	4	SF	
TGS223Z066		01 57 26.75 -27 57 39.1	1.8	18.16	2.9	0.295	0.0822	4	SF	
TGS224Z121		01 58 20.67 -28 11 41.5	2.2	17.99	7.2		0.1360	4	Aa	
TGS223Z022	ESO 414-018	01 58 42.43 -27 57 04.4	13.2	15.54	3.3	0.278	0.0583	4	SF?	Bright galaxy – correct ID
TGS224Z246		02 04 02.12 -27 06 57.5	3.0	17.83	3.4		0.1139	5	Aa	
TGS311Z013		02 31 05.08 -28 03 31.4	4.9	19.05	13.2		0.2171	5	Aa	Extended radio source
TGS311Z207		02 31 52.46 -28 59 57.1	13.6	19.31	25.9		0.1455	3	Aa	
TGS391Z166	ESO 416-001	02 32 33.94 -29 41 43.6	1.6	15.58	24.5	2.842	0.0171	4	SF	
TGS391Z127		02 34 00.19 -30 28 40.7	12.9	18.79	18.0		0.0615	4	SF	Double radio source – not this ID
TGS312Z212		02 34 15.55 -29 13 16.6	2.2	18.86	80.1		0.2037	3	??	Extended radio source
TGS312Z107		02 34 29.98 -28 40 18.7	6.1	19.32	188.1		0.2185	3	Aa	Extended radio source
TGS312Z194		02 35 14.30 -29 50 46.8	0.8	19.19	9.0		0.1986	4	Aa	
TGS312Z186		02 35 19.90 -29 09 50.9	4.4	18.66	44.7		0.1468	4	Ae	
TGS312Z171*		02 36 06.53 -29 07 38.0	14.5	19.21	10.2		0.1763	4	SF	Extended radio source – not this ID
TGS232Z060		02 36 32.03 -28 18 22.1	7.6	16.84	3.2	0.324	0.0590	4	SF	
TGS233Z122		02 36 40.56 -27 23 13.6	13.0	18.85	3.3		0.0869	4	Aa	
TGS232Z156		02 38 04.97 -27 13 52.0	5.6	19.28	6.1		0.2446	4	Aa	
TGS232Z027*	IC 1826	02 39 03.62 -27 26 33.6	6.3	13.20	9.8	2.229	0.0046	4	SF	Extended radio source
TGS233Z084		02 39 14.78 -27 37 17.1	7.6	18.40	3.8		0.0648	4	Ae	
TGS233Z202		02 39 55.19 -27 01 41.8	4.4	17.95	7.4			0	??	
TGS233Z196		02 40 07.88 -27 05 41.8	7.2	18.32	2.2		0.1030	4	Aa	
TGS312Z004		02 40 12.64 -28 27 01.5	3.0	19.22	3.5		0.1921	4	Aa	
TGS233Z189		02 40 36.80 -26 52 17.5	9.9	18.87	44.0		0.1572	4	??	
TGS234Z274*		02 41 12.13 -27 07 00.5	11.1	17.80	17.7		0.1097	4	Aa	Extended radio source – not this ID
TGS313Z100		02 41 23.41 -28 30 24.0	7.9	17.07	17.0		0.1474	4	Aae	Extended radio source
TGS313Z081		02 41 56.21 -28 38 35.9	4.2	17.73	105.8		0.1220	4	Aae	Extended radio source
TGS234Z066		02 43 59.58 -27 45 42.7	1.8	18.90	25.2		0.1512	4	Ae	
TGS234Z197		02 44 02.30 -26 50 07.9	6.1	17.92	21.1		0.1092	4	Aa	Extended radio source
TGS314Z129		02 44 22.99 -28 25 23.3	11.7	19.39	2.6		0.2389	4	Aa	
TGS234Z186		02 44 31.03 -26 33 56.8	7.4	18.00	4.6		0.1393	4	Aa	

Table 1. Candidate 2dFGRS/NVSS radio sources (continued).

(1) 2dFGRS name	(2) Other name	(3) Position α (J2000) δ		(4) Offset (arcsec)	(5) b_J (mag)	(6) $S_{1.4}$ (mJy)	(7) $S_{60\mu m}$ (Jy)	(8) Redshift z	(9) Q	(10) Class	(11) Comments
TGS314Z122		02 44 59.86	-29 02 05.5	0.9	17.71	98.1		0.1440	4	Aa	Extended radio source
TGS314Z116		02 45 15.33	-28 45 21.0	5.3	19.31	8.2		0.2355	4	Aa	Extended radio source
TGS520Z069		02 45 24.54	-33 53 14.0	1.3	17.97	22.8		0.1541	4	Aae?	
TGS520Z068		02 45 29.39	-33 25 48.9	9.8	19.11	3.7		0.2138	4	Aa	
TGS314Z110		02 45 35.74	-28 41 40.2	3.0	17.41	5.1		0.0820	4	Aa	
TGS234Z027	IC 1845	02 45 37.07	-27 57 38.3	2.3	14.49	9.5	1.079	0.0235	4	SF	
TGS235Z125	ESO 416-016	02 45 58.40	-28 16 10.5	2.6	14.76	9.6	0.932	0.0243	4	SF	
TGS314Z092		02 46 35.70	-28 55 38.1	3.1	19.17	13.2		0.2134	4	Aa	
TGS234Z163		02 46 35.92	-27 00 05.2	10.3	16.86	4.3		0.0251	4	SF	Bright galaxy – correct ID
TGS235Z101*		02 47 05.18	-27 32 36.4	11.1	17.47	81.2		0.1340	4	Aa	Extended radio source – correct ID
TGS521Z353		02 47 25.13	-34 03 09.6	14.5	18.52	2.9		0.1075	4	Aa?	
TGS578Z085		02 47 37.80	-34 15 04.7	3.7	18.46	2.8		0.1811	4	Aa	
TGS235Z069		02 47 39.84	-27 25 12.9	11.7	18.17	3.8		0.2306	4	Aa	
TGS521Z351		02 47 55.22	-34 01 18.5	3.2	18.99	197.7		0.2473	4	Aa	Extended radio source
TGS160Z339		02 48 10.58	-26 33 32.6	1.4	18.64	7.1		0.1186	4	Aa	
TGS314Z038		02 48 11.58	-28 40 18.7	1.2	18.68	3.7		0.1034	4	SF	
TGS394Z119		02 48 32.56	-29 41 43.4	0.7	17.95	58.8		0.0811	4	Ae	Extended radio source
TGS236Z095	ESO 416-024	02 48 42.08	-27 27 38.3	1.8	15.38	4.6	0.558	0.0237	4	SF	
TGS467Z191	IC 1859	02 49 03.88	-31 10 22.7	1.1	14.17	18.3	0.828	0.0200	4	SF	Extended radio source
TGS236Z091		02 49 07.73	-28 04 22.3	4.7	16.99	3.3	0.250	0.0552	4	SF	
TGS521Z210		02 49 26.93	-32 53 10.7	1.9	17.11	12.3		0.0991	4	Aa	
TGS394Z089		02 49 48.32	-30 23 11.9	1.6	18.74	3.5		0.1878	4	Aa	
TGS521Z174		02 50 00.58	-33 24 15.7	11.1	18.74	2.6		0.2006	4	Aa	
TGS236Z065		02 50 46.97	-27 19 28.6	2.3	17.62	9.8		0.1420	4	Aa	Extended radio source
TGS521Z145		02 50 53.94	-33 45 59.9	9.5	18.67	3.3		0.1829	4	Aa	
TGS579Z274		02 50 59.58	-34 06 02.8	6.0	18.24	2.2		0.0981	4	Aa	
TGS236Z194	ESO 480-005	02 51 08.62	-26 56 49.1	4.7	15.54	4.0	0.489	0.0237	4	SF	
TGS161Z131		02 51 09.40	-25 24 19.9	13.7	18.33	2.9		0.1069	4	Aa	
TGS315Z064	ESO 416-037	02 51 18.32	-28 11 57.8	6.0	14.91	16.9	1.557	0.0177	4	SF	Extended radio source
TGS161Z120		02 51 26.95	-25 16 40.1	9.5	18.67	3.7		0.1555	4	??	
TGS315Z038		02 52 09.54	-28 17 28.2	3.2	17.24	63.5		0.1366	5	Aa	Extended radio source
TGS521Z091		02 52 21.42	-33 33 39.2	7.8	18.81	3.9		0.1093	3	Aa?	
TGS162Z116		02 52 21.44	-25 48 33.6	4.6	19.01	6.2		0.2361	4	Aa	
TGS394Z023	ESO 416-040	02 52 27.10	-30 46 35.8	3.9	14.24	7.9	0.343	0.0230	4	SF	Extended radio source
TGS236Z171		02 52 43.46	-27 17 33.7	3.7	18.49	7.0		0.1648	4	Aa	
TGS236Z167		02 52 59.27	-26 45 37.9	0.8	16.98	84.3		0.0898	5	Ae	
TGS521Z059		02 53 06.51	-33 28 04.4	9.8	18.21	21.1		0.2448	4	??	Extended radio source
TGS162Z298		02 53 44.43	-26 16 13.6	13.3	19.44	2.2		0.1550	3	Aa?	
TGS315Z010		02 53 57.68	-28 58 41.0	14.1	18.47	5.9		0.0000	5	star	
TGS162Z056		02 54 20.28	-25 04 17.6	8.9	18.14	26.0		0.1361	5	Aa	Extended radio source

Table 1. Candidate 2dFGRS/NVSS radio sources (continued).

(1) 2dFGRS name	(2) Other name	(3) Position α (J2000)	(4) Offset (arcsec)	(5) b_J (mag)	(6) $S_{1.4}$ (mJy)	(7) $S_{60\mu\text{m}}$ (Jy)	(8) Redshift z	(9) Q	(10) Class	(11) Comments
TGS162Z037	ESO 480-012	02 54 44.91 -25 06 40.8	3.9	15.75	5.9	1.060	0.0161	5	SF	
TGS395Z125		02 54 50.66 -31 01 46.3	9.8	19.34	3.2		0.3009	4	Aa	
TGS162Z018	ESO 480-013	02 55 19.62 -25 32 39.0	1.4	16.47	4.5	0.709	0.0285	5	SF	
TGS237Z129		02 55 06.35 -28 09 33.2	12.9	19.17	4.0		0.2754	4	Aa	
TGS522Z219		02 55 30.42 -33 15 30.9	8.7	18.34	2.6	0.164	0.1098	4	SF?	
TGS522Z301		02 55 37.01 -34 13 51.9	4.9	18.05	2.4	0.241	0.0918	4	SF	
TGS237Z119	ESO 417-005	02 56 13.06 -28 02 31.9	3.0	14.64	5.7	0.452	0.0415	5	SF	
TGS316Z135		02 56 26.72 -29 16 38.5	3.1	16.70	2.6		0.1009	4	SF	
TGS163Z327		02 57 39.94 -25 54 17.4	1.0	17.99	18.7		0.1368	4	Aa	Extended radio source
TGS522Z138		02 57 45.61 -33 28 56.1	4.9	19.18	3.9		0.3351	4	Ae?	
TGS163Z135		02 57 55.95 -25 29 42.3	4.9	17.85	3.6		0.1412	4	Ae	
TGS522Z070		02 59 42.54 -32 59 29.9	13.6	18.41	3.2		0.1464	4	SF	
TGS522Z018		03 00 57.00 -32 50 29.0	5.2	17.07	3.6		0.0938	4	Ae?	
TGS316Z048		03 00 59.51 -29 24 52.0	3.4	18.91	48.4		0.1803	4	Aa	Extended radio source
TGS522Z009		03 01 19.67 -33 23 51.9	2.4	16.69	21.1		0.1345	4	Aa	Extended radio source
TGS316Z040		03 01 24.00 -28 39 41.3	4.2	16.45	4.6	0.398	0.0534	4	SF	
TGS163Z237		03 01 25.16 -25 58 24.1	2.4	19.23	3.9		0.1370	4	Aa	
TGS523Z006		03 01 29.98 -33 24 04.4	4.5	17.93	25.0		0.1337	4	Aa	Extended radio source
TGS163Z234		03 01 35.91 -26 50 57.1	5.8	19.03	3.3		0.2209	3	Aa	
TGS396Z098		03 01 56.77 -31 20 32.8	2.1	19.40	7.0		0.2477	4	Aa	Extended radio source
TGS238Z241		03 02 11.44 -27 07 26.3	1.6	18.20	10.7	0.918	0.2214	4	SF?	
TGS396Z091		03 02 16.99 -31 10 46.0	7.3	18.71	9.6		0.0602	4	SF?	
TGS163Z212		03 02 27.48 -26 04 38.1	9.0	18.27	4.1		0.1411	4	Aa	
TGS469Z192		03 03 09.99 -31 02 42.8	4.1	18.22	4.1		0.1917	4	Aa?	
TGS238Z070		03 03 18.49 -27 37 18.7	12.2	19.23	9.9		0.2615	4	Aa	Extended radio source – not this ID
TGS396Z054		03 03 46.87 -29 40 26.5	6.1	18.50	3.3		0.1805	4	Aa	
TGS164Z091		03 03 55.86 -25 49 31.4	7.6	18.83	2.4		0.1608	4	Aa	
TGS238Z206		03 04 13.08 -26 46 18.9	9.7	18.14	15.6		0.0008	4	star	
TGS238Z047	ESO 417-012	03 04 19.43 -27 41 33.6	3.3	16.52	5.3	0.741	0.0215	4	SF	
TGS238Z046		03 04 24.17 -27 36 39.6	13.8	19.11	27.1			2	Ae?	
TGS317Z111		03 04 30.16 -29 09 29.3	11.2	19.27	3.2		0.0000	4	star	
TGS238Z180		03 04 51.80 -26 54 32.3	6.9	17.16	3.1	0.186	0.1255	4	SF	
TGS164Z087	MRC 0302-258	03 04 54.07 -25 39 46.7	1.9	18.69	344.4			2	??	Extended radio source
TGS238Z036	ESO 417-015	03 05 07.98 -27 20 13.3	9.6	15.03	2.8	0.251	0.0203	4	SF	
TGS164Z077		03 05 15.34 -25 31 32.7	8.4	18.52	5.2		0.1442	4	SF	
TGS396Z015		03 05 18.09 -30 34 05.7	6.9	19.34	9.8		0.2065	4	Aa	Extended radio source
TGS238Z030		03 05 31.24 -27 48 52.5	3.1	17.21	5.5	0.482	0.0653	4	SF	
TGS239Z196	ESO 480-030	03 05 52.89 -27 13 51.5	8.6	14.80	3.5	0.301	0.0219	4	SF	
TGS164Z162		03 06 02.67 -26 07 31.6	0.2	17.49	46.6		0.1440	4	Aa	Extended radio source
TGS164Z151		03 06 24.69 -26 05 55.2	2.8	19.04	10.0		0.2203	4	Aa	Extended radio source

Table 1. Candidate 2dFGRS/NVSS radio sources (continued).

(1) 2dFGRS name	(2) Other name	(3) Position α (J2000)	(4) Offset (arcsec)	(5) b_J (mag)	(6) $S_{1.4}$ (mJy)	(7) $S_{60\mu m}$ (Jy)	(8) Redshift z	(9) Q	(10) Class	(11) Comments
TGS397Z204		03 06 58.42 -30 10 38.0	0.3	19.44	10.8		0.2482	4	Aa	
TGS397Z171		03 07 41.94 -30 28 42.2	3.7	16.62	2.5		0.0678	4	Aa	
TGS164Z013		03 08 31.16 -25 27 45.7	13.9	18.07	3.8	0.269	0.0929	4	Aae	
TGS318Z156		03 08 35.19 -28 47 49.7	6.9	18.28	2.8	0.496	0.0687	4	SF	
TGS239Z089		03 08 48.74 -27 52 35.6	5.4	18.79	4.3		0.2216	4	SF?	
TGS239Z061		03 10 00.89 -28 06 27.8	1.6	18.94	3.3		0.1580	4	Aa?	
TGS397Z053		03 10 23.43 -30 14 02.3	2.3	16.98	3.6	0.299	0.1045	4	SF?	
TGS470Z153		03 11 17.71 -31 10 21.7	5.6	17.79	9.6		0.0600	4	Ae	Extended radio source
TGS165Z303		03 11 28.89 -25 04 46.2	1.9	17.78	97.9		0.1625	4	Aa	Extended radio source
TGS240Z082		03 11 54.21 -27 23 31.4	0.5	17.72	11.0		0.1269	4	Aae	Extended radio source
TGS397Z016*		03 11 59.92 -31 00 16.2	5.4	18.99	5.2	0.229	0.1726	4	Ae	
TGS239Z018		03 12 16.28 -27 53 39.3	10.7	16.71	2.7	0.191	0.0701	4	SF	Bright galaxy – correct ID
TGS165Z257	ESO 481-010	03 12 17.38 -26 13 15.1	13.9	16.26	2.7	0.209	0.0753	4	SF	Bright galaxy – correct ID
TGS239Z227*	ESO 481-012	03 12 26.61 -27 08 18.5	9.4	15.28	6.1	0.468	0.0645	4	SF	
TGS318Z046		03 12 27.36 -29 20 32.0	5.8	18.48	4.9		0.1544	4	Aa	
TGS240Z211		03 13 30.24 -27 08 23.6	0.6	18.17	42.1		0.1395	4	Aae	
TGS165Z186		03 13 30.59 -26 40 16.2	5.1	18.34	5.8		0.1424	4	Aa	
TGS398Z133		03 13 34.09 -31 14 35.0	13.3	18.50	6.9		0.0664	4	Aa	
TGS398Z122		03 13 43.98 -31 21 48.5	3.5	19.29	13.6		0.2387	4	Aa	
TGS241Z059		03 13 51.27 -27 35 47.1	11.3	19.41	3.5		0.1392	3	Aae	
TGS398Z068		03 14 52.47 -31 28 54.4	4.5	18.87	76.0		0.2225	4	Aa	Extended radio source
TGS165Z065		03 15 10.93 -25 52 02.6	2.9	18.75	9.3		0.2175	4	Aa	
TGS398Z011		03 16 55.01 -30 56 16.1	10.6	16.57	2.6	0.222	0.0414	4	SF	Bright galaxy – correct ID
TGS240Z013		03 16 55.17 -27 50 26.5	0.4	18.94	3.3		0.2238	4	Aae	
TGS398Z009		03 16 59.68 -30 40 46.1	12.2	16.83	2.6		0.0650	4	SF	Bright galaxy – correct ID
TGS319Z013		03 17 02.80 -28 51 28.5	2.1	18.69	4.2		0.1224	4	Aa	
TGS166Z273		03 18 06.80 -26 00 23.8	4.5	19.41	89.0		0.1624	3	Aa	Extended radio source
TGS241Z101		03 20 55.37 -27 30 40.4	1.8	17.80	12.7		0.1276	4	Aa	
TGS166Z108		03 21 11.63 -26 09 13.3	6.7	17.23	3.0	0.297	0.0801	4	SF	
TGS166Z029		03 23 05.10 -26 38 18.2	12.1	16.99	3.8		0.0705	4	Aa	Bright galaxy – correct ID
TGS167Z303		03 24 51.89 -25 31 38.7	1.5	16.91	3.7		0.0708	4	Aa	
TGS167Z279	NGC 1327	03 25 23.22 -25 40 45.8	7.9	15.15	3.8	0.625	0.0428	4	SF?	
TGS167Z246	MCG -04-09-010	03 26 01.39 -25 44 31.3	4.3	15.55	3.3	0.379	0.0416	3	SF	
TGS167Z203		03 26 37.08 -25 43 52.6	6.7	17.78	4.1	0.530	0.0897	4	SF	
TGS167Z160		03 27 25.39 -26 43 01.2	14.1	19.08	3.1		0.2034	3	Aa?	
TGS167Z061		03 29 07.79 -26 35 55.5	4.7	18.92	6.6		0.1722	3	Ae	
TGN284Z105		09 52 50.92 -01 58 17.6	8.8	18.20	3.1		0.0561	4	SF	
TGN092Z279		09 52 52.41 -04 50 00.6	13.4	18.68	68.4		0.1708	3	Aa	Extended radio source – not this ID
TGN284Z103		09 52 56.95 -00 47 30.8	1.9	17.93	25.0		0.0898	4	Aa	Extended radio source
TGN419Z231		09 53 16.10 +00 40 01.7	13.5	18.41	3.2		0.0935	3	Aa?	

Table 1. Candidate 2dFGRS/NVSS radio sources (continued).

(1) 2dFGRS name	(2) Other name	(3) Position α (J2000)	(4) Offset (arcsec)	(5) b_J (mag)	(6) $S_{1.4}$ (mJy)	(7) $S_{60\mu m}$ (Jy)	(8) Redshift z	(9) Q	(10) Class	(11) Comments
TGN419Z222		09 53 20.33 +01 22 31.8	13.7	17.52	3.4		0.0956	4	SF?	
TGN152Z225		09 53 29.35 -03 14 11.9	1.4	15.96	4.9	0.461	0.0581	4	SF	
TGN351Z183		09 53 30.38 +00 26 54.3	2.1	17.29	12.0		0.0802	3	Aa	
TGN092Z235		09 53 34.37 -05 15 18.3	14.1	18.95	2.8		0.0931	3	??	
TGN419Z202		09 53 37.86 +00 35 18.4	1.7	18.21	2.5		0.0915	4	Aa	
TGN152Z205		09 54 00.68 -04 20 38.1	13.9	18.26	17.9		0.1082	4	SF	Extended radio source – not this ID
TGN092Z201		09 54 03.46 -05 38 19.0	9.1	19.42	6.7		0.1586	4	Aa	
TGN284Z051*		09 54 07.38 -01 36 27.9	2.9	18.22	79.0		0.1065	5	Aa	Double radio source
TGN092Z198		09 54 08.78 -04 41 02.0	8.5	17.34	2.7		0.0686	4	SF	
TGN351Z147		09 54 21.51 +00 09 11.1	8.1	18.99	2.7		0.1507	4	Aa	
TGN034Z178		09 54 22.26 -06 30 49.1	0.7	19.44	31.5		0.2469	4	Aa	Extended radio source
TGN152Z171		09 54 36.77 -04 15 10.9	2.7	18.85	4.9	0.387	0.2371	3	Ae?	
TGN092Z135		09 55 06.67 -05 41 39.6	6.1	17.11	4.9	0.606	0.0708	4	Ae	
TGN215Z250		09 55 09.16 -02 43 07.1	7.2	18.48	5.9		0.1632	4	Aa	
TGN152Z123		09 55 38.89 -04 20 18.2	4.6	15.64	3.3	0.256	0.0439	4	SF	
TGN152Z302		09 56 05.64 -04 30 38.2	8.1	17.75	6.1	0.453	0.0358	4	SF	
TGN215Z203		09 56 11.16 -01 52 20.6	14.2	17.56	13.4		0.0373	4	SF	
TGN352Z229		09 56 23.63 -00 10 15.7	9.9	19.40	6.1		0.1580	3	??	
TGN035Z041		09 56 25.26 -06 05 42.1	10.4	18.96	4.5		0.2175	4	Aa	
TGN419Z056		09 56 40.94 +02 10 13.6	2.7	17.24	2.7	0.221	0.0319	3	SF	
TGN092Z035		09 56 50.53 -05 59 11.4	1.6	19.34	13.2		0.0001	4	star	
TGN152Z068		09 57 03.18 -04 14 47.4	14.7	19.13	25.1		0.0001	3	star	
TGN285Z123		09 57 09.04 -01 52 44.7	7.1	18.84	4.3		0.1219	5	Aa	
TGN351Z006		09 57 09.24 +00 00 32.1	2.8	18.01	11.4		0.1255	4	Aa	Extended radio source
TGN285Z117		09 57 10.20 -02 04 17.2	4.5	19.44	5.3		0.2817	3	Aa?	
TGN420Z238		09 57 21.14 +00 42 21.7	4.3	18.43	5.8		0.0873	4	SF	
TGN352Z178		09 57 34.67 +00 14 18.4	7.2	19.29	27.2		0.1605	4	Aa	Extended radio source
TGN152Z279		09 57 59.61 -04 30 14.7	6.7	17.61	4.5		0.0567	3	SF	
TGN093Z297		09 58 17.57 -04 38 11.8	9.8	17.95	3.1		0.1572	3	Aa	
TGN216Z148		09 58 20.84 -03 13 41.7	6.1	17.92	4.1		0.0832	4	Aa	
TGN215Z012	CGCG 008-005	09 58 31.09 -02 49 21.1	8.5	14.79	3.5	0.202	0.0474	4	SF	
TGN420Z200		09 58 35.24 +00 44 34.2	1.5	17.60	6.8	0.923	0.0652	4	SF	
TGN215Z144		09 58 47.31 -02 09 39.9	4.6	18.10	3.7		0.0913	4	Aa	
TGN035Z160		09 59 19.80 -06 28 22.4	1.3	17.36	22.1		0.1471	4	Aa	Extended radio source
TGN216Z253		09 59 33.98 -02 08 51.9	11.0	19.11	6.8		0.0007	4	star	
TGN285Z018		09 59 39.04 -01 14 53.4	2.9	18.14	11.8		0.1376	5	Aa	
TGN093Z186		09 59 52.12 -05 46 59.7	5.4	16.35	7.7		0.0616	4	Ae	Extended radio source
TGN420Z110		10 00 05.26 +01 20 59.3	13.5	19.43	9.9		0.2203	4	Aa	Double radio source – not this ID
TGN352Z063		10 00 06.88 +00 13 09.1	6.0	19.24	3.3		0.1910	4	Aa	
TGN352Z050		10 00 25.17 +00 14 57.2	11.1	18.79	19.0		0.2202	4	Aa	Extended radio source – correct ID

Table 1. Candidate 2dFGRS/NVSS radio sources (continued).

(1) 2dFGRS name	(2) Other name	(3) Position α (J2000)	(4) Offset (arcsec)	(5) b_J (mag)	(6) $S_{1.4}$ (mJy)	(7) $S_{60\mu\text{m}}$ (Jy)	(8) Redshift z	(9) Q	(10) Class	(11) Comments
TGN093Z139		10 00 32.23 -06 06 02.3	1.5	18.84	117.1		0.2734	4	Aa	Extended radio source
TGN420Z082		10 00 45.52 +01 39 26.5	12.9	19.11	4.4		0.2206	3	Aa	
TGN286Z189		10 00 46.01 -01 41 53.6	12.1	17.19	3.3	0.398	0.0375	4	SF	
TGN353Z151		10 01 52.81 -00 07 32.3	4.0	17.13	38.4		0.0335	4	Aa	Extended radio source
TGN153Z038		10 02 08.80 -04 13 55.5	6.6	17.17	3.8		0.0938	4	Aa	
TGN286Z109		10 02 41.77 -01 20 09.4	2.9	19.34	15.3		0.1779	4	Aa	Extended radio source
TGN353Z089		10 03 01.36 -00 09 55.8	13.1	19.23	3.1		0.0449	3	SF?	
TGN154Z224		10 03 11.61 -03 22 17.9	5.7	19.19	4.5		0.2157	5	Aa	
TGN421Z210		10 03 12.77 +01 08 55.6	8.1	18.22	2.6		0.0681	4	SF	
TGN286Z081*		10 03 27.09 -01 32 46.7	6.5	16.79	23.8	0.855	0.0460	4	SF	Extended radio source
TGN216Z011		10 03 37.17 -02 48 35.8	2.2	18.75	9.8		0.1395	4	Aa	Extended radio source
TGN286Z063		10 04 04.98 -00 32 54.2	8.2	19.33	4.5		0.2887	4	??	
TGN217Z240		10 04 24.22 -02 25 29.7	7.3	15.94	3.8	0.335	0.0201	5	SF	
TGN217Z221		10 05 02.03 -02 08 17.5	13.0	19.44	9.2		0.1881	4	Aa	Extended radio source – correct ID
TGN286Z025		10 05 02.74 -00 42 33.6	6.2	19.00	4.8		0.1961	4	Aa	
TGN286Z023		10 05 03.76 -01 17 54.9	10.2	18.89	2.9		0.1848	4	Aae?	
TGN421Z119		10 05 12.28 +00 37 54.9	7.6	18.58	3.0		0.0623	4	SF	
TGN353Z009		10 05 13.49 +00 33 39.6	10.6	19.19	16.4		0.1787	4	Aa	Extended radio source – not this ID
TGN353Z006		10 05 21.49 +00 05 18.4	1.1	19.43	9.0		0.1793	4	Aa	
TGN286Z008		10 05 22.30 -01 33 53.4	1.5	16.99	3.6	0.349	0.0459	4	SF	
TGN286Z007		10 05 27.14 -00 52 29.0	4.9	19.33	4.1		0.2059	3	Aa	
TGN353Z002		10 05 33.43 +00 17 59.1	1.9	19.05	10.4		0.2143	4	Aa	
TGN421Z097		10 05 50.22 +00 37 58.4	5.6	16.13	24.4		0.0209	4	Aa	
TGN421Z096		10 05 51.77 +01 26 47.9	1.5	18.76	17.9		0.1230	4	Aa	Extended radio source
TGN155Z252		10 07 00.84 -04 03 25.3	9.6	19.32	4.7			1	??	
TGN218Z083		10 07 19.01 -02 54 27.0	5.4	18.09	2.8		0.1934	4	SF	
TGN154Z014		10 07 49.16 -03 58 29.0	4.6	18.92	12.1		0.2510	3	Aa	
TGN217Z154	IC 592	10 07 58.73 -02 29 50.3	12.4	15.71	6.9	0.501	0.0203	5	SF	Extended radio source – correct ID
TGN155Z230		10 08 17.44 -03 46 05.6	8.9	14.32	2.8	0.345	0.0205	4	SF	
TGN218Z230		10 08 18.11 -02 31 35.6	3.1	15.85	3.3	0.379	0.0201	4	SF	
TGN218Z228		10 08 20.45 -02 17 07.1	2.8	17.01	10.6		0.0652	4	Aa	
TGN155Z223	MCG -01-26-026	10 08 33.63 -04 28 40.1	0.2	14.78	250.7		0.0510	5	Aa	
TGN421Z004		10 08 55.39 +01 44 19.5	4.9	16.99	6.7		0.0456	4	Aa?	Extended radio source
TGN155Z280		10 08 59.58 -04 53 20.7	1.5	19.10	8.1		0.2172	4	Aa	Extended radio source
TGN422Z122*		10 09 51.56 +01 13 27.8	8.5	16.67	29.2	0.279	0.0459	4	Ae?	Triple radio source
TGN422Z102		10 10 04.98 +01 53 03.6	8.3	18.27	5.7		0.0951	4	Aa	
TGN219Z136		10 11 04.83 -02 02 35.7	1.8	19.36	7.0		0.1980	4	Aa	
TGN422Z002		10 12 30.06 +01 57 33.4	4.5	18.11	23.7		0.1225	4	Aa?	Extended radio source
TGN096Z333		10 12 51.62 -05 35 36.8	8.1	16.54	4.0	0.426	0.0381	4	SF	
TGN155Z327		10 13 02.61 -04 37 01.5	5.5	18.75	4.2		0.1395	4	SF	

Table 1. Candidate 2dFGRS/NVSS radio sources (continued).

(1) 2dFGRS name	(2) Other name	(3) Position α (J2000)	(4) Offset (arcsec)	(5) b_J (mag)	(6) $S_{1.4}$ (mJy)	(7) $S_{60\mu m}$ (Jy)	(8) Redshift z	(9) Q	(10) Class	(11) Comments
TGN219Z100		10 13 02.84 -03 27 07.1	7.2	17.16	3.5		0.0411	4	Ae?	
TGN219Z259		10 13 55.30 -01 51 09.4	13.5	16.92	3.2		0.0594	3	SF	
TGN038Z253		10 13 55.48 -06 05 30.5	14.4	18.22	15.1		0.0875	4	SF	Extended radio source – not this ID
TGN219Z066		10 14 21.44 -02 50 28.6	3.7	17.60	6.8		0.0614	4	SF	Extended radio source
TGN096Z274		10 14 21.78 -05 55 26.2	7.2	18.55	4.4		0.1622	4	Aa	
TGN097Z244		10 16 28.80 -05 56 45.4	10.0	19.10	2.7		0.1454	4	SF	
TGN097Z223		10 16 54.52 -05 52 14.7	8.9	15.57	4.7		0.0389	4	Aa?	
TGN219Z179		10 16 58.43 -02 22 29.5	11.3	16.91	3.8	0.316	0.0466	4	SF	Bright galaxy – correct ID
TGN097Z192		10 17 25.25 -05 12 29.7	9.3	16.92	5.8	0.414	0.0540	4	SF?	
TGN156Z159		10 17 32.66 -04 32 03.0	11.5	16.73	2.9		0.0393	3	SF	Bright galaxy – correct ID
TGN156Z153		10 17 37.69 -04 13 21.2	5.8	19.44	8.5		0.2142	3	Aa	
TGN423Z108		10 17 42.23 +01 12 36.3	11.2	18.98	27.4		0.0782	4	SF?	Extended radio source – not this ID
TGN219Z152		10 17 45.37 -02 22 17.4	5.4	16.44	3.5			1	??	
TGN220Z065		10 18 12.28 -03 08 44.3	8.3	17.31	4.4	0.287	0.0498	5	SF	
TGN220Z258		10 18 03.32 -01 54 20.4	1.4	17.24	14.8		0.0607	4	Aa	Extended radio source
TGN097Z126		10 18 37.90 -04 43 08.9	13.2	18.00	2.8		0.1264	4	SF	
TGN156Z104		10 18 49.38 -03 35 46.6	1.1	18.84	30.7		0.2105	3	Aa	Extended radio source
TGN097Z073		10 19 23.40 -06 10 07.5	1.7	18.20	4.1		0.1622	4	Aa	
TGN156Z046*		10 19 39.18 -04 04 01.4	9.5	16.05	7.8		0.0391	4	Ae	Extended radio source
TGN424Z142		10 21 32.73 +01 11 20.7	9.7	17.63	2.9		0.0941	4	SF	
TGN424Z101	IC 605	10 22 24.12 +01 11 55.1	1.0	15.17	8.8	0.698	0.0219	4	SF	
TGN358Z083		10 23 24.75 +00 52 50.9	8.9	18.90	3.2			2	??	
TGN098Z023		10 23 29.33 -06 08 32.6	0.8	19.20	10.1		0.1458	4	Aa	Extended radio source
TGN099Z348		10 23 36.91 -04 51 14.8	6.1	16.31	5.6		0.0390	4	SF	
TGN424Z034		10 23 54.38 +01 56 29.6	3.5	18.94	9.8			2	??	
TGN221Z023	CGCG 009-018	10 23 56.51 -03 10 54.5	2.9	14.32	7.8		0.0188	4	SF?	Extended radio source
TGN222Z318		10 24 07.26 -02 03 46.2	3.6	16.07	12.2		0.0528	4	Aa	
TGN099Z317	IC 608	10 24 21.20 -06 02 21.5	4.1	14.95	5.9		0.0375	4	SF	
TGN425Z165		10 24 42.58 +01 10 19.8	6.9	18.96	5.9		0.1491	4	Aa	
TGN222Z132		10 25 26.77 -03 05 36.1	3.8	16.74	3.5		0.0505	4	SF?	
TGN222Z108		10 26 06.27 -02 46 32.3	0.8	16.05	3.3		0.0571	4	Aae	
TGN222Z097		10 26 23.23 -02 49 01.5	13.3	18.34	30.1		0.0577	4	SF?	Extended radio source – not this ID
TGN158Z250	CGCG 009-035	10 26 28.54 -03 40 55.6	7.4	15.36	5.1		0.0388	4	Aa	
TGN158Z232	IC 614	10 26 51.88 -03 27 52.2	1.6	15.22	7.0		0.0346	4	Ae	
TGN099Z110		10 27 15.51 -05 10 57.1	8.0	19.42	3.4		0.2045	3	Aae	
TGN099Z108		10 27 16.80 -05 38 47.4	1.5	17.99	4.2		0.1547	4	SF	
TGN222Z218		10 27 35.27 -02 16 13.6	0.6	18.99	5.1		0.2178	4	Ae	
TGN158Z190		10 27 44.98 -03 51 49.0	6.7	16.88	3.6		0.0311	4	SF	
TGN158Z162		10 28 20.58 -04 24 21.1	4.5	15.06	3.5		0.0307	4	SF	
TGN223Z133		10 28 52.99 -03 14 45.6	8.6	17.93	3.5		0.0356	3	SF	

Table 1. Candidate 2dFGRS/NVSS radio sources (continued).

(1) 2dFGRS name	(2) Other name	(3) Position α (J2000)		(4) Offset (arcsec)	(5) b_J (mag)	(6) $S_{1.4}$ (mJy)	(7) $S_{60\mu m}$ (Jy)	(8) Redshift z	(9) Q	(10) Class	(11) Comments
TGN100Z170	MCG -01-27-010	10 29 58.96	-04 59 03.9	9.4	15.06	4.6		0.0291	4	SF	
TGN158Z038		10 30 17.35	-03 36 13.2	8.0	17.78	3.2		0.0616	4	Aae	
TGN100Z141		10 30 26.22	-05 19 00.3	3.2	16.92	7.8		0.0627	4	SF	Extended radio source
TGN100Z050		10 31 34.35	-05 30 43.8	4.4	18.71	4.7		0.1859	4	Aa	
TGN042Z009		10 31 52.82	-06 27 00.9	0.7	18.28	27.5		0.1676	4	Aa	
TGN100Z232		10 34 25.79	-05 54 30.7	8.3	18.29	3.6		0.1674	3	Aa	
TGN294Z262		10 34 38.21	-00 51 10.8	3.0	16.82	2.9		0.0739	5	SF	
TGN293Z129		10 35 23.15	-01 37 09.8	13.6	16.81	2.8		0.0238	3	SF	Bright galaxy – correct ID
TGN101Z286		10 36 42.77	-06 03 28.0	5.4	18.71	9.4		0.1333	4	Aa	Extended radio source
TGN361Z125		10 36 47.17	-00 40 57.5	2.9	18.89	12.8		0.0960	4	Aa	Extended radio source
TGN361Z107		10 37 05.71	-00 42 32.4	3.8	18.75	3.8		0.0822	3	Ae	
TGN225Z128	IC 627	10 37 19.85	-03 21 28.8	1.6	14.50	17.9		0.0318	4	SF?	Extended radio source
TGN295Z289		10 38 13.32	-01 22 28.5	2.6	17.45	4.2		0.0875	5	SF	
TGN294Z142		10 38 36.18	-00 45 52.7	1.9	16.51	4.7		0.0756	4	Ae?	
TGN101Z130		10 38 47.16	-05 56 40.8	5.7	17.15	3.1		0.1308	5	Ae	
TGN102Z346		10 39 48.95	-05 48 11.4	11.7	18.94	3.5		0.2489	4	SF?	
TGN160Z216		10 40 02.51	-03 59 08.5	2.1	17.44	27.7		0.1346	4	Aa	Extended radio source
TGN160Z187		10 40 12.67	-04 04 11.7	5.3	17.87	11.7		0.1301	4	Aa	Extended radio source
TGN160Z169		10 40 24.32	-03 06 34.9	4.7	18.53	3.7		0.1474	4	Aa	
TGN160Z156		10 40 32.56	-04 33 29.3	5.2	19.03	4.0		0.1581	4	Ae	
TGN294Z022		10 41 01.70	-00 44 47.8	12.1	18.17	2.7		0.1385	4	Aa	
TGN160Z102		10 41 15.61	-04 20 46.9	5.7	17.58	3.6		0.0825	3	SF?	
TGN160Z067		10 41 42.85	-03 40 02.3	12.0	18.53	3.1		0.1484	4	Aa	
TGN226Z110		10 42 10.48	-03 23 28.1	1.5	19.06	21.0		0.2317	4	Ae	
TGN160Z003		10 43 22.16	-03 56 08.0	2.9	19.18	3.5		0.1767	4	Aa	
TGN161Z310		10 43 27.23	-04 58 05.3	4.1	16.84	3.0		0.0434	4	SF	
TGN161Z178		10 45 34.04	-04 17 21.3	13.2	18.43	2.5		0.1417	4	SF	
TGN161Z167		10 45 42.81	-04 16 34.5	11.3	19.12	24.9		0.1282	4	SF?	Extended radio source – not this ID
TGN161Z158		10 45 57.89	-04 04 39.8	11.4	18.15	4.3		0.0777	4	SF	
TGN162Z320		10 46 17.63	-03 56 33.1	10.8	19.34	4.4		0.2565	4	Aa	
TGN161Z113		10 46 35.00	-04 32 37.0	0.4	18.96	12.9		0.2591	4	Aa	
TGN162Z302		10 47 25.29	-03 55 46.1	3.9	18.58	5.8		0.0678	3	SF?	
TGN162Z295		10 47 36.50	-04 46 06.6	7.8	17.16	2.5	0.272	0.0612	4	SF	
TGN162Z289		10 47 42.71	-04 46 56.3	7.4	17.69	3.6		0.1114	4	Ae	
TGN162Z276		10 47 55.40	-04 32 27.2	1.3	16.37	132.0		0.0783	4	Aa	Extended radio source
TGN162Z245		10 48 16.16	-03 55 26.5	4.2	19.35	3.3		0.2636	4	Aa	
TGN228Z216		10 49 28.59	-02 27 30.6	2.3	19.37	8.3		0.1990	4	Aa	
TGN103Z089		10 49 55.50	-05 33 25.3	7.4	16.02	5.1		0.0658	4	SF	
TGN162Z033		10 51 21.95	-04 16 55.5	4.0	18.39	8.2		0.1356	4	Aa	
TGN103Z006		10 52 28.58	-05 04 45.3	3.4	17.82	2.6	0.221	0.1270	4	SF?	

Table 1. Candidate 2dFGRS/NVSS radio sources (continued).

(1) 2dFGRS name	(2) Other name	(3) Position α (J2000)	(4) Offset (arcsec)	(5) b_J (mag)	(6) $S_{1.4}$ (mJy)	(7) $S_{60\mu\text{m}}$ (Jy)	(8) Redshift z	(9) Q	(10) Class	(11) Comments
TGN298Z263		10 52 53.74 -01 53 15.8	6.1	16.36	5.7	0.952	0.0261	4	SF	
TGN163Z340		10 52 58.84 -03 17 30.4	4.5	17.51	5.2	0.319	0.0710	4	SF	
TGN229Z124		10 53 07.24 -02 49 47.1	0.1	19.38	28.0		0.2145	4	Aa	
TGN162Z332		10 53 27.62 -04 05 34.9	3.9	16.57	5.1	0.267	0.0481	4	Aae?	
TGN366Z219		10 53 40.41 +00 09 02.9	0.6	17.24	11.5		0.1083	4	Aa	
TGN163Z266		10 54 30.38 -04 10 09.4	3.7	15.30	11.8		0.0219	4	Aa	
TGN163Z203		10 55 20.37 -03 50 43.3	5.2	17.64	5.1	0.752	0.0484	4	SF?	
TGN163Z202		10 55 20.43 -03 47 29.2	4.6	17.63	22.6		0.1124	4	Aa	Extended radio source
TGN229Z094		10 55 30.27 -03 25 30.4	1.3	17.15	5.4	0.433	0.0702	4	SF	
TGN104Z182		10 55 36.77 -05 31 13.1	4.7	18.62	8.3		0.2067	4	Aa	
TGN163Z159		10 55 56.66 -03 53 23.7	4.1	16.21	7.1		0.0476	4	SF	
TGN104Z157		10 56 00.52 -05 23 18.2	8.0	17.90	3.1		0.1110	4	Aa	
TGN298Z089		10 56 21.57 -00 53 21.5	12.3	17.03	3.4		0.0754	4	SF?	
TGN163Z123		10 56 48.86 -03 37 25.4	1.8	18.67	19.2		0.1818	4	Aa	Extended radio source
TGN163Z109		10 57 02.20 -04 15 51.7	9.2	15.94	3.1	0.293	0.0336	3	SF?	
TGN229Z228		10 57 06.43 -02 13 01.1	9.8	18.34	4.3		0.1863	4	Aa	
TGN105Z314		10 57 34.80 -05 53 27.1	10.9	17.88	3.9		0.1099	4	SF	
TGN366Z106		10 57 42.46 -00 20 13.1	13.9	17.40	3.6		0.0837	4	Aa	
TGN105Z301		10 57 45.73 -05 39 57.9	1.4	18.89	4.8		0.1871	4	Aa	
TGN164Z290	MCG -01-28-008	10 57 52.57 -04 21 45.2	2.6	14.69	13.4		0.0220	4	Ae?	
TGN105Z279		10 58 03.84 -06 15 38.0	3.0	15.32	54.0		0.0484	4	Aa	Extended radio source
TGN164Z276	MCG -01-28-011	10 58 05.66 -04 45 32.4	1.1	15.15	5.0		0.0224	4	SF	
TGN299Z237		10 58 17.48 -01 47 47.7	10.8	18.25	4.5		0.1315	4	Ae	
TGN105Z257		10 58 19.57 -05 08 37.9	8.5	16.12	2.8	0.570	0.0325	4	Ae	
TGN434Z168		10 58 26.55 +00 34 29.8	8.3	19.07	2.7		0.0852	4	SF?	
TGN229Z166		10 58 35.35 -02 35 53.3	1.3	16.22	205.9	1.304	0.0357	4	Ae	
TGN164Z255		10 58 39.31 -03 30 16.6	1.7	15.82	32.5	0.401	0.0661	4	SF	Extended radio source
TGN299Z119*		10 59 28.87 -01 01 39.7	12.6	18.23	7.1		0.1861	4	Aa	Extended radio source - not this ID
TGN105Z178		10 59 33.42 -05 07 55.6	1.7	18.34	19.4		0.1840	4	Aa	Extended radio source
TGN105Z155		10 59 51.65 -06 09 01.3	1.2	15.16	16.6		0.0311	4	Aae	
TGN105Z122		11 00 11.35 -05 22 54.5	8.6	15.86	4.4	0.512	0.0325	4	SF	
TGN105Z105		11 00 20.72 -05 00 29.1	3.9	15.91	6.2		0.0684	4	Aa	
TGN105Z098		11 00 25.97 -06 22 33.1	2.4	18.52	14.0		0.1070	4	Ae	
TGN164Z114		11 01 28.84 -04 16 12.5	1.9	16.44	4.5	0.395	0.0687	4	SF	
TGN299Z059		11 01 36.08 -00 55 22.4	3.9	19.33	4.3		0.1590	4	Aa	
TGN300Z167		11 01 43.89 -00 49 27.7	5.2	17.93	2.9		0.0436	3	SF?	
TGN164Z100		11 01 46.04 -04 07 11.9	5.8	17.98	3.1		0.1232	4	Aae	
TGN367Z019		11 02 17.19 +00 57 59.4	5.6	18.03	4.4	0.277	0.1023	4	Aae	
TGN164Z065		11 02 18.46 -04 15 49.2	13.5	18.39	21.4		0.0003	4	star	
TGN164Z061		11 02 22.21 -04 43 21.7	1.7	16.97	11.3		0.0685	4	SF?	

Table 1. Candidate 2dFGRS/NVSS radio sources (continued).

(1) 2dFGRS name	(2) Other name	(3) Position α (J2000)	(4) Offset (arcsec)	(5) b_J (mag)	(6) $S_{1.4}$ (mJy)	(7) $S_{60\mu\text{m}}$ (Jy)	(8) Redshift z	(9) Q	(10) Class	(11) Comments
TGN164Z053		11 02 34.95 -04 48 35.2	14.4	18.83	2.8		0.1529	4	Ae?	
TGN105Z005		11 02 37.93 -05 17 12.7	2.8	16.21	3.8	0.292	0.0630	4	SF?	
TGN164Z023		11 03 13.57 -04 32 36.0	5.0	16.64	4.0	0.285	0.0400	4	SF	
TGN367Z088		11 04 03.10 -00 09 26.3	6.4	18.31	2.8		0.0863	4	SF	
TGN165Z324		11 04 20.83 -04 07 52.5	2.0	18.90	3.0		0.1825	4	Aa	
TGN230Z013		11 04 46.29 -03 06 48.8	4.6	17.84	4.3		0.0879	4	Aa	
TGN165Z299		11 04 47.18 -03 44 42.4	2.0	18.97	7.4			1	??	
TGN106Z185		11 05 07.44 -04 58 26.0	4.6	16.64	4.6	0.427	0.0539	4	SF	
TGN231Z285		11 05 36.51 -02 08 32.9	14.7	17.87	8.8	0.960	0.1585	4	Aa	
TGN230Z003		11 05 38.10 -02 57 59.6	7.6	19.14	3.4		0.1229	3	Aae?	
TGN165Z203		11 06 14.85 -04 25 52.7	4.0	19.22	37.9			1	??	Extended radio source
TGN165Z189		11 06 19.52 -03 45 43.0	3.1	17.51	10.7		0.0674	4	SF?	Extended radio source
TGN231Z068		11 06 26.14 -03 22 03.8	1.6	18.75	5.6		0.1837	4	Ae	
TGN231Z064		11 06 33.29 -03 24 51.2	11.7	18.80	28.1		0.2625	4	Ae	
TGN165Z119*		11 07 01.86 -04 08 20.3	5.7	18.06	5.1		0.1244	4	Ae	
TGN165Z107		11 07 13.14 -04 47 41.7	5.6	18.98	2.6		0.1007	4	??	
TGN231Z211		11 07 17.58 -01 57 05.0	5.5	16.42	2.8		0.0671	4	Ae	
TGN165Z054		11 07 51.81 -03 54 37.8	9.9	17.42	3.8		0.1222	4	SF?	
TGN231Z143	CGCG-11-010	11 09 35.20 -02 35 59.8	8.7	15.46	2.9	0.276	0.0314	4	SF	
TGN109Z350		11 15 51.58 -05 19 21.2	2.9	17.34	2.3		0.0627	4	SF	
TGN233Z225		11 15 57.80 -02 10 15.4	5.7	16.44	2.3		0.0797	4	SF?	
TGN233Z035		11 16 29.22 -03 08 43.5	7.2	18.78	4.1		0.1589	4	??	
TGN050Z119	MCG-01-29-006	11 16 56.25 -06 13 11.0	1.0	14.27	7.9	0.672	0.0252	4	SF	
TGN234Z240	IC 680	11 17 54.65 -01 56 47.8	4.9	14.42	13.1	0.580	0.0419	4	Aae?	Extended radio source
TGN303Z102	UGC 06311	11 17 54.87 -02 05 32.4	6.6	14.30	7.0	0.670	0.0251	4	SF?	Extended radio source
TGN168Z211		11 17 59.97 -04 51 08.7	9.2	15.75	3.1		0.0258	4	SF	
TGN109Z315		11 18 30.45 -06 22 34.8	5.1	17.31	4.2		0.0884	4	SF	
TGN234Z037		11 19 59.23 -02 47 22.8	7.2	16.41	3.8		0.0252	4	Ae?	
TGN234Z028	CGCG 011-064	11 20 20.75 -02 54 59.5	4.7	14.76	3.1		0.0254	4	SF?	
TGN109Z153		11 20 38.26 -04 44 56.8	1.3	15.22	26.2	4.925	0.0248	4	SF	Extended radio source
TGN234Z011	CGCG 011-076	11 21 12.22 -02 59 02.8	1.7	14.88	35.3	5.222	0.0252	4	SF	
TGN304Z086*		11 21 54.27 -01 43 34.0	6.1	18.97	11.9		0.1410	5	SF	
TGN234Z134		11 21 58.35 -02 40 51.0	10.6	15.44	6.9	0.739	0.0255	4	SF	Bright galaxy – correct ID
TGN109Z029		11 22 21.57 -05 11 15.8	14.8	18.74	6.5		0.1023	3	Aa	
TGN109Z025*		11 22 25.36 -05 12 13.8	4.6	17.40	62.8		0.0961	4	Aa	Extended radio source
TGN109Z024*		11 22 27.06 -05 11 43.1	7.2	16.61	94.7		0.0987	3	Aa	Extended radio source
TGN235Z087		11 22 51.73 -02 54 39.7	6.4	15.79	11.3		0.0463	5	SF	
TGN235Z217		11 23 56.00 -02 42 20.6	6.4	16.84	3.1		0.1167	4	SF	
TGN235Z203		11 24 27.12 -02 42 58.9	5.3	17.89	3.3		0.1431	4	Aa	
TGN235Z026		11 24 59.82 -02 50 56.9	3.5	18.73	8.7		0.2330	4	Aa	